Dipl.-Ing. Georg Witek

# SCALE-UP OF THE PRODUCTION OF MONOFUNCTIONAL POLYSILOXANES

## DISSERTATION

zur Erlangung des Grades eines

Doktors der technischen Wissenschaften

erreicht an der

Technischen Universität Graz

Univ.-Prof. Dipl.-Chem. Dr.rer.nat. Frank Uhlig

Institut für Anorganische Chemie

Univ.-Prof. Dipl.-Ing. Dr.techn. Matthäus Siebenhofer

Institut für Thermische Verfahrenstechnik und Umwelttechnik

Technische Universität Graz


2010

**EIDESSTATTLICHE ERKLÄRUNG**

Ich erkläre an Eides statt, dass ich die vorliegende Arbeit selbständig verfasst, andere als die angegebenen Quellen/Hilfsmittel nicht benutzt, und die den benutzten Quellen wörtlich und inhaltlich entnommene Stellen als solche kenntlich gemacht habe.

Graz, am …….. ....……
(Datum) (Unterschrift)

**STATUTORY DECLARATION**

I declare that I have authored this thesis independently, that I have not used other than the declared sources / resources, and that I have explicitly marked all material which has been quoted either literally or by content from the used sources.

Graz, …….. ....……
(Date) (Signature)

# Acknowledgment

This work is dedicated to my family: My wife Verena, my son Lorenz as well as to all other children my wife and I might get in the future and our pets Mokka and Cino. I also thank my parents, Helga and Jörg, my brother Markus as well as my parents- and brother-in-law, Sieglinde, Alfred and Christopher for all their help and support in my life.

I gratefully acknowledge Frank Uhlig and Matthäus Siebenhofer for supervising my PhD Thesis as well as for all their additional help and support.

Kristina Schrempf is gratefully acknowledged for her Diploma Thesis, Bachelor Thesis and for various student laboratory courses under my supervision.

Claus del Negro (formerly Pschera) is gratefully acknowledged for his Diploma Thesis under my supervision.

Dilek Halici, Merit Bodner and Michael Lammer are gratefully acknowledged for their Bachelor Thesis and various student laboratory courses under my supervision. I also acknowledge Sandra Pötz, Lisa Schickhofer, Rita Ambach and Saša Đurović for their student laboratory courses under my supervision.

I thank all associates and colleagues from the Institut für Anorganische Chemie (IfAC) for their help, support and of course their friendship. Kristina Schrempf, Sarah Meyer, Sandra Wiesenhofer, Margot Brandstätter, Oxana Mishchenko, Johann “Houns” Pichler and Stefan Pichler are gratefully acknowledged for sharing the laboratory, office and some spare time with me. Kathrin Schittelkopf, Petra Wilfling, Susanna Neuhold, Birgit Ehmann, Thomas Mitterfellner and Roland Fischer are acknowledged for helpful discussions, NMR and technical support. I acknowledge Maria Theresia “Resi” Koller, Barbara Seibt, Monika Filzwieser, Astrid Falk and Thomas Schalk for help and support.

I thank the associates of the Institut für Thermische Verfahrenstechnik und Umwelttechnik (TVTUT) for help and support. Especially I acknowledge Enes Aksamija for CFD calculations, Hannes Noll, Rene Fras and Herta Luttenberger for technical support.

I acknowledge Josefine Hobisch and Christian Slugovc from the Institut für Chemische Technologie von Materialien (ICTM) for SEC measurements as well as Robert Saf from the same institution for MALDI-TOF-MS measurements.

I gratefully acknowledge Hansjörg Weber from the Institut für Organische Chemie for NMR support and for organizing Badminton games and tournaments.

*Wer Humor hat,*

*der hat beinahe schon Genie.*

(Arthur Schnitzler)

# Table of Contents

# Abstract

Target of this work is the continuous ring-opening polymerization (ROP) of hexamethylcyclotrisiloxane ($D_3$) for the production of linear, monofunctional oligo- and polydimethylsiloxanes (PDMS) in a range of ten to sixty Si-O units and a narrow molecular weight distribution. The polymerization is initiated by *tert*-butyllithium (t-BuLi) and stopped by chlorodimethylsilane (CDMS) or chlorotrimethylsilane (CTMS). The polymerization is performed in polar aprotic media using THF as solvent (Figure 1).

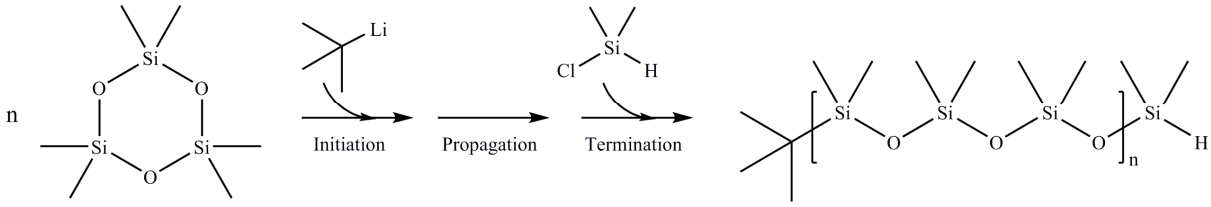


**Figure 1.** Ring-opening polymerization (ROP) of hexamethylcyclotrisiloxane ($D_3$) initiated with *tert*-butyllithium (t-BuLi) and stopped with chlorodimethylsilane (CDMS)

In a first step the three individual reactions – initiation, propagation and termination – were separately characterized in batch experiments. All three reactions are exothermic, the enthalpy change of reaction ($\Delta_R H$) was found to be -206.6 kJ mol$^{-1}$ for the initiation, -31.1 kJ mol$^{-1}$ for the propagation and -98.7 kJ mol$^{-1}$ for the termination reaction.

The Arrhenius parameters of the initiation and propagation reaction were determined. The kinetics of the termination reaction could not be obtained. The initiation reaction obeys second order kinetics, the frequency factor ($k_0$) and the activation energy ($E_A$) were found to be $k_0 = 1.39 \cdot 10^9$ L mol$^{-1}$ s$^{-1}$ and $E_A = 45.8$ kJ mol$^{-1}$. The propagation reaction was divided into two kinetic regions: oligomerization and polymerization, both obey first order kinetics in respect to the monomer as shown by the method of initial rates. The Arrhenius parameters were found to be $k_0 = 1.75 \cdot 10^6$ s$^{-1}$ and $E_A = 54.7$ kJ mol$^{-1}$ for the oligomerization and $k_0 = 8.01 \cdot 10^5$ s$^{-1}$ and $E_A = 53.3$ kJ mol$^{-1}$ for the polymerization reaction.

The polydispersity index (PDI) of the PDMS was found to be $\leq 1.2$ as determined by size exclusion chromatography (SEC) measurements. Furthermore, the ROP is highly selective towards the monomer $D_3$ in comparison to higher analogs ($D_4$) and side product formation resulting from backbiting or rearrangement was found to be insignificant.

Furthermore, the influence of matrix ions on the ROP of $D_3$ was studied. It could be shown that the admixture of various metal halogenides significantly decreases the rate of polymerization.

In a second step, a plug flow reactor (PFR) consisting of PTFE tubing was used for continuous experiments. The PTFE-PFR was coiled up a tube to induce radial mixing along

the reactor due to Dean vortices. Figure 2 shows a picture of the simulated reactor which was used for CFD calculation.

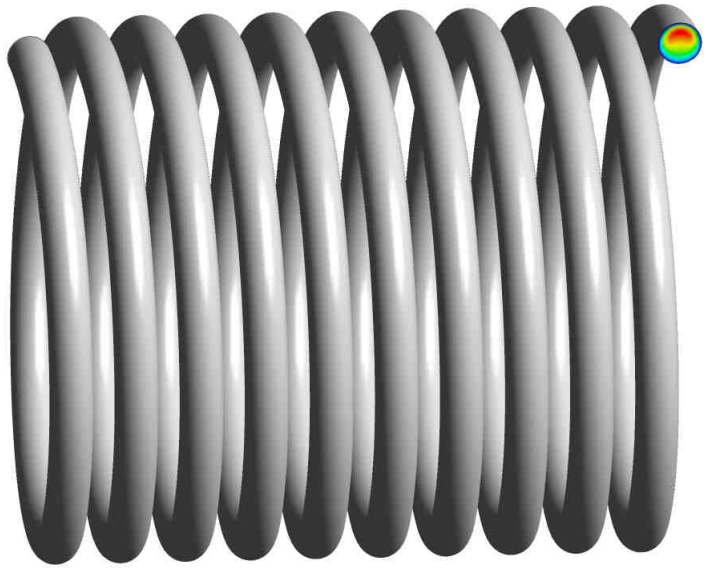

**Figure 2.** PTFE-PFR (CFD simulation) for continuous polymerization of $D_3$

First the residence time distribution (RTD) of the experimental setup was investigated. The Bodenstein number (Bo) seemingly showed uncommon behavior as its value decreased with increasing flow rate. This effect is caused by the instability of the flux resulting in the formation of two toroidal eddies starting at 3.0 mL $min^{-1}$ as shown by CFD simulations. From these results it is expected that Bo-number passes a minimum to increase at higher flow rate again.

Continuous ROP of $D_3$ was successfully performed. PDMS with narrow molecular weight distributions (PDI $\leq$ 1.2) were obtained and a strong dependence of the molecular weight to the flow rate (= residence time) was achieved. The PDMS chain lengths decreased with increasing flow rate. At low flow rate the molecular weight also showed dependence on the curvature radius of the coiled PTFE-PFR.

# Kurzfassung

Zielvorgabe für diese Dissertation war die kontinuierliche Ring-Öffnungspolymerisation (ROP) von Hexamethylcyclotrisiloxan ($D_3$) für die Produktion von linearen, monofunktionellen Oligo- und Polydimethylsiloxanen (PDMS) in einem Bereich von zehn bis sechzig Si-O Einheiten und niedrigen Molmassenverteilungen. Die Polymerisation wird durch *tert*-Butyllithium (t-BuLi) initiiert und durch Zugabe von Chlordimethylsilan (CDMS) oder Chlortrimethylsilan (CTMS) gestoppt. Die Polymerisationsreaktion wurde in polaren, aprotischen Medien durchgeführt, das Hauptlösungsmittel war THF (Abbildung 1).

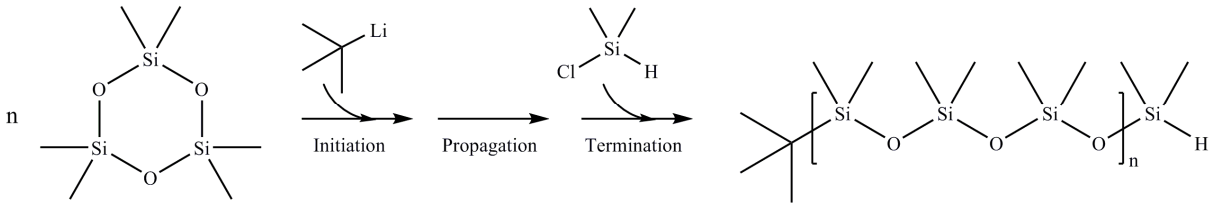


**Abbildung 1.** Ring-Öffnungspolymerisation (ROP) von Hexamethylcyclotrisiloxan ($D_3$) initiiert durch *tert*-Butyllithium (t-BuLi) und gestoppt mit Chlordimethylsilan (CDMS)

Im ersten Schritt wurden die drei Einzelreaktionen – Initiations-, Kettenfortpflanzungs- und Kettenabbruchsreaktion – separat in diskontinuierlichen Ansätzen charakterisiert. Alle drei Reaktionen sind durch Exothermie gekennzeichnet, die Reaktionsenthalpie ($\Delta_R H$) ist -206,6 kJ mol$^{-1}$ für die Initiationsreaktion, -31,1 kJ mol$^{-1}$ für die Kettenfortpflanzungsreaktion und -98,7 kJ mol$^{-1}$ für die Kettenabbruchsreaktion.

Die Arrhenius Parameter für die Initiations- und Kettenfortpflanzungsreaktion wurden bestimmt. Die Kinetik der Kettenabbruchsreaktion konnte nicht gemessen werden. Die Initiationsreaktion gehorcht einer Kinetik 2. Ordnung und der Stoß- oder Frequenzfaktor ($k_0$) und die Aktivierungsenergie ($E_A$) sind $k_0 = 1{,}39 \cdot 10^9$ L mol$^{-1}$ s$^{-1}$ und $E_A = 45{,}8$ kJ mol$^{-1}$. Die Kettenfortpflanzungsreaktion wurde in zwei Bereiche unterteilt: die Oligomerisations- und die Polymerisationsreaktion, beide gehorchen einer Kinetik 1. Ordnung in Bezug auf das Monomer. Die wurde durch die Methode der Initial Rate bestätigt. Die Arrhenius Parameter der Oligomerisation sind $k_0 = 1{,}75 \cdot 10^6$ s$^{-1}$ und $E_A = 54{,}7$ kJ mol$^{-1}$ und die der Polymerisation $k_0 = 8{,}01 \cdot 10^5$ s$^{-1}$ und $E_A = 53{,}3$ kJ mol$^{-1}$.

Der Polydispersitätsindex (PDI) der hergestellten PDMS wurde durch Messungen mittels Gelpermeationschromatographie (GPC) bestimmt und dieser war $\leq 1{,}2$. Die ROP ist durch höchste Selektivität bezüglich des Monomers $D_3$ im Vergleich zu höheren cyclischen Oligosiloxanen ($D_4$) gekennzeichnet und die Nebenproduktbildung durch Backbiting- oder Umlagerungsreaktionen ist vernachlässigbar.

Zusätzlich wurde der Einfluss von Fremdmetallionen auf die ROP von $D_3$ untersucht. Es konnte gezeigt werden, dass der Zusatz von unterschiedlichen Metallhalogeniden eine drastische Abnahme der Polymerisationsgeschwindigkeit zur Folge hat.

In einem weiteren Schritt wurden kontinuierliche Experimente in einem Rohrreaktor (RR) bestehend aus einem PTFE-Schlauch durchgeführt. Der PTFE-RR wurde auf einem Rohr aufgewickelt um die radiale Durchmischung entlang des Reaktors durch Dean Wirbel zu verbessern. Abbildung 2 zeigt eine Simulation des Reaktors die für CFD Rechnungen verwendet wurde.

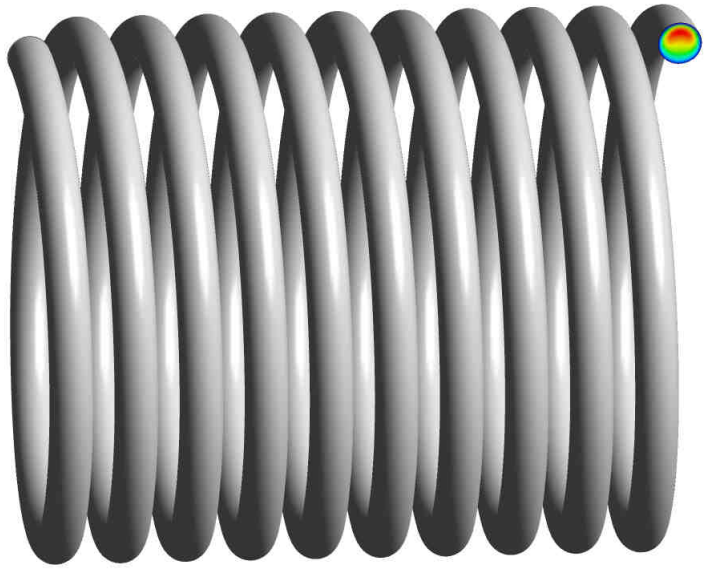

**Abbildung 2.** PTFE-RR (CFD Simulation) für kontinuierliche Polymerisationsexperimente

Zuerst wurde die Verweilzeitverteilung (VZV) des experimentellen Versuchsaufbaus untersucht. Die Bodensteinzahl (Bo) zeigt ein scheinbar ungewöhnliches Verhalten, ihr Wert sank mit zunehmender Flussrate. Dieser Effekt wird durch Instabilität der Strömung verursacht und resultiert, wie aus CFD Simulationen hervorgeht, in der Ausbildung von zwei toroidalen Wirbeln beginnend bei 3,0 mL $min^{-1}$. Aus diesen Ergebnissen folgt auch, dass die Bo-Zahl bei höheren Flussraten wieder ansteigt.

Die kontinuierliche ROP von $D_3$ wurde erfolgreich durchgeführt. PDMS mit engen Molmassenverteilungen (PDI $\leq$ 1,2) wurden hergestellt und es gab einen starken Zusammenhang zwischen dem Molekulargewicht und der Flussrate. Mit steigender Flussrate sank wie erwartet die Kettenlänge der PDMS. Es konnte gezeigt werden, dass bei niedrigen Flussraten der Krümmungsradius des PTFE-RR einen Einfluss auf das Molekulargewicht hat.

# 1. Introduction

Silicones, in particular polydimethylsiloxanes (PDMS), have high industrial importance due to their outstanding stability at high temperature, UV irradiation, weathering and their hydrophobic properties. In general all physical properties show low temperature dependence. Polysiloxanes consist of silicon atoms which are linked via oxygen atoms. Polymeric methylsilicone structures can be described using the letters M, D, T and Q as shown in Figure 3. These letters represent the functionality of each siloxane unit; e.g. M represents monofunctional and therefore terminal siloxane units, D difunctional, T trifunctional and Q tetrafunctional (quaternary) units, respectively. The characteristic properties of silicones strongly depend on the quantity of these building blocks within the material. Silicon rubbers, resins, oils and fats are common industrial products.

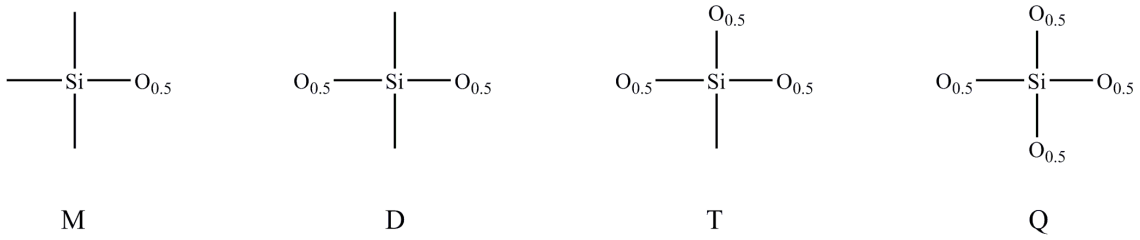


**Figure 3.** General building blocks for poly(methylsiloxanes)

Linear polyorganosiloxanes are mainly produced by the reaction of the corresponding dichlorodiorganosilanes either with water (hydrolysis) or methanol (methanolysis). The continuous hydrolysis of dichlorodimethylsilane for the production of common silicon oil is shown in Figure 4.[1]

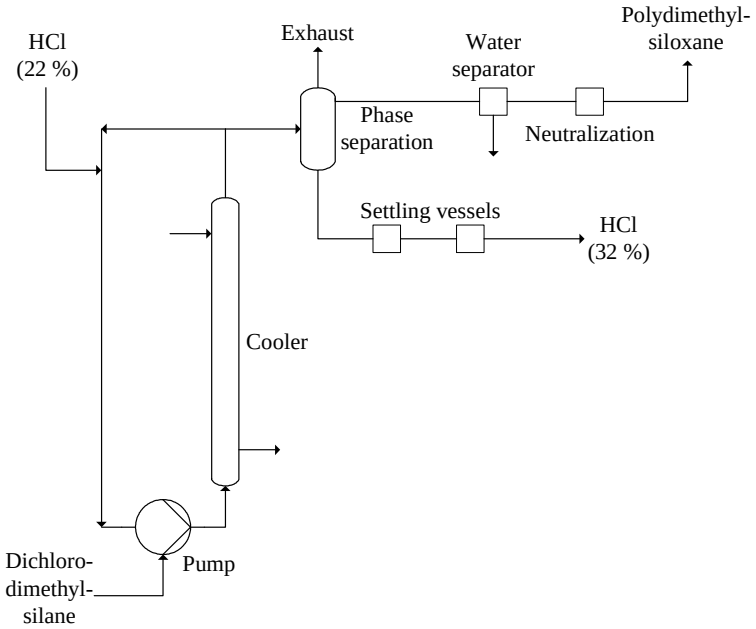


**Figure 4.** Continuous hydrolysis of dichlorodimethylsilane in a circulation apparatus[1]

In this synthesis large amounts of hydrogen chloride are produced in a highly exothermic reaction. In contrary, methanolysis allows the recovery of chlorine as chloromethane. This compound can be subsequently reacted with silicon in the Müller-Rochow Process for the production of dichlorodimethylsilane. In the hydrolysis and methanolysis cyclic oligosiloxanes such as hexamethylcyclotrisiloxane ($D_3$), octamethylcyclotetrasiloxane ($D_4$) or higher analogs ($D_5$, $D_6$, …) are produced as side products. The industrially most important monomers are $D_3$ and $D_4$, their molecular structure is shown in Figure 5.

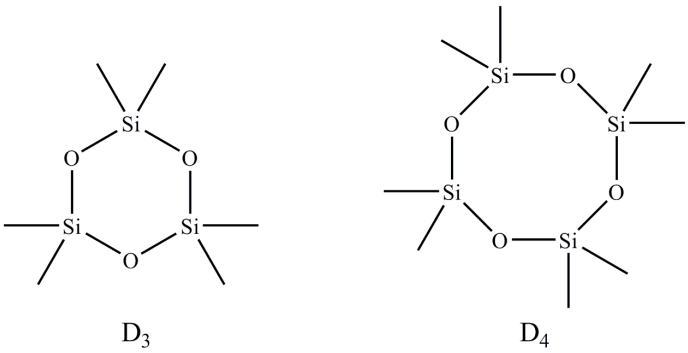


**Figure 5.** The industrially most important monomers for polymerization: Hexamethylcyclotrisiloxane ($D_3$) and octamethylcyclotetrasiloxane ($D_4$)

Selective cyclization is obtained by performing the hydrolysis or methanolysis with potassium hydroxide and other process aids at elevated temperature. The base catalyzes cleavage and formation of the Si-O bond, the low boiling cyclic oligomers are continuously removed from the process by distillation.[1,2]

Ring-opening polymerization (ROP) of cyclic oligosiloxanes leads to linear polysiloxanes. This polymerization is promoted by both cationic and anionic catalysts and initiators. Common reagents for this process are potassium hydroxide and sulfuric acid. A typical polymerization is performed at 140°C with a few ppm potassium hydroxide. Hydroxyl terminated chains are produced in the presence of water and accordingly trimethylsilyl-terminated chains are obtained when e.g. $MD_2M$ is added.[1] A general scheme of the anionic ROP of cyclic oligosiloxanes initiated and catalyzed by hydroxide ions is shown in Figure 6.

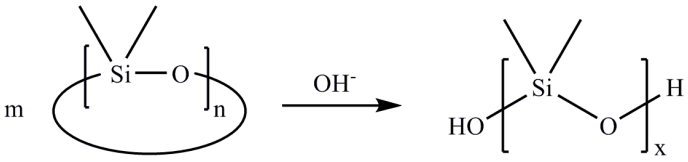


**Figure 6.** General scheme of the anionic ROP of cyclic oligosiloxanes initiated and catalyzed by hydroxide ions

# 2. Definition of the Project

Target of this project is the development of a continuously operated reactor system for the production of linear monofunctional PDMS. Chain lengths of about 10 to 60 Si-O units with a narrow molecular weight distribution are desired. Hexamethylcyclotrisiloxane ($D_3$) is used as the monomer, *tert*-butyllithium (t-BuLi) as the initiator for the ring-opening polymerization (ROP) and chlorodimethylsilane (CDMS) as the end capping reagent. Starting from these substances PDMS chains which solely contain one terminal functional group (Si-H) are produced (Figure 7).

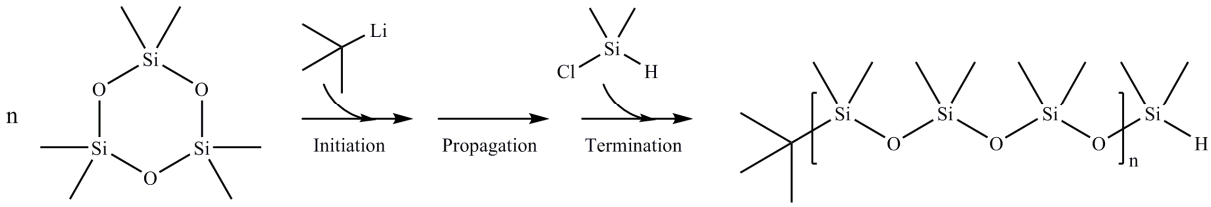


**Figure 7.** Ring-opening polymerization (ROP) of hexamethylcyclotrisiloxane ($D_3$) initiated with *tert*-butyllithium (t-BuLi) and stopped with chlorodimethylsilane (CDMS)

In this project the kinetics and the thermodynamic properties were investigated. With this data a continuously operated reactor in lab-scale was modeled and operated. These results are essential for further process design and optimization.

# 3. Literature Overview

Linear monofunctional PDMS have a great industrial potential. However, there are only few processes described in literature for the continuous production of these materials on an industrial scale. Wacker Chemie GmbH patented a process for the production of low molecular weight mono- and difunctional organosiloxanes using methyllithium as initiator in 1988[3]. The synthesis of lithiumsiloxanolates and linear polysiloxanes was already patented in the United States in 1969 by General Electric Company[4].

The ROP of cyclic oligosiloxanes (primarily $D_3$ and $D_4$) is the method of choice for the synthesis of monofunctional silicones. This polymerization is promoted by both anionic and cationic initiators and catalysts; however in current literature the anionic route is more frequently described. One of the first publications focusing on the ROP of cyclic oligosiloxanes for the production of monofunctional PDMS with a narrow molecular weight distribution was reported by Zilliox et al.[5] in 1975, followed by an increasing research interest[6-8].

## 3.1. The Initiation Reaction

Common anionic initiators for the production of monofunctional PDMS are organolithium reagents such as methyllithium[9], *n*-, *-sec*- and *tert*-butyllithium[10] or a corresponding Grignard reagent[11]. Initiators which already contain a silicon atom are trimethylsilylmethyllithium[12,13] (Figure 8 (a)) and hexamethyldisilazyllithium[14] (Figure 8 (b)). More complex initiator systems are aluminum-tetraphenylporphorin complexes[15], phosphazene bases in combination with methanol[16] (Figure 8 (c)) or the superbase hexapyrrolidinediphosphazenium hydroxide[17]. The uncharged iminooligophosphazene also serves as an active promoter when used together with organolithium reagents[17,18].

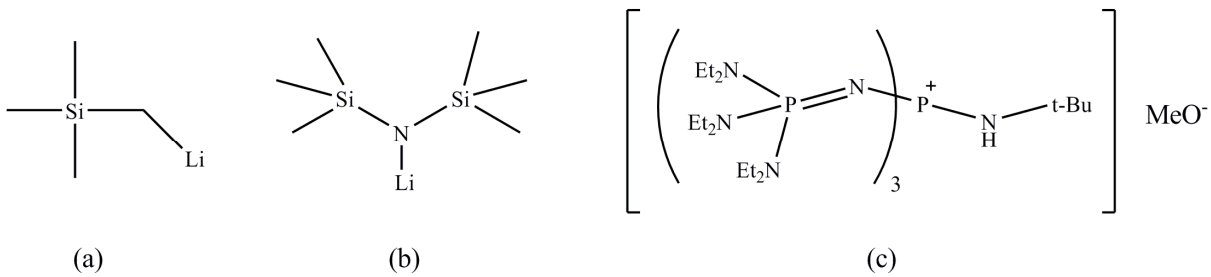


**Figure 8.** Initiators for the ROP of cyclosiloxanes: (a) trimethylsilylmethyllithium[19], (b) hexamethyldisilazyllithium[14] and (c) a phosphazene base in combination with methanol[19]

With an increased molar ratio of organolithium reagents to one single monomer unit the number of siloxane units is adjustable as shown in Figure 9.[10] Newer results showed that *sec*- and *n*-butyllithium form different populations of initiator species prior to propagation[20]. However, when using excess $D_3$ as monomer in polar media only the ring-opening reaction and subsequent polymerization occur. Hence, chain lengths of a multiple of three are produced in the kinetically controlled regime[21].

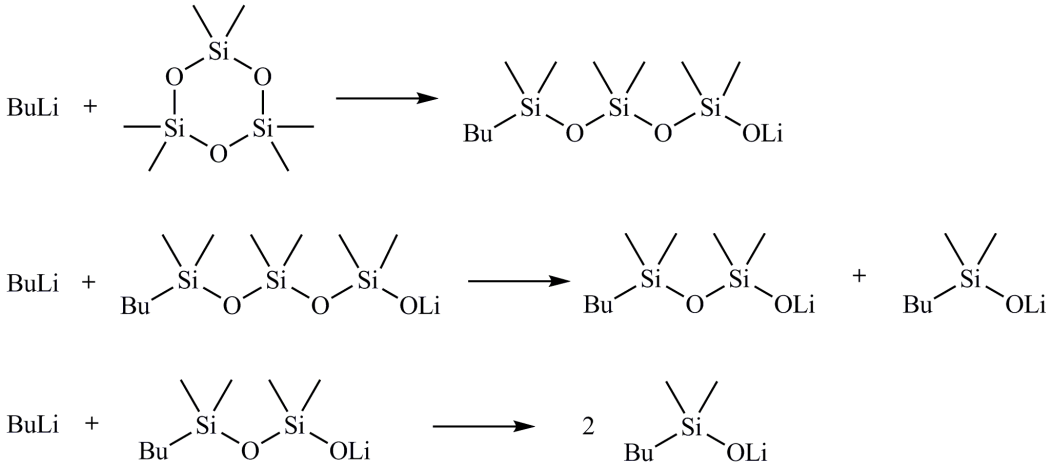


**Figure 9.** Increased ratio of initiator (BuLi) to monomer ($D_3$)

Cationic polymerization is carried out with strong protic or Lewis acids.[1] Besides sulfuric acid, mixtures of acylchlorides and antimony pentachloride ($RCOCl/SbCl_5$) or perfluoroalkane sulfonic acids such as trifluoromethanesulfonic acid (TfOH) are used as initiators. The cationic ROP generally suffers a significantly higher side product formation compared to the anionic polymerization.[22]

## 3.2. The Propagation Reaction

The ROP strongly depends on the used cyclic oligosiloxane. The reversibility of the polymer formation is suppressed when using the monomer $D_3$ due to the ring strain of the molecule (10.5 kJ $mol^{-1}$ [23]). Hence, the polymerization of $D_3$ is primarily controlled by kinetics. At high conversion the polymer starts to decompose when the reaction is not quenched, equilibrating with the formation of cyclic oligosiloxanes.[21,24]

The ring strain of higher cyclic analogs of type $D_n$ ($n > 3$) is significantly lower compared to $D_3$ (e.g. $D_4 = D_5 = 1.0$ kJ $mol^{-1}$ [23]) and the polymerization of these monomers is basically controlled by thermodynamics.[21,24] Typical polymer formation of the monomers $D_3$ and $D_4$ is shown in Figure 10.

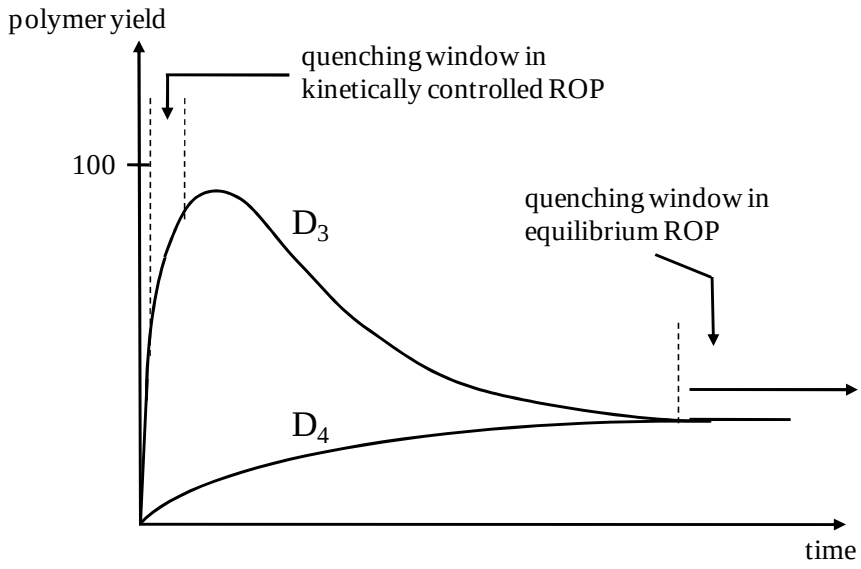


**Figure 10.** Characteristic polymer formation (quenching windows) for the anionic ROP of $D_3$ and $D_4$[1]

The rate of reaction of the anionic ROP of cyclic oligosiloxanes is increased when using polar aprotic solvents such as THF. The solvent molecules stabilize the transitional state of polymerization and aggregation of ion pairs is inhibited.[25] In literature anionic ROPs are typically performed in pure THF[26] or in mixtures with aromatics[27] or (cyclo)alkanes[20].

The ROP of $D_3$ initiated by strong bases such as organolithium reagents proceeds automatically. When using weaker initiators (alcohols, water) or monomers other than cyclotrisiloxanes the conditions of polymerization have to be rather drastic or a catalyst has to be added. Potassium hydroxide and sulfuric acid are industrially important catalysts. In literature the use of N-heterocyclic carbenes[28], tris(pentafluorophenyl)borane[29], biscatecholsiliconates[30] or potassiumcarbonate supported on alumina[31] is described. Attempts using rare earth compounds as catalysts have not been successful[32].

## 3.3. The Termination Reaction

Anionic ring-opening polymerization of cyclic oligosiloxanes initiated by organolithium reagents requires an adequate termination reaction to yield the desired monofunctional polymer. Depending on the purpose of the substance an appropriate chlorosilane (e.g. chlorodimethylsilane for subsequent hydrosilylation reactions) is essential. With this strategy a broad range of functional groups (vinyl, allyl, chloride, epoxy, alkoxy, …) is accessible. Hydroxy groups (silanols) are generally not desirable as they may suffer from consecutive condensation reactions.

## 3.4. Hybrid Materials

Polysiloxanes are interesting building blocks for the production of novel inorganic-organic hybrid materials such as block-copolymers, graft-copolymers or core-shell particles as shown in Figure 11. Therewith, the properties of organic polymers (mechanical stability, low-specific weight, …) and polysiloxanes (UV-protection, hydrophobicity, …) are combined in one single material. Several routes for accessing these substances are reported in literature and described in this section.

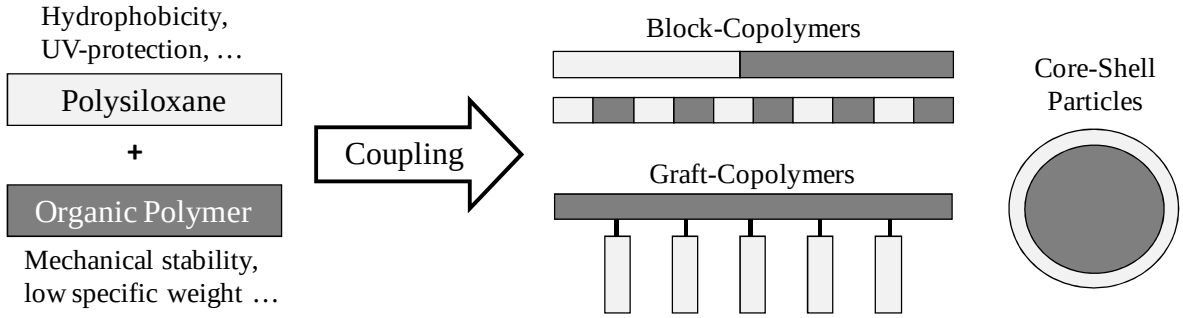


**Figure 11.** General scheme of inorganic-organic hybrid materials

The hydrosilylation reaction of monofunctional polysiloxanes for the synthesis of macromolecular initiators for organic polymerization reactions is of high interest. With these macroinitiators block copolymers of type AB or ABC are accessible.[33,34]

A different approach is the use of pre-modified cyclic oligosiloxanes for ring-opening polymerization. These cycles may vary by either altered substituents or ring atoms. Differently substituted cyclotrisiloxanes such as trimethyltrivinyl-[35] or pentamethylvinylcyclotrisiloxane[35], pentamethyl-[36,37], *tert*-butyltetramethyl-[37] or tetramethylphenylcyclotrisiloxane[37] were synthesized as shown in Figure 12.

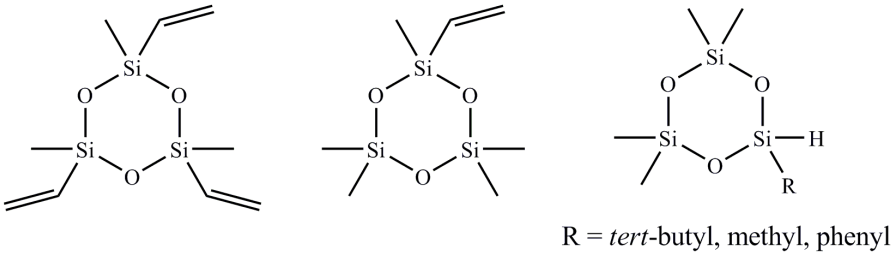


**Figure 12.** Differently substituted cyclotrisiloxanes for the production of hybrid materials

Cyclic compounds containing different ring atoms are shown in Figure 13. These cycles may be cyclocarbosiloxanes such as 2,2,4,4,6,6,8,8-octamethyl-1,5-dioxa-2,4,6,8-tetrasilacyclooctane[37,38], 2,2,4,4-tetramethyl-1,3,5-trioxa-2,4-disilacyclononane[37] and 2,2,5,5-tetramethyl-1-oxa-2,5-disilacyclopentane[39] or cyclosiloxazanes such as nonamethyl-1,3,5-

trioxa-7-aza-2,4,6,8-tetrasilacyclooctane[40] and heptamethyl-1,3-dioxa-5-aza-2,4,6-trisilacyclohexane[40].

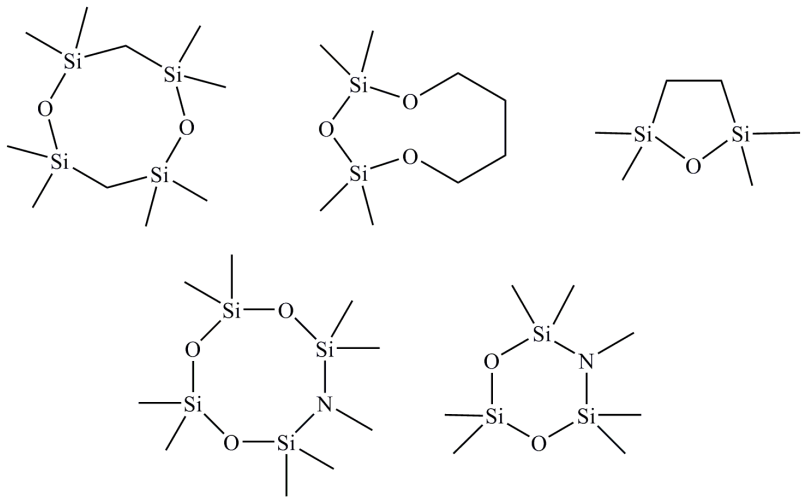


**Figure 13.** Cyclic siloxanes with different ring atoms for the production of hybrid materials

In general, hybrid materials containing polysiloxane moieties have a large range of different applications due to the unique physical and chemical properties of these substances. Besides the usage as foam stabilizers, leveling agents in paints, release aids and additives for cosmetics and polishing agents[1], biomedical applications[41,42], modifications of catalysts[43] or materials with bactericidal properties[44] are of great interest.

There is no limit for the variety of capable organic substances and polymers for the synthesis of hybrid materials with polysiloxanes. Block-copolymers with common monomers like styrene[5], methacrylates[33], butadiene[45] or siloxane containing polyesters and polyamides[46], polyethers[47] and polycarbonates[48,49] are reported in literature.

# 4. Fundamentals

In this section the principles of process design are described. These are the kinetics and thermodynamic characteristics of a chemical reaction and the basic fluid dynamic properties of a chemical reactor. Furthermore, the basics of polymer characterization are described.

## 4.1. Kinetics

The rate of a chemical reaction ($r_A$) and its temperature dependence are essential for reactor design and modeling. The basic equation for constant volume of reactant *A* is given with the differential Equation 1. The change of the concentration of component *A* with reaction time is proportional to a temperature dependent rate coefficient ($k_{(T)}$) and to the concentration of all substances ($c_A$, $c_B$, …) involved in the reaction to the power of a specific constant (*a*, *b*, …). The sum of these constants identifies the overall order of reaction. The exponents are not necessarily equal to the stoichiometric coefficients of the chemical reaction or a natural number.

$$r_A = \frac{dc_A}{dt} = -k_{(T)} \cdot c_A^a \cdot c_B^b \cdot ... \tag{1}$$

The temperature dependence of $k_{(T)}$ is described by the Arrhenius Equation 2.

$$k_{(T)} = k_0 \cdot e^{\frac{-E_A}{R \cdot T}} \tag{2}$$

$E_A$ is called the activation energy and $k_0$ the pre-exponential or frequency factor. These constants are primarily calculated from the logarithm of Equation 2 as stated in Equation 3.

$$\ln(k_{(T)}) = \ln(k_0) - \frac{1}{T} \cdot \frac{E_A}{R} \tag{3}$$

### 4.1.1. Method of Initial Rates

The method of initial rates is an appropriate method for the determination of the order of a certain reaction. For its calculation, the reaction rate of a common reaction is simplified according to Equation 4, where $c_A$ equals the concentration of reactant A, *av* is the average value, *t* the reaction time, *k* the rate constant and *n* the order of the reaction.

$$\frac{\Delta c_A}{\Delta t} = -k \cdot c_{A,av}^n \tag{4}$$

From Equation 5 the order ($n$) is calculated or fitted. For its determination only the concentration change of reactant A ($\Delta c_A$), the reaction time ($t$) and therefore a minimum of two experiments with two different concentrations of component A are required.

$$\ln\left(-\frac{\Delta c_A}{\Delta t}\right) = \ln\left(c_{A,av}\right)\cdot n + \ln\left(k\right) \tag{5}$$

## 4.2. Thermodynamics

The standard enthalpy change of reaction ($\Delta_R H^0$) is the change of enthalpy which occurs when one mole of a substance is reacted under standard conditions. It equals the sum of the standard enthalpies of formation ($\Delta_F H_i^0$) of all components i according to their stoichiometric coefficient ($\upsilon$) – products have positive and reactants negative coefficients (Hess's law, Equation 6).

$$\Delta_R H^0 = \sum_i \upsilon_i \cdot \Delta_F H_i^0 \tag{6}$$

If $\Delta_R H^0$ is > 0, the reaction is considered as endothermic and it consumes energy in the form of heat. If $\Delta_R H^0$ is < 0 the reaction releases heat and is denoted as exothermic.

$\Delta_R H^0$ of a fast chemical reaction is adequately determined with an adiabatic calorimeter by recording the change of the temperature of the system during the reaction at constant pressure (Equation 7). The heat of reaction ($Q_R$) and therefore the enthalpy change of reaction ($\Delta_R H$) of the component i is calculated from the temperature at start ($T_S$) and end ($T_E$) of the reaction and with the knowledge of the heat capacity of the system ($C_{Sys}$).

$$Q_R = \Delta_R H \cdot n_i = - C_{Sys} \cdot (T_E - T_S) \tag{7}$$

## 4.3. Chemical Reactors

There are three basic cases for an ideal reactor in single-phase: a) the batch reactor (BR), b) the continuously stirred tank reactor (CSTR) and c) the plug flow reactor (PFR). Target of this work is the development of a continuously fed reactor, a boundary which is not given with a BR. Furthermore, when considering a continuously operated polymerization reaction with ionic initiation the PFR is the reactor of choice[50]. Hence, in this work only the PFR is discussed in detail.

### 4.3.1. Ideal Plug Flow Reactor[51]

Plug flow conditions are characterized by homogeneity of the reaction medium over the cross section of the reactor without any mixing in axial direction. Hence, the concentration of a reactant is a function of the reactor length ($L$) and constant for a certain reaction time ($t$) as shown in Figure 14.

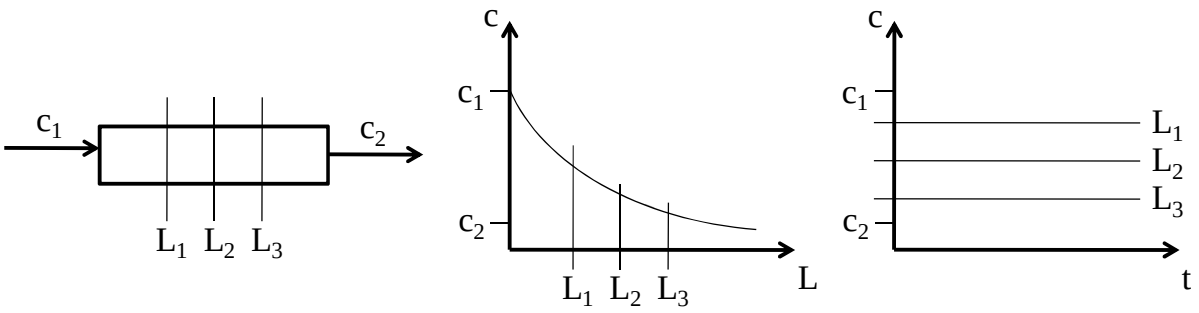


**Figure 14.** Concentration profiles for an ideal plug flow reactor

A differential element of the reactor volume ($V_R$) is shown in Figure 15 where $F_A$ represents the molar flow of reactant A, $F_{A,0}$ the initial molar flow, $r_A$ the rate of reaction, $k$ the rate constant, $n$ the order of the reaction, $c_A$ the concentration of component A, $c_{A,0}$ the initial concentration of component A and $X_A$ the conversion of component A (1 = in, 2 = out). The differentials of these parameters are appropriately described with the prefix $d$.

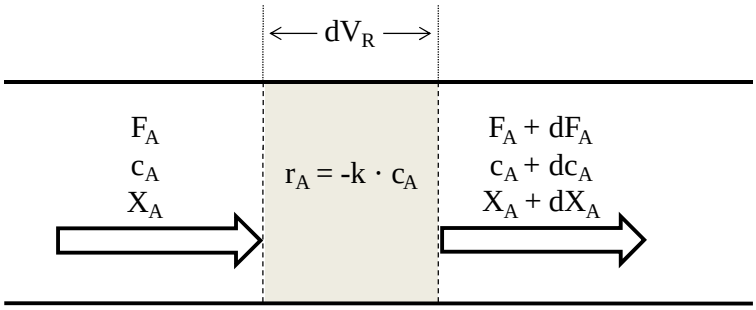


**Figure 15.** Differential balance of a plug flow reactor

For constant volume the mass balance of reactant A is given with Equation 8.

$$F_A = F_A + dF_A + (-r_A) \cdot dV_R \tag{8}$$

The change of the molar flow of component A is a function of its conversion as stated in Equation 9.

$$dF_A = -F_{A,0} \cdot dX_A \tag{9}$$

The rate of reaction is according to Equation 10.

$$-r_A = k \cdot c_A^n \tag{10}$$

The concentration of reactant A is according to Equation 11.

$$c_A = c_{A,0} \cdot (1 - X_A) \tag{11}$$

Therefore the reactor volume ($V_R$) is calculated as a function of the conversion of reactant A according to Equation 12.

$$V_R = -\frac{F_{A,0}}{k \cdot c_{A,0}^n} \cdot \int_{X_{A,1}}^{X_{A,2}} \frac{dX_A}{(1 - X_A)^n} \tag{12}$$

Hence, assuming first order kinetics (n = 1) and no conversion at the reactor inlet ($X_{A,1} = 0$ and $X_{A,2} = X_A$) $V_R$ is given with Equation 13.

$$V_R = -\frac{F_{A,0}}{k \cdot c_{A,0}} \cdot \int_0^{X_A} \frac{dX_A}{1 - X_A} \tag{13}$$

The integrated form of Equation 13 is given with Equation 14.

$$V_R = -\frac{F_{A,0} \cdot \ln(1 - X_A)}{k \cdot c_{A,0}} \tag{14}$$

### 4.3.2. Non-ideal Plug Flow Reactor[52]

The ideal isothermal reactor types provide all basic equations for fundamental reactor design. However, non-ideal reactors generally differ from these models caused by different issues such as mixing, mass and/or heat transfer as well as enthalpy effects.

The residence time distribution (RTD) is an adequate method for characterization of a non-ideal reactor system. With the knowledge of the retention time of every single molecule a real conversion rate is easily calculated. In this work the dispersion model was used. In this model the RTD results from axial back-mixing effects heterodyning an ideal plug flow. These effects may result from convective mixing in axial direction due to turbulences and vortices, inhomogeneous velocity profile along the cross section of the reactor or molecular diffusion. The axial back mixing is characterized by the axial dispersion coefficient ($D_{ax}$) a parameter which has the same dimension as the diffusion coefficient.[50]

## 4.4. Dimensional Analysis

In this work the dimensionless numbers, Bodenstein number, Péclet number, Reynolds number and Dean number, are used for basic characterization of a real reactor system.

### 4.4.1. Bodenstein and Péclet Number (Bo, $Pé_{ax}$)[50]

The Bodenstein number (*Bo*) and Péclet number ($Pé_{ax}$) are used for characterizing the ideality of hydraulic flow patterns of a reactor, where *u* represents the flow velocity, *L* the length of the reactor, *d* the tube diameter and $D_{ax}$ the axial dispersion coefficient. If Bo = 0 ($D_{ax}$ >> u·L; u·d) the reactor is ideally mixed and corresponds with an ideal CSTR and if Bo = ∞ ($D_{ax}$ << u·L; u·d) the reactor is equal to an ideal PFR. Definitions are given with Equation 15 to Equation 17.

$$Bo = \frac{u \cdot L}{D_{ax}} \tag{15}$$

$$Pé_{ax} = \frac{u \cdot d}{D_{ax}} \tag{16}$$

$$Bo = Pé_{ax} \cdot \frac{L}{d} \tag{17}$$

### 4.4.2. Reynolds Number (Re)[53]

The Reynolds number (*Re*) represents the ratio of inertial to viscous forces. For a Newtonian fluid *Re* may be defined as shown in Equation 18 where *u* is the flow velocity, *L* a characteristic length (diameter of the tube) and $\upsilon$ the kinematic viscosity.

$$\mathrm{Re} = \frac{u \cdot L}{\upsilon} \tag{18}$$

### 4.4.3. Dean Number (De)[53,54]

The Dean effect – secondary circulation perpendicular to the main flow – occurs for flow through a curved tube or coil. De-number is defined as shown in Equation 19.

$$De = \mathrm{Re} \cdot \sqrt{\frac{d}{D}} \tag{19}$$

*d* is the diameter of the tube or coil and *D* the diameter of the curvature according to Figure 16.

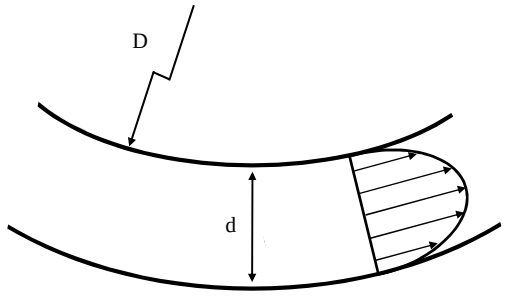


**Figure 16.** Dimensions *d* and *D* for the flow regime in a curved pipe or coil[55]

The critical Dean number ($De_{crit}$) for formation of secondary circulation is given in Equation 20.[56]

$$De_{crit} = 54 \tag{20}$$

## 4.5. Polymer Characterization

The number average molecular mass ($M_n$) the mass average molecular mass ($M_w$) and the polydispersity index (*PDI*) are used to characterize the mass distribution of polymers. Definitions are given with Equations 21 to 23, where $n_i$ is the number of polymers with the molecular mass $M_i$.

$$M_n = \frac{\sum M_i \cdot n_i}{\sum n_i} \tag{21}$$

$$M_w = \frac{\sum M_i^2 \cdot n_i}{\sum M_i \cdot n_i} \tag{22}$$

$$PDI = \frac{M_w}{M_n} \tag{23}$$

The PDI has a value $\geq 1$ and indicates the molecular weight distribution of a polymer. When the polymer approaches uniform chain length, the PDI approaches unity. Most common methods for determination of the polydispersity of polymers are light scattering measurements, mass spectrometry and size exclusion chromatography (SEC).

# 5. Results and Discussion

## 5.1. The ROR of $D_3$ and $D_4$

The ROR of $D_3$ initiated by t-BuLi was performed in THF. CDMS was used for successful end capping forming 1-*tert*-butyl-1,1,3,3,5,5,7,7-octamethyltetrasiloxane **(1)** by elimination of lithium chloride. The general procedure is shown in Figure 17.

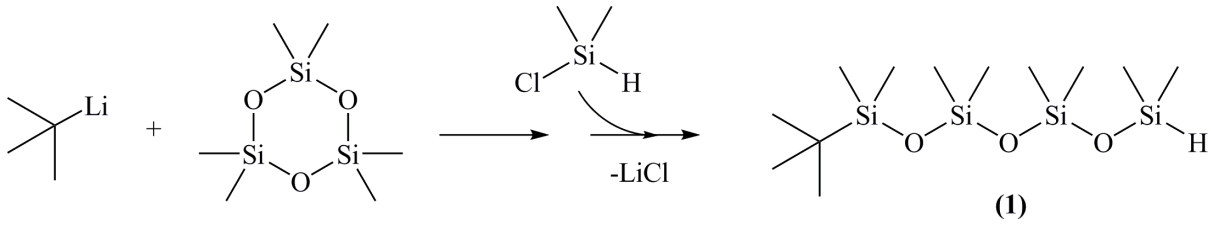


**Figure 17.** ROR of $D_3$ initiated with t-BuLi and terminated with CDMS

The $^1$H NMR spectrum of **(1)** is shown in Figure 18 to Figure 20.

$^1$H NMR (300 MHz, 25°C, $CDCl_3$) $\delta$ / *ppm*: 0.037 ($C_4H_9$-Si(C**H$_3$**)$_2$-O, s, 6H); 0.054-0,064 (O-(Si(C**H$_3$**)$_2$-O)$_2$, 2s, 12H); 0.180-0.190 (O-Si(C**H**$_3$)$_2$-H, d, 6H); 0.873 ($C_4$**H**$_9$-Si, s, 9H); 4.674-4.730 (Si-**H**, m, 1H)

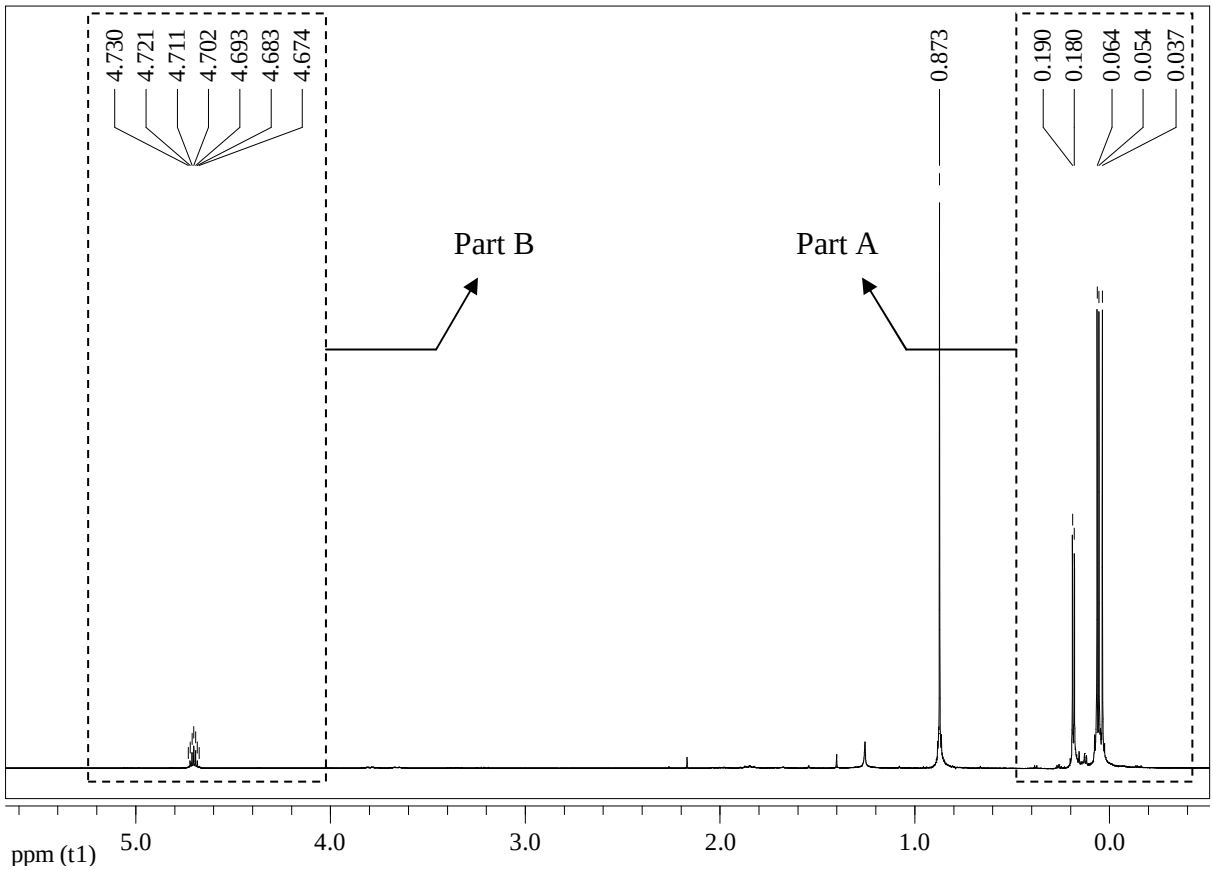


**Figure 18.** $^1$H NMR spectrum of **(1)**: total spectrum

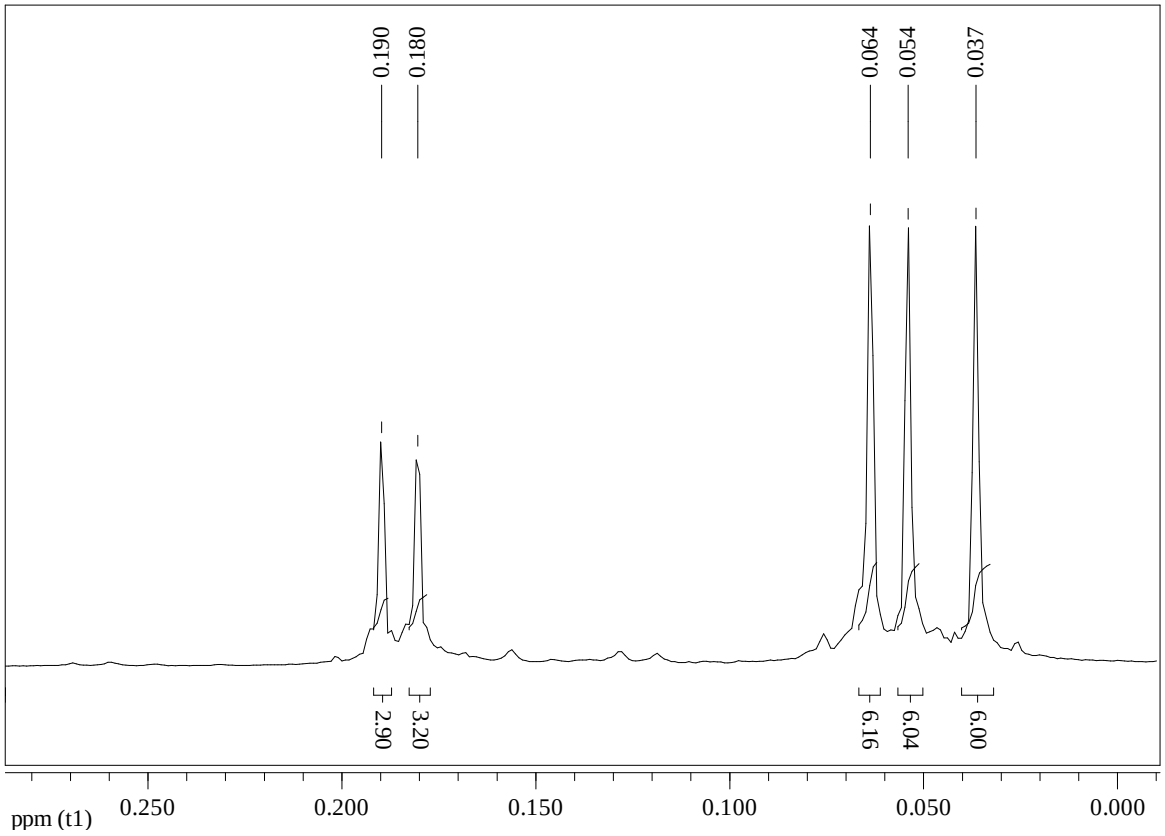


**Figure 19.** $^{1}$H NMR spectrum of **(1)**: Part A, methyl groups

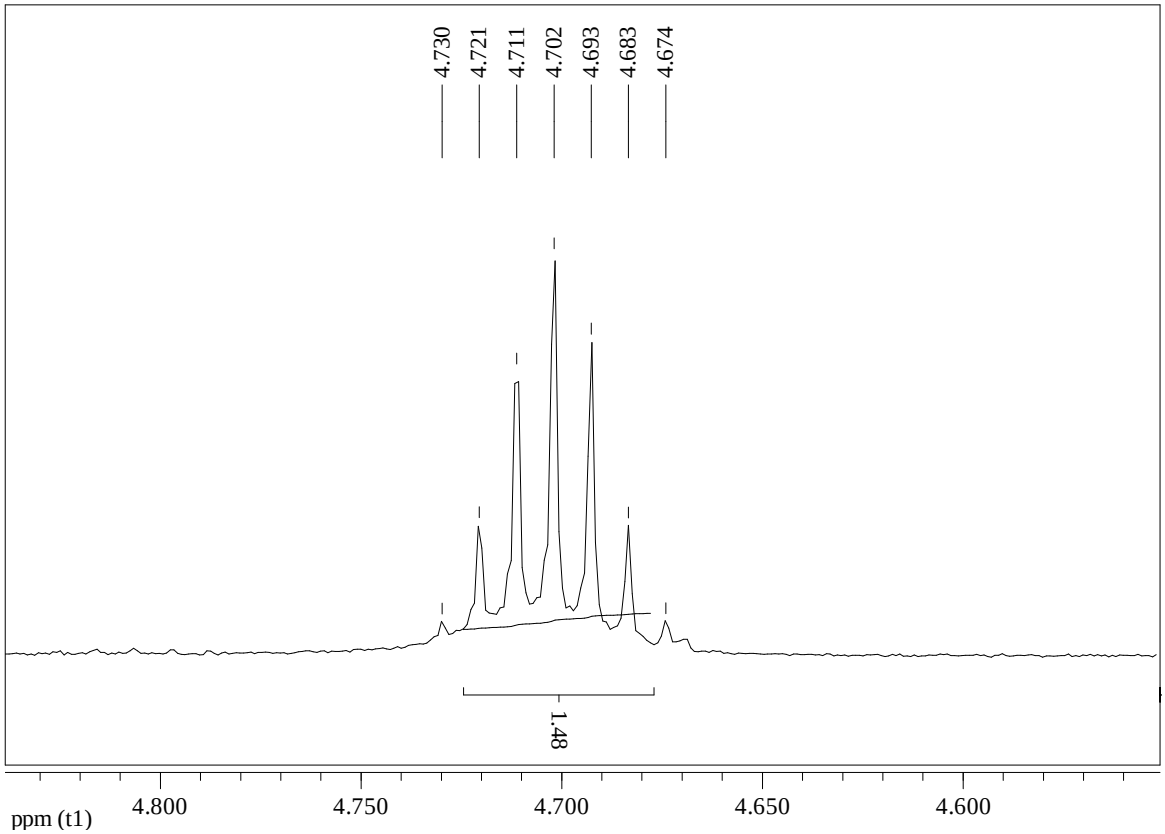


**Figure 20.** $^{1}$H NMR spectrum of **(1)**: Part B, hydride functional group

The $^{29}$Si NMR spectrum of **(1)** is shown in Figure 21.

$^{29}$Si NMR (300 MHz, 25°C, $CDCl_3$) *δ / ppm*: -24,637 - -22.777 (O-(**Si**$(CH_3)_2$-O)$_2$, 2s); -9.526 (**Si**-H, s); 7.532 ($C_4H_9$-**Si**, s)

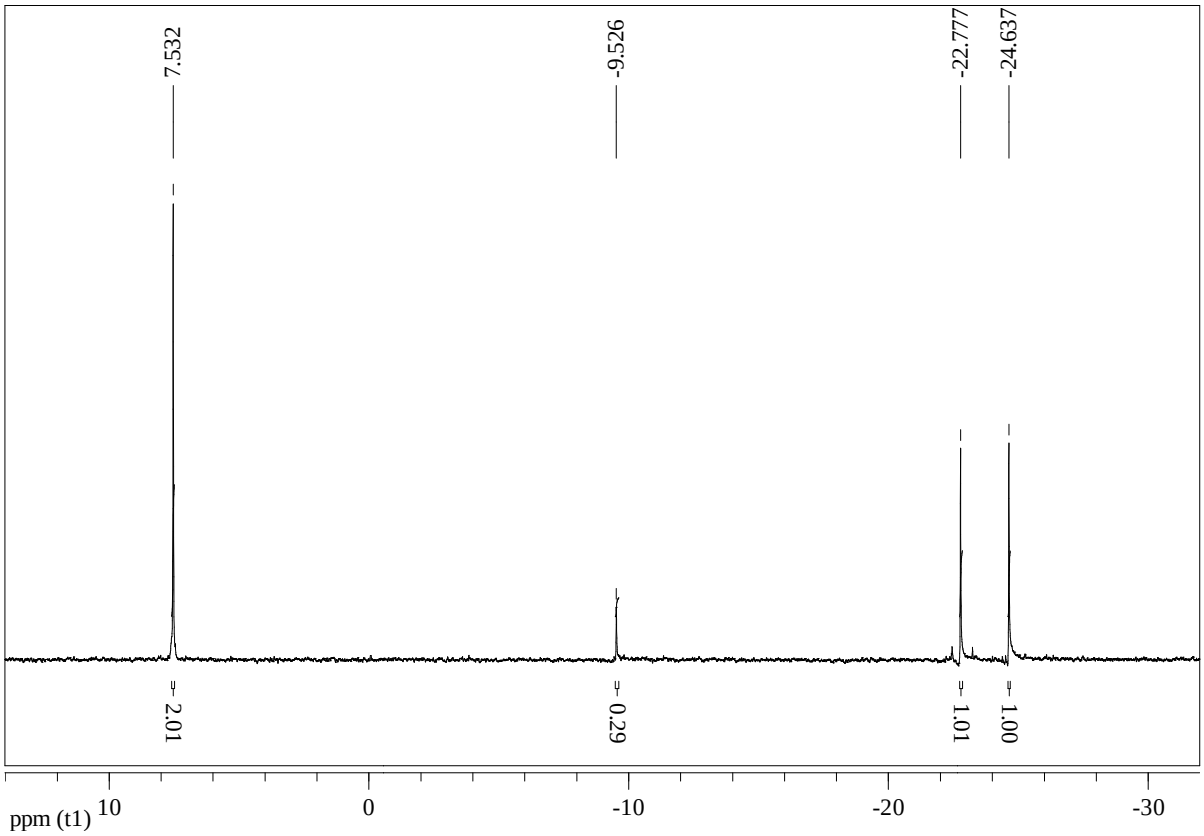


**Figure 21.** $^{29}$Si NMR spectrum of **(1)**

All peak intensities in the $^1$H NMR spectrum are in great correlation to each other except the hydride function. This effect is due to the overlap of the background noise and the broad multiplet (septet, 4.674 ppm to 4.730 ppm) signal (Figure 20). Generally, also the $^{29}$Si NMR spectrum has quantitative integrals, however, the *tert*-butyl group (7.532 ppm) increases and the hydride group (-9.526 ppm) decreases the signal intensity (Figure 21).

The IR spectrum of **(1)** is shown in Figure 22. The most characteristic peak in the IR spectrum is the strong Si-H band in the range between 2280 cm$^{-1}$ and 2080 cm$^{-1}$ (B), this functional group is also found between 950 cm$^{-1}$ and 800 cm$^{-1}$ (B'). The peaks at 1260 cm$^{-1}$ (D) and between 865 cm$^{-1}$ and 750 cm$^{-1}$ (D') are attributed to the Si-$CH_3$ of the M and D units. The Si-O-Si chain results in a broad and strong band between 1130 cm$^{-1}$ and 1000 cm$^{-1}$ (E).[23] The multiplet in the range between 2960 cm$^{-1}$ and 2850 cm$^{-1}$ is attributed to the C-H valence stretch of the alkyl groups (A). Furthermore, the *tert*-butyl group (C) is a small, but sharp band at 1365 cm$^{-1}$.[57] The IR spectrum excellently shows the well segregated hydride functional group peak at 2128 cm$^{-1}$; however, this method cannot be used for any quantitative analysis.

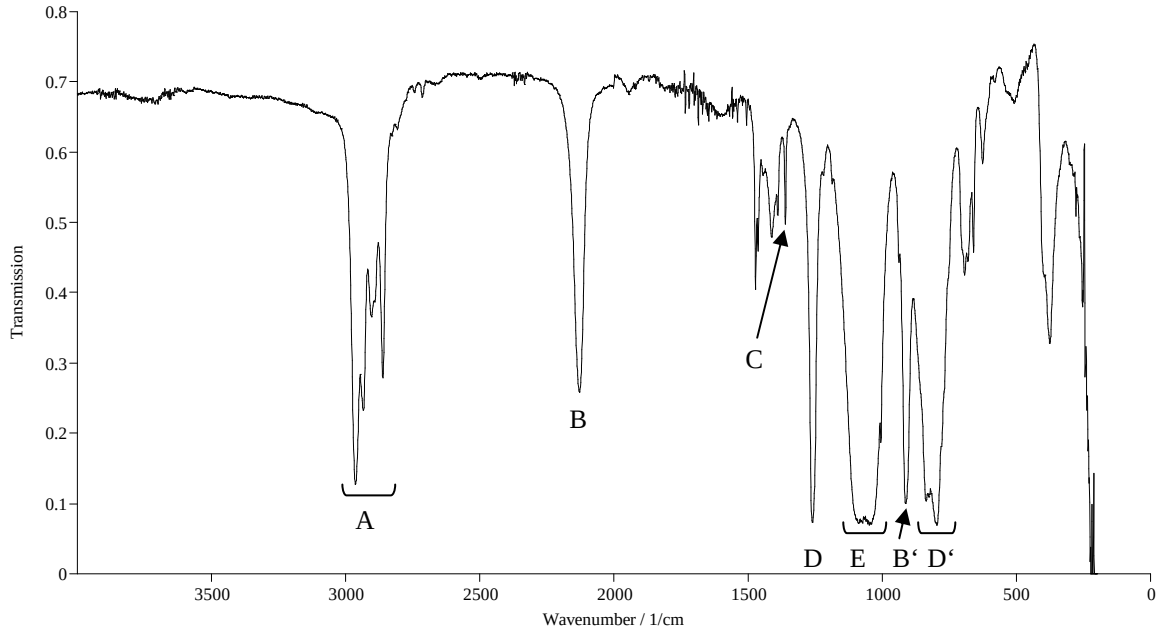


**Figure 22.** IR spectrum of **(1)**

### 5.1.1. Kinetics of the ROR of $D_3$

$D_3$ conversion is calculated by the ratio of reacted to unreacted $D_3$ molecules. A characteristic $^1H$ NMR spectra array is shown in Figure 23 where the peak intensity of $D_3$ is diminishing with increasing time.

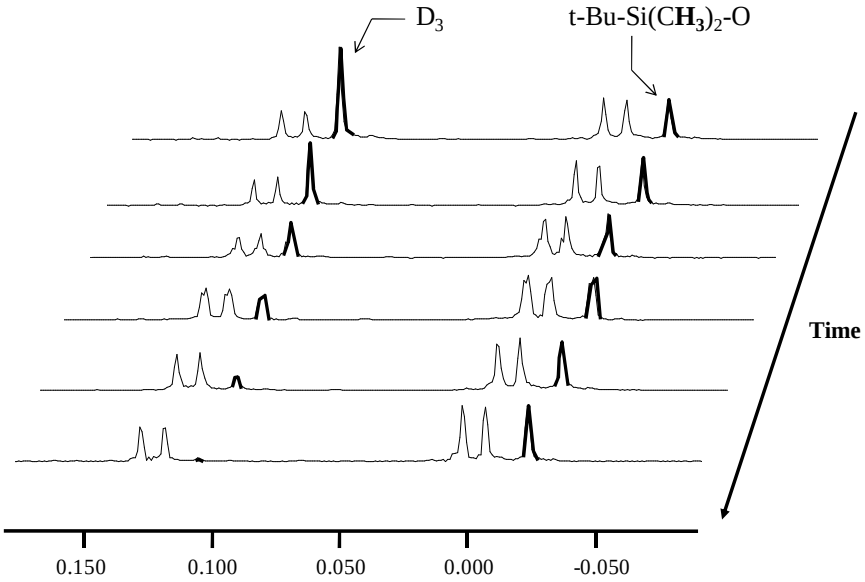


**Figure 23.** $^1H$ NMR array of the ROR of $D_3$ initiated by t-BuLi

Conversion curves of the ROR of $D_3$ initiated by t-BuLi in a temperature window starting from -70°C and ending with -45°C are shown Figure 24. The reaction obeys second order kinetics (x = 2) in respect to $D_3$ according to the simplification given in Equation 24 to Equation 27. The second order rate constants of the ROR are shown in Figure 25; however, the rate constants were generally calculated with the software TableCurve 2D 5.0: Eqn 8102 [Decay2_].

$$-\frac{dc_{D_3}}{dt} = k \cdot c_{D_3}^{n} \cdot c_{t-BuLi}^{m} \tag{24}$$

$$c_{D_3} = c_{t-BuLi} \tag{25}$$

$$x = n + m \tag{26}$$

$$-\frac{dc_{D_3}}{dt} = k \cdot c_{D_3}^{x} \tag{27}$$

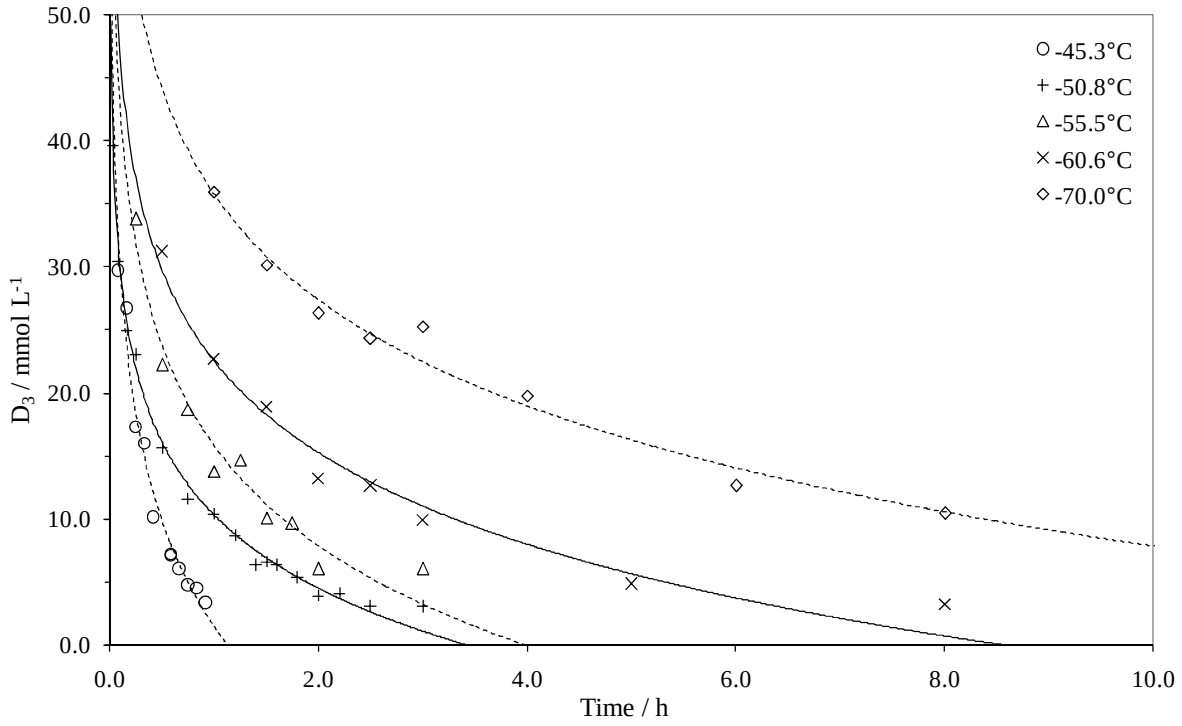


**Figure 24.** Typical conversion curves of the ROR of $D_3$ initiated by t-BuLi and quenched with CDMS in THF in a temperature range between -70°C and -45°C

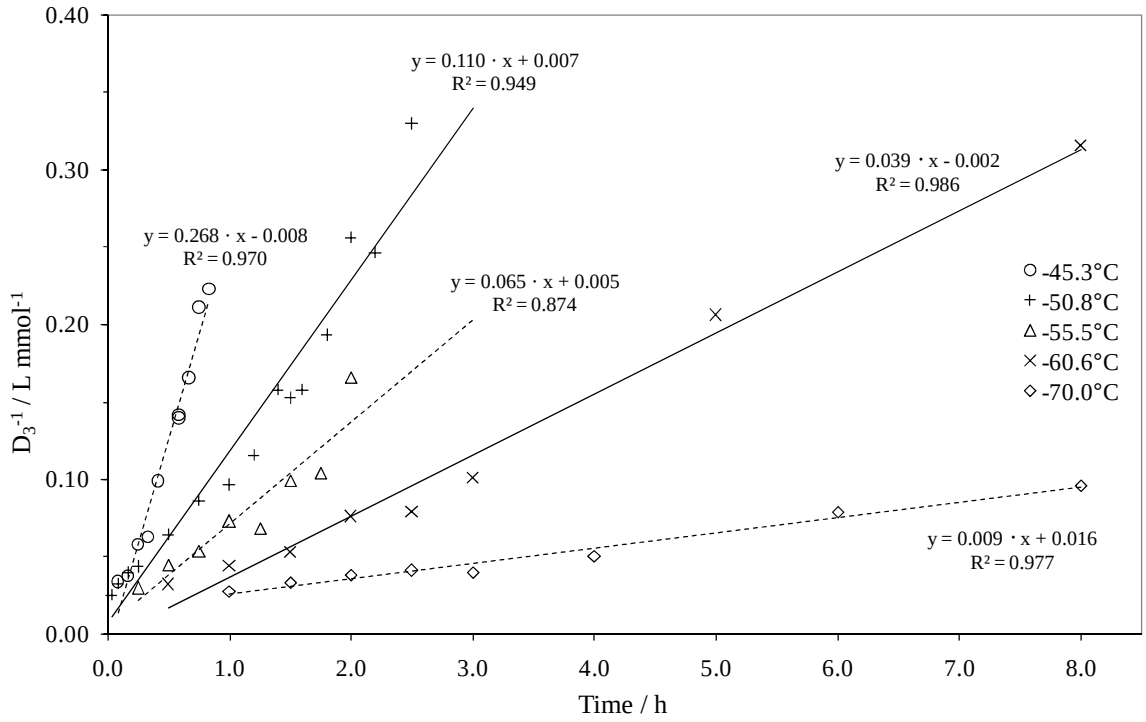


**Figure 25.** Second order rate constants of the ROR of $D_3$ initiated by t-BuLi

Seven different temperature levels were considered for determination of the temperature dependence of the rate of reaction. The parameters are summarized in Table 1.

**Table 1.** Rate constants (TableCurve: Eqn 8102) and temperatures of the ROR of $D_3$ initiated by t-BuLi

| T / °C | $T^{-1}$ / $K^{-1}$ | $k_{(T)}$ / L $mol^{-1}$ $s^{-1}$ | $ln(k_{(T)})$ / - |
|---|---|---|---|
| -40.8 | $4.30 \cdot 10^{-3}$ | $7.14 \cdot 10^{-2}$ | -2.64 |
| -45.3 | $4.39 \cdot 10^{-3}$ | $4.50 \cdot 10^{-2}$ | -3.10 |
| -50.7 | $4.49 \cdot 10^{-3}$ | $2.50 \cdot 10^{-2}$ | -3.69 |
| -50.8 | $4.50 \cdot 10^{-3}$ | $2.53 \cdot 10^{-2}$ | -3.68 |
| -55.5 | $4.59 \cdot 10^{-3}$ | $1.50 \cdot 10^{-2}$ | -4.20 |
| -60.6 | $4.70 \cdot 10^{-3}$ | $7.65 \cdot 10^{-3}$ | -4.87 |
| -70.0 | $4.92 \cdot 10^{-3}$ | $2.42 \cdot 10^{-3}$ | -6.02 |

The Arrhenius plot of the ROR of $D_3$ initiated by t-BuLi is shown in Figure 26.

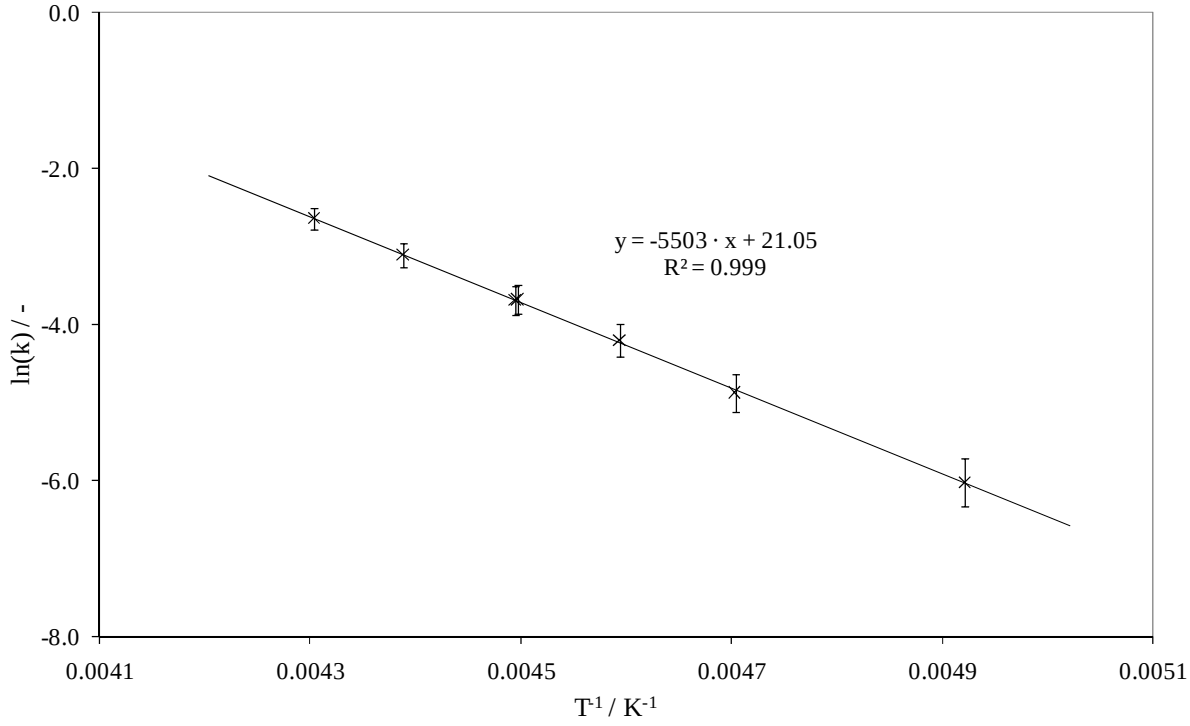


**Figure 26.** Arrhenius plot of the ROR of $D_3$ initiated by t-BuLi

The Arrhenius parameters were found to be $\mathbf{k_0 = 1.39 \cdot 10^9\ L\ mol^{-1}\ s^{-1}}$ and $\mathbf{E_A = 45.8\ kJ\ mol^{-1}}$ (Table 2). An error of 5.0 % is estimated according to literature[58].

**Table 2.** Arrhenius parameters of the ROR of $D_3$ initiated by t-BuLi

| Parameter | Value | Error |
|---|---|---|
| $\mathbf{E_A}$ / kJ mol$^{-1}$ | 45.8 | ± 2.3 |
| $\mathbf{k_0}$ / L mol$^{-1}$ s$^{-1}$ | $1.39 \cdot 10^9$ | $\pm 6.93 \cdot 10^7$ |

The monomer $D_4$ does not react forming the corresponding linear oligosiloxane **(2)** under the same reaction conditions as it does $D_3$, even when extending the temperature window to room temperature with reaction times of about 2 h (Figure 27). For this reaction more drastic conditions are needed[59]. The difference of the reactivity is attributed to the ring strain of the molecule $D_4$ which is ten times lower than the ring strain of the six membered ring. Hence, the ROR of cyclic oligosiloxanes is highly selective towards the monomer $D_3$.

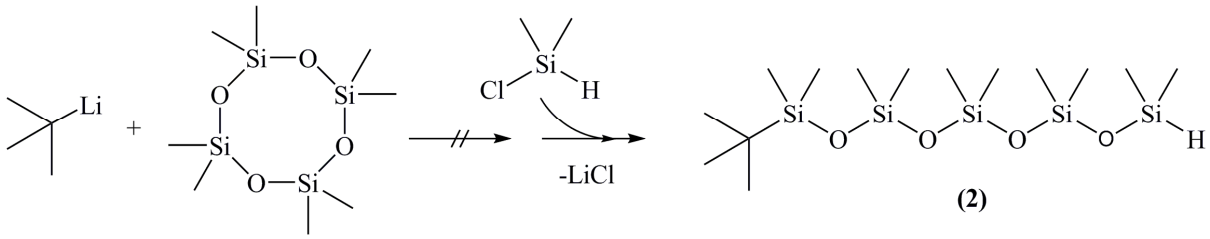


**Figure 27.** ROR of $D_4$ initiated with t-BuLi using the same reaction conditions as with the monomer $D_3$

### 5.1.2. Thermodynamics of the ROR of $D_3$

For reactor design the consumed or evolved heat of reaction is an essential parameter. As it can be seen in Figure 28 the ROR of $D_3$ initiated by t-BuLi is a highly exothermic reaction. For characterization of the temperature curve standard balanced analysis was applied[60].

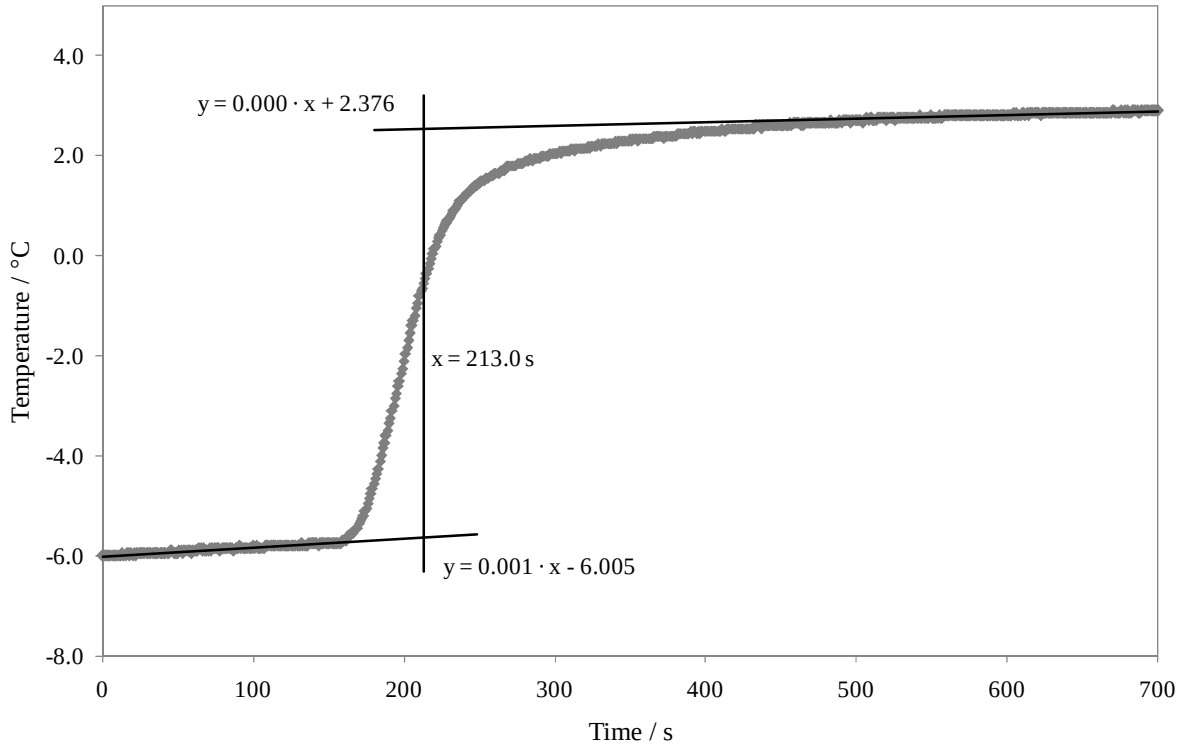


**Figure 28.** Temperature curve of the ROR of $D_3$ initiated by t-BuLi

$\Delta_R H$ of the ROR of $D_3$ initiated by t-BuLi was determined to be **-206.6 kJ mol$^{-1}$** with a standard deviation of 2.6 % (Table 3).

**Table 3.** $\Delta_R H$ of the ROR of $D_3$ initiated by t-BuLi

| Experiment No. | $\Delta_R H$ / kJ mol$^{-1}$ |
|---|---|
| # 1 | -212.0 |
| # 2 | -201.3 |
| # 3 | -206.5 |
| **Average** | **-206.6** |
| **Deviation** | **5.4** |

In accordance to the results of the experiments for determining the kinetics, $\Delta_R H$ of the ROR of $D_4$ initiated by t-BuLi could not be measured.

## 5.2. The ROP of $D_3$

In this section a general polymer characterization, kinetic studies and the determination of the enthalpy change of reaction of linear PDMS of type **(3)** with $2 \leq n \leq 25$ (Figure 29) are described. Due to reasons of simplification the trimethylsilyl terminated chains were mainly used in order to prevent any oxidative side effects a hydride function might suffer. Deviations or any other consequences caused by the change of the chlorosilane (CDMS vs. CTMS) are assumed to be insignificant.

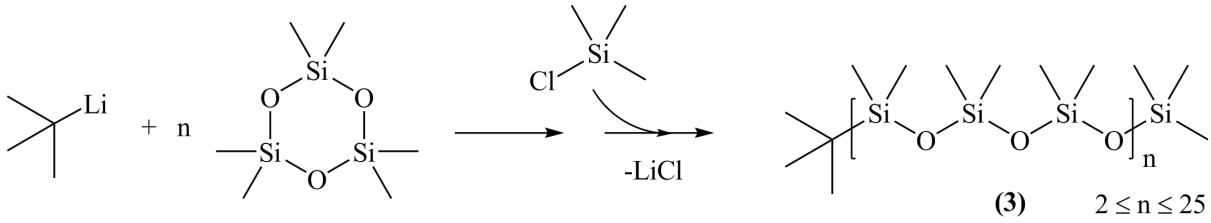


**Figure 29.** ROP of $D_3$ initiated by t-BuLi and stopped by CTMS

### 5.2.1. General Polymer Characterization

Determination of the monomer conversion was mainly performed by $^1$H NMR spectroscopy (300 MHz, 25°C, $CDCl_3$) using the ratio of reacted ($\delta$ = 0.0 ppm) to unreacted molecules $D_3$ ($\delta$ = 0.1 ppm) or equimolar amounts of benzene ($\delta$ = 7.3 ppm) as internal standard. This method was compared to gravimetric (grav) and SEC ($M_n$) measurements. The results of these three analyses were consistent. A typical result is given in Table 4, where *n* represents the number of reacted $D_3$ molecules. PDMS with a molecular weight distribution of PDI ≤ 1.2 are producible.

**Table 4.** Comparison of the analytical methods

| | |
|---|---|
| **$D_{3,0}$ / mmol $L^{-1}$** | 482.1 |
| **$D_3$ : t-BuLi / mol $mol^{-1}$** | 31 : 1 |
| **Temperature / °C** | -1.0 |
| **Reaction time / h** | 7.0 |
| **$n_{NMR}$ / -** | 21.9 |
| **$n_{grav}$ / -** | 21.9 |
| **$n_{SEC}$ / -** | 23.6 |
| **PDI / -** | 1.197 |

Figure 30 shows a MALDI-TOF-MS ($Ag^+$) of a linear PDMS produced by the anionic ROP of $D_3$ initiated by t-BuLi and stopped by addition of CTMS. The isotope pattern of this spectrum is given in Chapter 8.1.2. The polydispersity calculated from the signal intensities of the mass

spectrum equals 1.1, a value which is even lower than the molecular weight distribution gained from SEC measurement. The inter-distance of the peak signals equals in approximation the molecular weight of $D_3$ (222.46 g mol$^{-1}$). In addition, as described in Chapter 5.1.1, the ROR of $D_4$ is not occurring at the applied reaction conditions, since the ring strain of the six membered ring provides the driving force for this polymerization. Hence, it is assumed that backbiting or any other side reactions are not occurring in the kinetically controlled regime as already reported in literature[17].

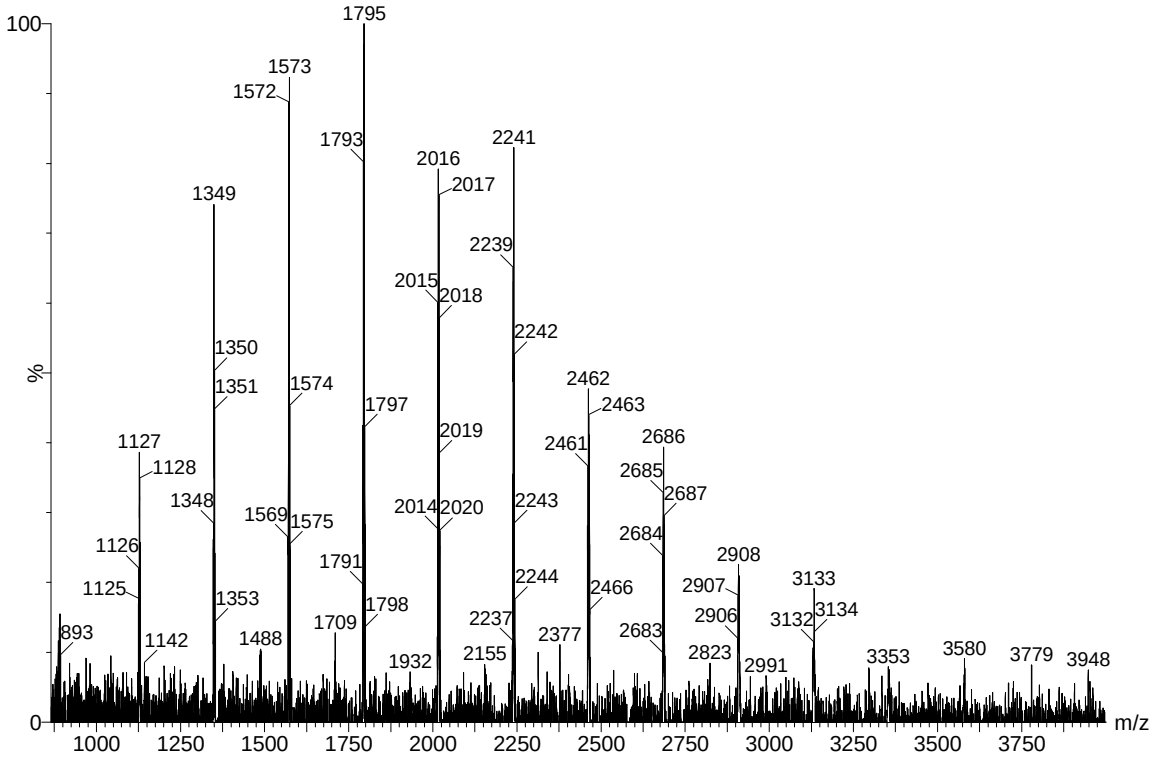


**Figure 30.** MALDI-TOF-MS of a linear PDMS produced from the ROP of $D_3$

The formation of the thermodynamically most stable cyclic oligosiloxane ($D_4$) due to backbiting reactions was not observed up to about 90 % to 95 % conversion according to $^{29}$Si NMR spectroscopy (Figure 31: no peak at at 19.4 ppm). At higher conversion the polymer starts to degrade as already elucidated in Figure 10 and $D_4$ is formed as the main side product. Furthermore, no consumption of $D_4$ in the ROP of $D_3$ from equimolar mixtures of these two cyclic oligosiloxanes in THF was detected. With these observations, the anionic ROP of $D_3$ in polar aprotic media is regarded as a highly selective polymerization reaction towards the monomer $D_3$ in the kinetically controlled regime. However, the polymerization reaction suffers side product formation when no termination reaction is performed and the degree of polymerization starts to decrease, ending up in the equilibrium controlled regime. Figure 31 shows a typical $^{29}$Si-INEPT NMR spectrum of a linear PDMS terminated with CTMS.

$^{29}$Si NMR (300 MHz, 25°C, $CDCl_3$) *δ / ppm*: -22.726 - -21.477 (O-(**Si**$(CH_3)_2$-O)$_n$, m); -8.686 (**$D_3$**, s); 7.071 (O-**Si**$(CH_3)_3$, s); 9.912 ($C_4H_9$-**Si**$(CH_3)_2$-O, s); 30.697 (Cl-**Si**$(CH_3)_3$, s)

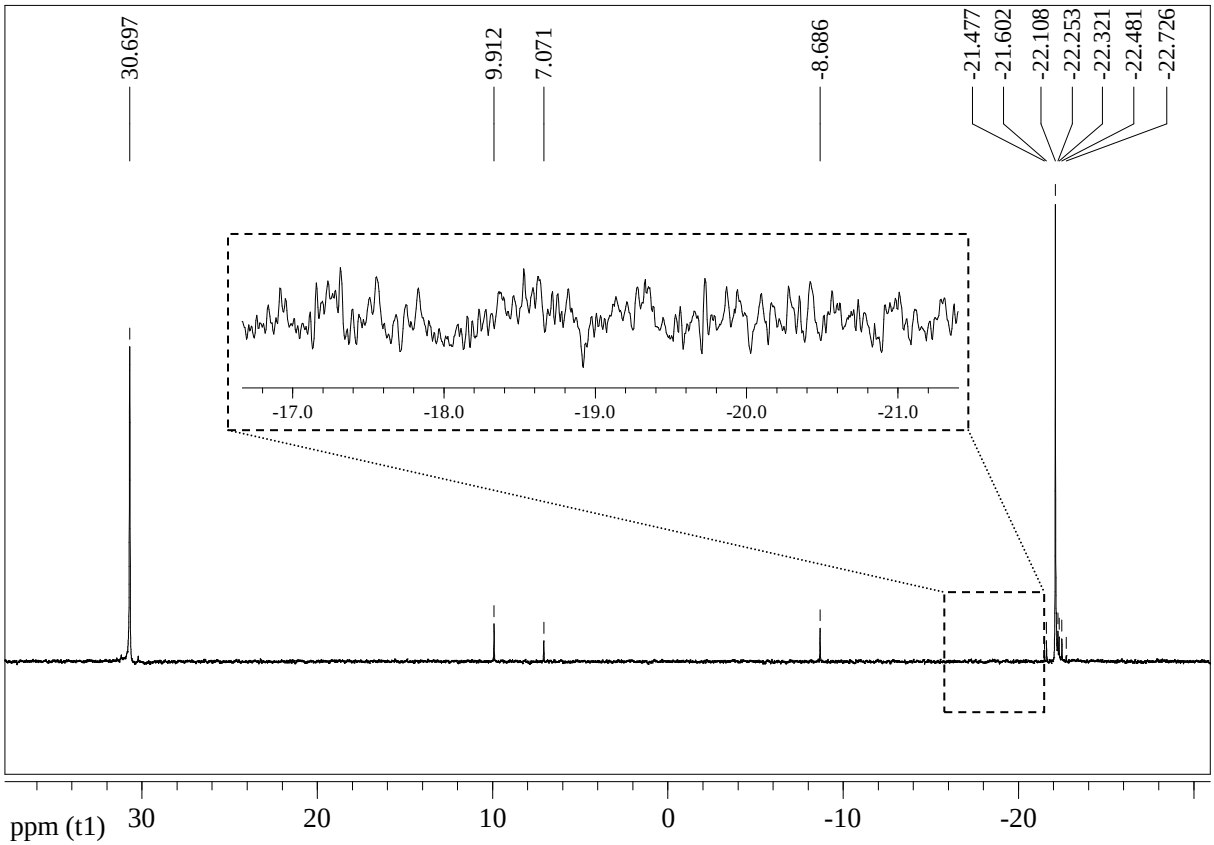


**Figure 31.** $^{29}$Si-INEPT NMR spectrum of a linear PDMS chain terminated with CTMS, $D_{3,0}$ : t-BuLi = 10 : 1, T = 10.0°C, monomer conversion $X_{D3}$ = 94.5 %

The viscosity and density of linear PDMS were determined in dependence on the chain length. The results are given in Table 5. Figure 32 shows the correlation[61] of the logarithm of the dynamic viscosity (η) and the logarithm of the molecular mass (M) of linear PDMS. The measurements (squares, solid line) show linear dependence and are in good agreement with adapted data* reported in literature[62] (circles, dashed line).

**Table 5.** Dynamic and kinematic viscosities and densities of various PDMS at 20.0°C and 50.0°C

| $(D_3)_n$ | $(Si\text{-}O)_x$ | 20.0°C | | | 50.0°C | | |
|---|---|---|---|---|---|---|---|
| | | Viscosity / mPa s | Viscosity / $mm^2\ s^{-1}$ | Density / $g\ mL^{-1}$ | Viscosity / mPa s | Viscosity / $mm^2\ s^{-1}$ | Density / $g\ mL^{-1}$ |
| 3.3 | 10.8 | 8.3034 | 8.9975 | 0.9229 | 4.7477 | 5.2926 | 0.8970 |
| 7.8 | 24.4 | 21.638 | 22.768 | 0.9504 | 12.043 | 13.021 | 0.9249 |
| 13.0 | 39.9 | 36.941 | 38.493 | 0.9588 | 19.675 | 21.071 | 0.9331 |
| 13.6 | 41.8 | 39.132 | 40.813 | 0.9597 | 21.724 | 23.283 | 0.9337 |
| 21.7 | 66.0 | 63.871 | 66.272 | 0.9638 | 35.381 | 37.712 | 0.9382 |

* Viscosities were given for 100°F (37.8°C) and 210°F (98.9°C), the values for 20°C were extrapolated from these data points.

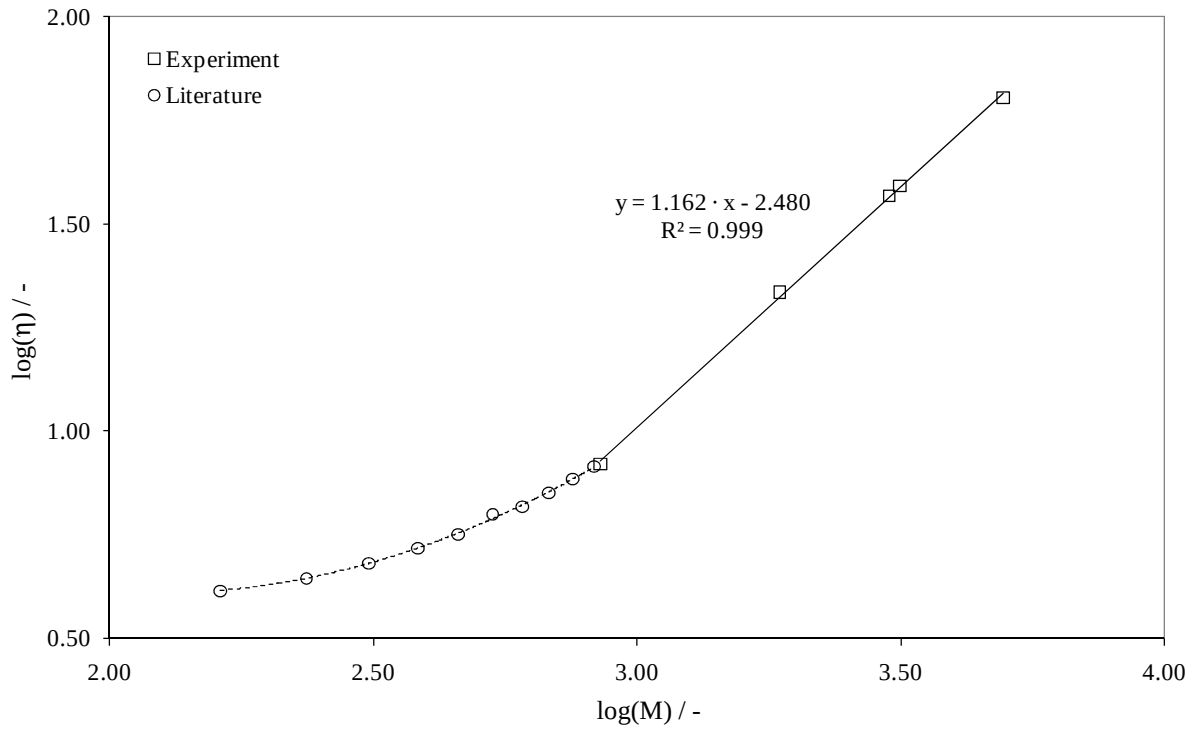


**Figure 32.** Correlation of the logarithm of the dynamic viscosity and the logarithm of the molecular mass of linear PDMS at 20.0°C

Figure 33 shows the density of the linear PDMS as a function of the number of Si-O units of the polymer chain at 20.0°C and 50.0°C.

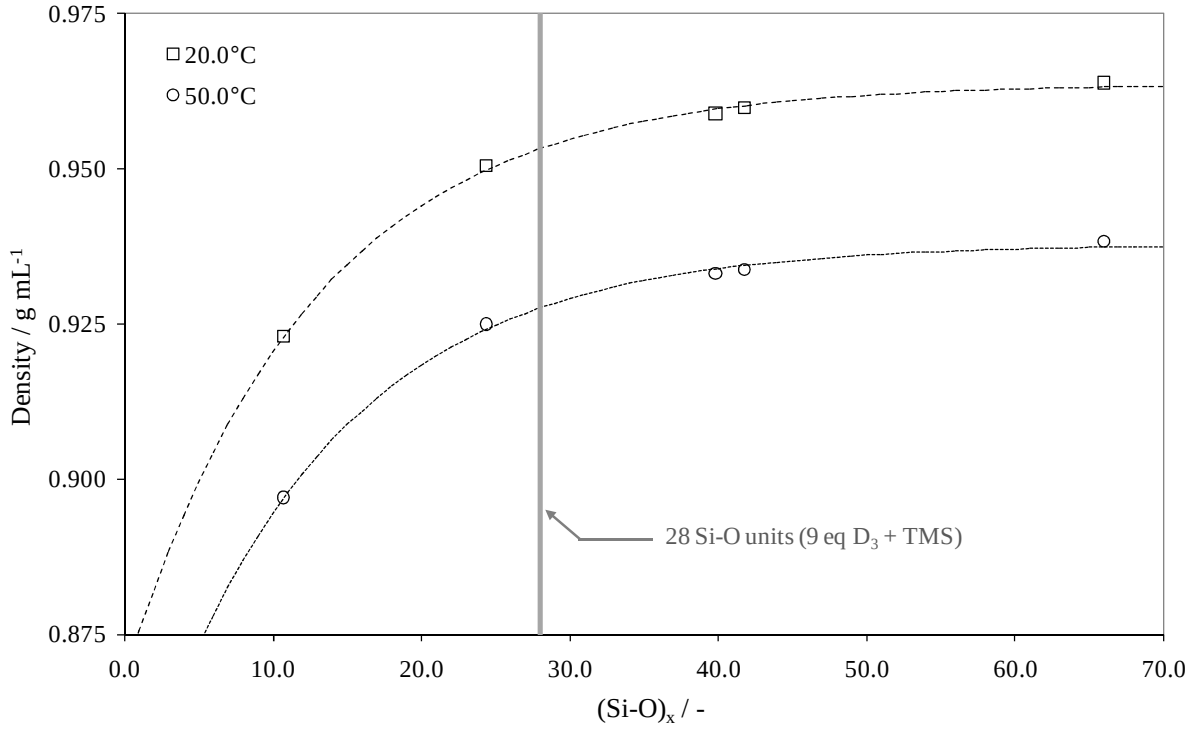


**Figure 33.** Density of linear PDMS at T = 20.0°C and T = 50.0°C

In the investigated molecular weight-range the density shows a significant dependence to the PDMS chain length (number of Si-O units) as represented by the dashed (20.0°C) and dotted (50.0°C) line. The density approximates 0.964 g $mL^{-1}$ for 20.0°C and 0.938 g $mL^{-1}$ for 50.0°C at higher degrees of polymerization. A thetic boundary dividing the plot into two sections was set (grey solid line) at a degree of polymerization of 28 (9 equivalents $D_3$ + TMS end group). At this point, the slopes of the two density curves start to diminish, dividing oligo- from polymerization. This interpretation is in accordance with the analysis of the rate constants of the ROP of $D_3$ (Chapter 5.2.2.2).

### 5.2.2. Kinetics of the Propagation Reaction

The determination of the kinetics of the ROP of $D_3$ was performed with different molar ratios of $D_3$ to t-BuLi in order to evaluate the dependence of the kinetics on the chain length of the growing PDMS chain (Table 6). The ROR of the first equivalent of the monomer $D_3$ forms the "active monomer" $D_3$* according to Equation 28. The ROR is several orders of magnitude faster than the ROP.

$$n_{D_3^*} = n_{D_3} - n_{t-BuLi} \tag{28}$$

**Table 6.** Molar ratios of the kinetic study of the ROP of $D_3$

| t-BuLi | $D_3$ | $D_3$* |
|---|---|---|
| 1 | 2 | 1 |
| | 4 | 3 |
| | 7 | 6 |
| | 10 | 9 |
| | 19 | 18 |

#### 5.2.2.1. Method of Initial Rates

The method of initial rates is an appropriate model for determination of the order of a chemical reaction. The ROP of $D_3$ was performed with molar ratios of $D_3$ : t-BuLi = 4 : 1 and 10 : 1 at 0°C, 10°C and 20°C and reaction times of 0.5 h and 1.0 h.

Figure 34 shows the ROP of $D_3$ for a molar ratio of $D_3$ : t-BuLi = 10 : 1 with reaction times of 1.0 h at 0.0°C and reaction times of 0.5 h at 10.0°C and 20.0°C.

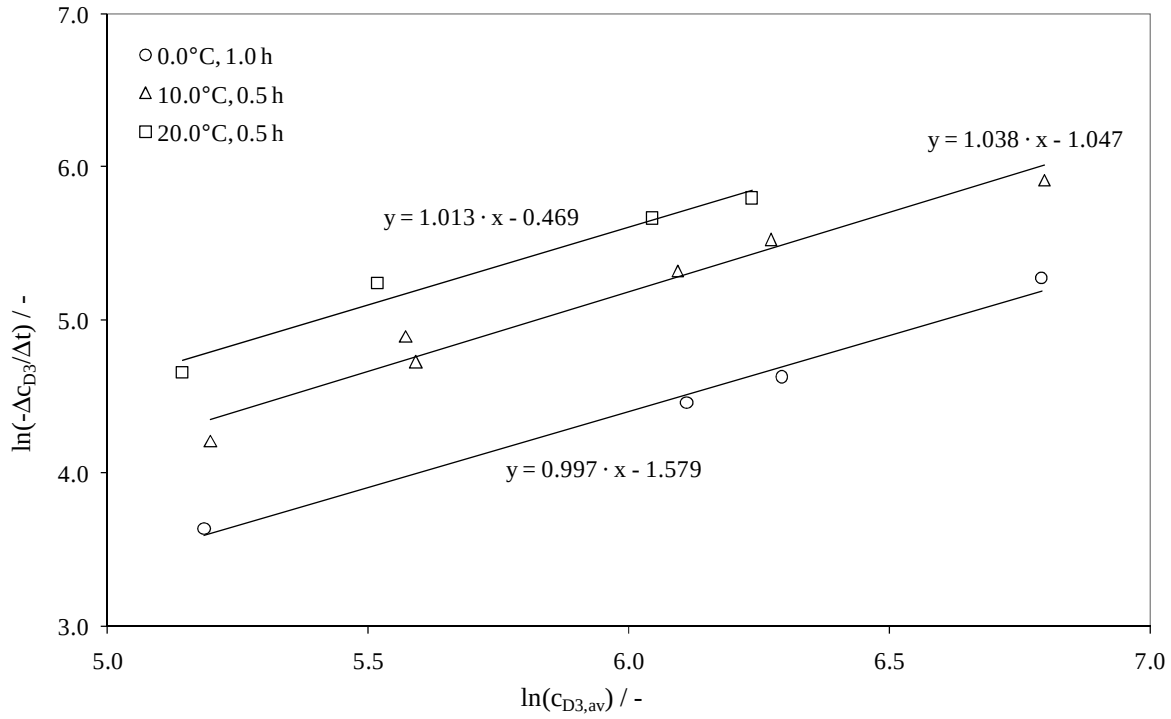


**Figure 34.** Method of initial rates for $D_3$ : t-BuLi = 10 : 1

Figure 35 shows the ROP of $D_3$ for a molar ratio of $D_3$ : t-BuLi = 4 : 1 with reaction times of 1.0 h at 0.0°C and reaction times of 0.5 h at 20.0°C.

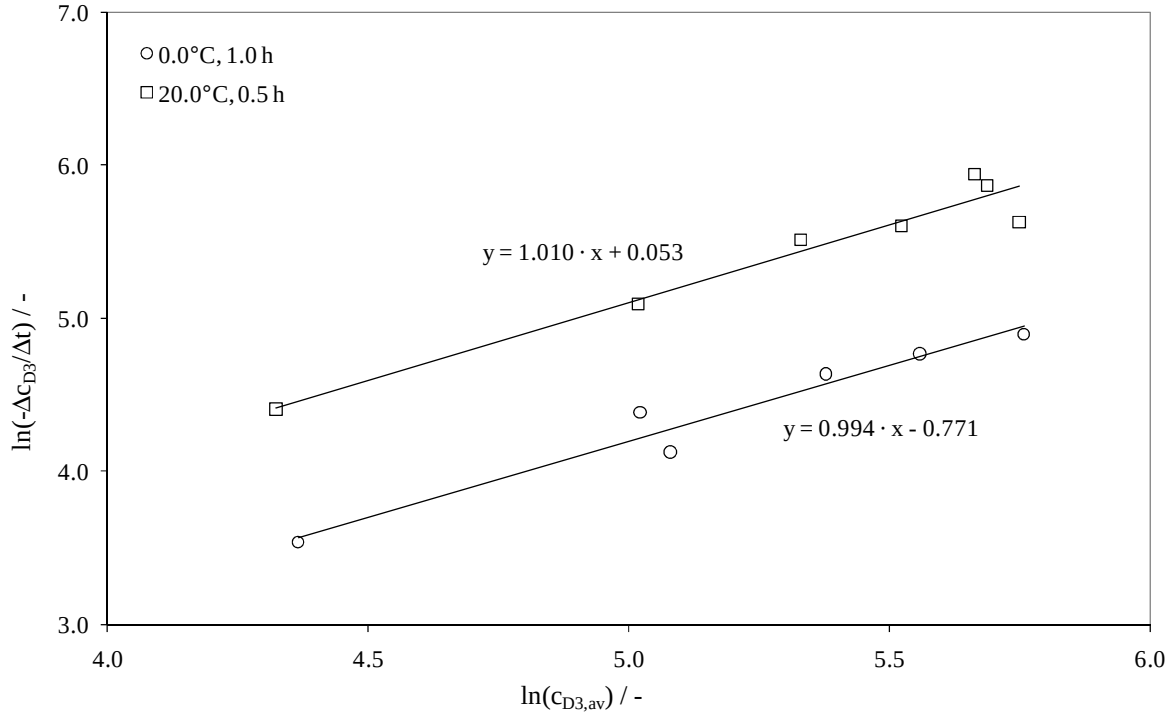


**Figure 35.** Method of initial rates for $D_3$ : t-BuLi = 4 : 1

The results are summarized in Table 7; the resulting order equals **n = 1.0** with a standard deviation of less than 2 %.

**Table 7.** Method of initial rates of the ROP of $D_3$

| $D_3$ : t-BuLi / mol mol$^{-1}$ | Temperature / °C | Reaction Time / h | Order n / - |
|---|---|---|---|
| 10:1 | 0.0°C | 1.0 | 0.997 |
| | 10.0°C | 0.5 | 1.038 |
| | 20.0°C | 0.5 | 1.013 |
| 4:1 | 0.0°C | 1.0 | 0.994 |
| | 20.0°C | 0.5 | 1.010 |
| **Average order n / -** | | | **1.0** |
| **Deviation / -** | | | **0.017** |

### 5.2.2.2. Rate Constants of the ROP of $D_3$

The rate constants of the ROP of $D_3$ were determined according to the molar ratios of $D_3$ : t-BuLi given in Table 6. The experiments were carried out in a temperature window of -10.0°C to about 35.0°C. The rate constants are summarized in Table 8 and Table 9, Figure 36 shows typical first order kinetics of the anionic ROP of $D_3$ initiated by t-BuLi with $D_3$ : t-BuLi = 7 : 1 at 0.0°C, 10.0°C, 20.0°C and 30.0°C.

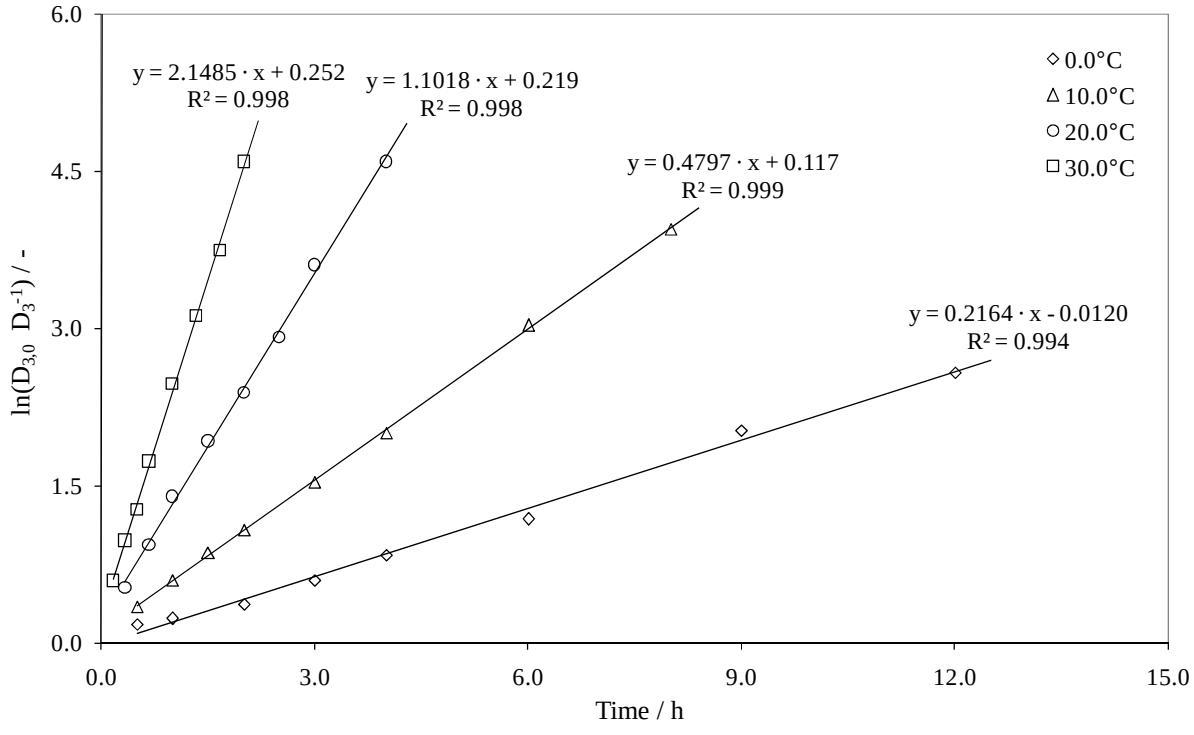


**Figure 36.** First order kinetics of the anionic ROP of $D_3$ ($D_3$ : t-BuLi = 7 : 1) at different temperatures

**Table 8.** Rate constants of the ROP of $D_3$ (I)

| $D_3$ : t-BuLi | T / °C | k / $h^{-1}$ |
|---|---|---|
| **1 : 2** | -10.0 | 0.0887 |
| | -0.79 | 0.2378 |
| | 0.00 | 0.1824 |
| | 10.1 | 0.4468 |
| | 14.8 | 0.7680 |
| | 14.9 | 0.7704 |
| | 19.9 | 0.978 |
| | 24.8 | 1.542 |
| | 29.8 | 2.190 |
| | 30.4 | 2.946 |
| | 32.1 | 3.060 |
| **1 : 4** | 10.0 | 0.5163 |
| | 20.0 | 1.0796 |
| | 30.0 | 2.1047 |

**Table 9.** Rate constants of the ROP of $D_3$ (II)

| $D_3$ : t-BuLi | T / °C | k / $h^{-1}$ |
|---|---|---|
| **1 : 7** | 0.0 | 0.2164 |
| | 10.0 | 0.4797 |
| | 20.0 | 1.1018 |
| | 30.0 | 2.1485 |
| **1 : 10** | 0.00 | 0.1918 |
| | 10.0 | 0.4302 |
| | 10.0 | 0.4741 |
| | 30.0 | 1.9128 |
| **1 : 19** | 0.00 | 0.1779 |
| | 20.0 | 0.9080 |
| | 20.0 | 0.9277 |

Figure 37 shows the Arrhenius evaluation of the acquired data. The fit of the whole set shows a highly accurate correlation according to the variance of $R^2 = 0.987$ (dashed line, italic equation). However, this correlation is significantly improved when the data set is split into two sections. The first section ($D_3$ : t-BuLi = 2 : 1, 4 : 1, 7 : 1, circles, upper solid line) representing the oligomerization of $D_3$ has an accuracy of $R^2 = 0.9905$ and the second ($D_3$ : t-BuLi = 10 : 1, 19 : 1, squares, lower solid line) representing further polymerization has an accuracy of $R^2 = 0.997$.

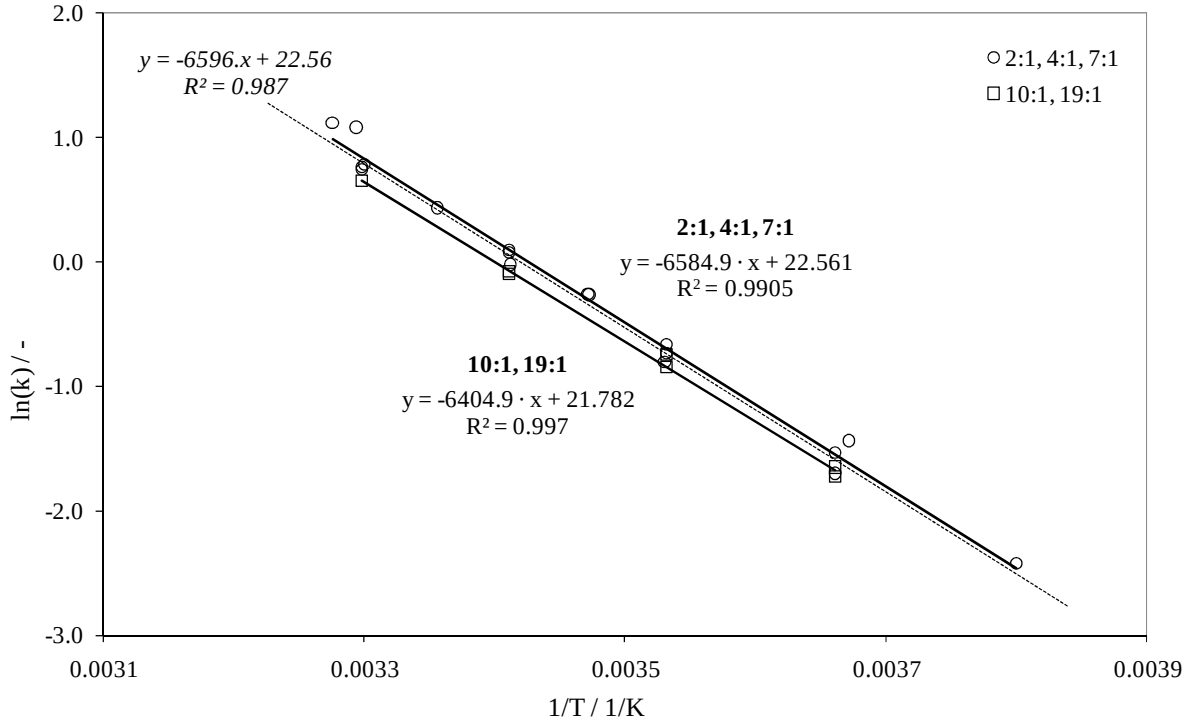


**Figure 37.** Arrhenius plot of the ROP of $D_3$ initiated by t-BuLi with different ratios of monomer to initiator

In consistency with the interpretation of the density curves (Figure 33) the consumption of the first to the eighth equivalent $D_3$ in the ROP is specified as oligomerization and any further propagation is defined as polymerization.

The Arrhenius parameters were found to be $\mathbf{k_0 = 1.75 \cdot 10^6\ s^{-1}}$ and $\mathbf{E_A = 54.7\ kJ\ mol^{-1}}$ for the oligomerization of $D_3$ and $\mathbf{k_0 = 8.01 \cdot 10^5\ s^{-1}}$ and $\mathbf{E_A = 53.3\ kJ\ mol^{-1}}$ for further polymerization (Table 10). An error of 5.0 % is estimated according to literature[58].

**Table 10.** Arrhenius parameters of the ROP of $D_3$ initiated by t-BuLi

| Type | Parameter | Value | Error |
|---|---|---|---|
| **$D_3$ 1-8 Oligomerization** | **$E_A$ / kJ mol$^{-1}$** | 54.7 | ± 2.7 |
| | **$k_0$ / s$^{-1}$** | $1.75 \cdot 10^6$ | $\pm 8.73 \cdot 10^4$ |
| **$D_3$ 9+ Polymerization** | **$E_A$ / kJ mol$^{-1}$** | 53.3 | ± 2.7 |
| | **$k_0$ / s$^{-1}$** | $8.01 \cdot 10^5$ | $\pm 4.00 \cdot 10^4$ |

### 5.2.2.3. The Influence of Matrix Ions on the ROP of $D_3$

The influence of various metal salts, especially elements of common stainless steel (Fe, Cr and Ni) on the anionic ROP of $D_3$ ($D_3$ : t-BuLi = 19 : 1) at 10°C and 20°C was investigated. In general, the admixture of a metal halogenide resulted in a significant decrease of the rate of reaction.

Figure 38 shows the monomer conversion of the anionic ROP of $D_3$ (crosses, solid line) and polymerization with addition of Cr(II) (squares, dotted line) and Cr(III) (rhombi, triangles and circles, dashed lines) chlorides at T = 10°C. Either Cr constituent has a significant influence on the rate of conversion, Cr(III) decreases polymer formation and Cr(II) even quenches polymerization completely. Cr complexes such as $Cr(acac)_3$ as well as $MnSO_4$ showed no influence on the rate of reaction. Admixture of several Fe-, Ni- or Mg-halogenides resulted in consistency to the Cr-doped experiments in decreased monomer consumption.

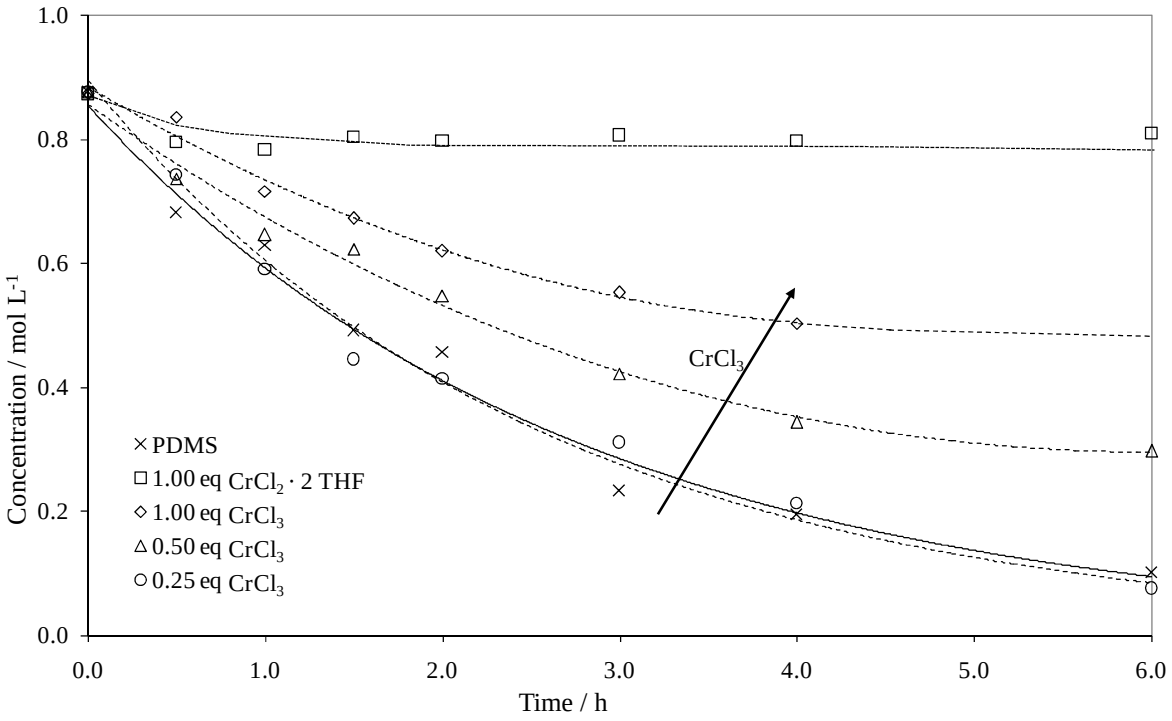


**Figure 38.** Influence of Cr(II) and Cr(III) on the anionic ROP of $D_3$ ($D_3$ : t-BuLi = 19 : 1) at 10.0°C

The addition of stainless steel internals (1.4301 (V2A) and 1.4571 (V4A)) did not cause decreased rate of the polymerization. However, interactions of reactive PDMS-compounds with stainless steel are reported in literature[63,64] and therefore, a negative influence of e.g. brazed joints in continuously fed reactors cannot be completely excluded, as shown by previous experiments[65].

### 5.2.3. Thermodynamics of the ROP of $D_3$

The polymerization of $D_3$ is a mildly exothermic reaction as shown by the corresponding temperature curve (Figure 39). For determination of $\Delta_R H$, a solution of $D_3$ in THF was added to the reaction mixture and therefore correction of the temperature curve was necessary. The corrected baseline (dashed line) was used instead of the lower baseline (lower solid line) for data calculation.

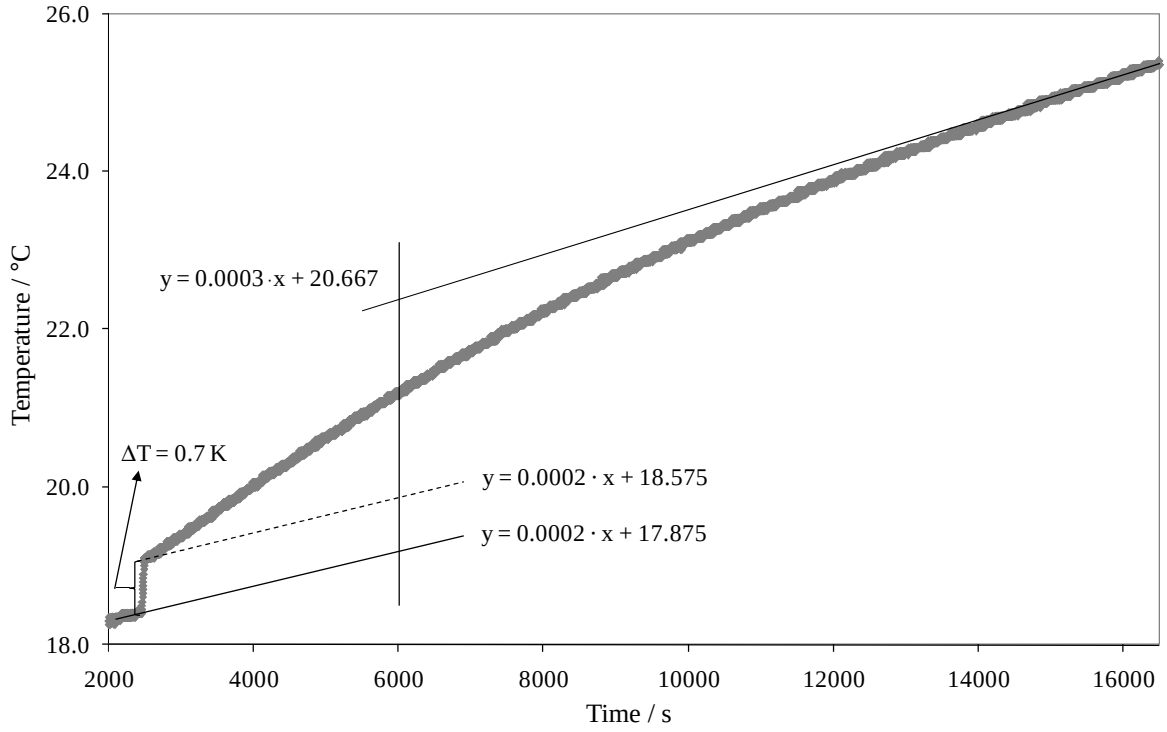


**Figure 39.** Temperature curve of the propagation reaction of $D_3$

$\Delta_R H$ of the propagation reaction of $D_3$ was found to be **-31.1 kJ mol$^{-1}$** with a standard deviation of 24.8 % (Table 11). A value of $\Delta_R H$ = -60.7 kJ mol$^{-1}$ is reported in literature[23]. The deviation may result from heat losses during processing because the reaction was not fast enough for this experimental setup.

**Table 11.** $\Delta_R H$ of the propagation reaction of $D_3$

| Experiment No. | $\Delta_R H$ / kJ mol$^{-1}$ |
|---|---|
| # 1 | -36.5 |
| # 2 | -25.6 |
| **Average** | **-31.1** |
| **Deviation** | **7.7** |

## 5.3. The Termination Reaction

The anionic ROP of $D_3$ initiated by t-BuLi is forming a linear terminal lithium silanolate as an intermediate which is simultaneously end capped by elimination of lithium chloride when a chlorosilane is added (Figure 17). In this reaction no other side products are formed and there are no competing reactions reported in literature to affect kinetic studies. Hence, only the thermodynamic characterization was performed by means of determination of $\Delta_R H$ by measuring the corresponding temperature curve. The termination reaction with CDMS as end capping reagent is an exothermic reaction as shown in Figure 40. $\Delta_R H$ of the termination reaction was found to be **-98.7 kJ mol$^{-1}$** with a standard deviation of 2.1 % (Table 12).

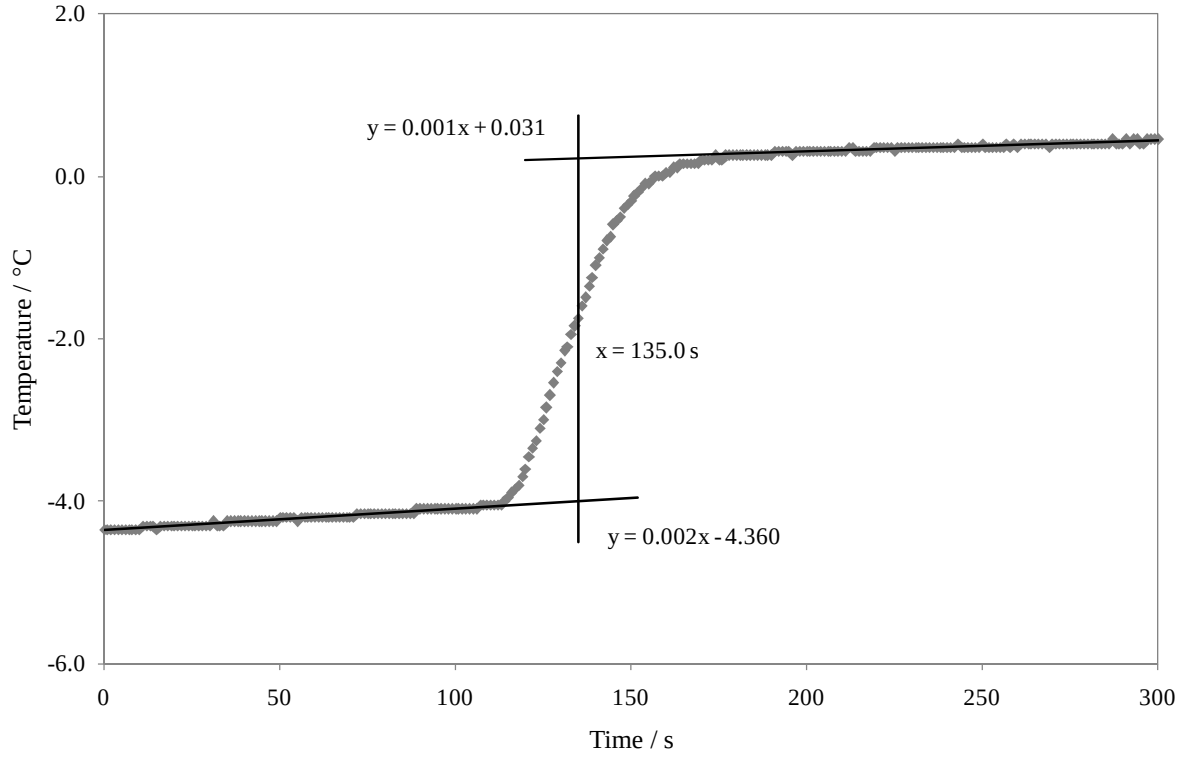


**Figure 40.** Typical temperature curve of the termination reaction with CDMS

**Table 12.** $\Delta_R H$ of the termination reaction with CDMS

| Experiment No. | $\Delta_R H$ / kJ mol$^{-1}$ |
|---|---|
| # 1 | -98.6 |
| # 2 | -99.8 |
| # 3 | -95.3 |
| # 4 | -99.3 |
| # 5 | -100.6 |
| **Average** | **-98.7** |
| **Deviation** | **2.1** |

## 5.4. Continuously Performed Experiments

As already stated in Chapter 4.3 for a continuously operated anionic polymerization reaction the PFR is the reactor of choice. At first, theoretical calculations of an ideal PFR were performed. Later on, the continuous production of linear PDMS with narrow molecular weight distributions is described. Preliminary polymerization reactions were carried out in a stainless steel PFR (SS-PFR) by C. Pschera.[65] In this work a PFR consisting of Teflon tubing (PTFE-PFR) was constructed and operated. The PTFE-PFR was coiled up a central tube to induce radial mixing along the reactor. The mixing effect was proven by CFD calculations.

### 5.4.1. Ideal PFR Calculations

With the determined polymerization kinetics and with the parameters given in Table 13 an ideal, isothermal PFR for the continuous ROP of $D_3$ was calculated. This dataset was chosen in order to develop the PTFE-PFR experiments described in Chapter 5.4.3. Two different stock solutions ($D_3$ stock and t-BuLi stock) are assumed which are mixed in a T-connector and the polymerization reaction occurrs subsequently according to Figure 41. The termination reaction is not considered at this point.

**Table 13.** Parameters for calculations of the ideal PFR

| Type | Parameter | Value |
|---|---|---|
| **Stock Solution** | **$D_3$ / mmol $L^{-1}$** | 500.0 |
| | **t-BuLi / mmol $L^{-1}$** | 320.0 |
| **Molar Flow Ratio** | **$D_3$ : t-BuLi / -** | 25 |
| **Volumetric Flow Ratio** | **$D_3$ : t-BuLi / -** | 16 |
| **Reaction Solution** | **$D_3$ / mmol $L^{-1}$** | 470.6 |
| | **t-BuLi / mmol $L^{-1}$** | 18.8 |
| **Temperature** | **T / °C** | 40.0 |

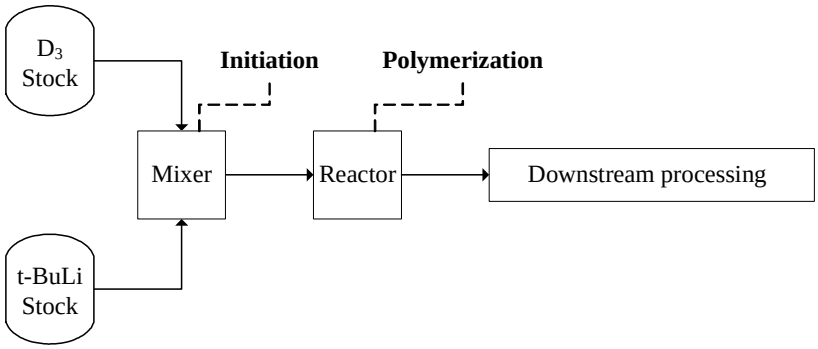


**Figure 41.** Flowsheet for calculations of the ideal PFR

Figure 42 shows the modeled concentration profile (squares, solid line) and the number of Si-O units (triangles, dashed line) of the growing PDMS chains in dependence on the mean residence time for an ideal PFR. The change from oligo- to polymerization is represented by the vertical dotted line; a significant influence on the concentration curve is not apparent.

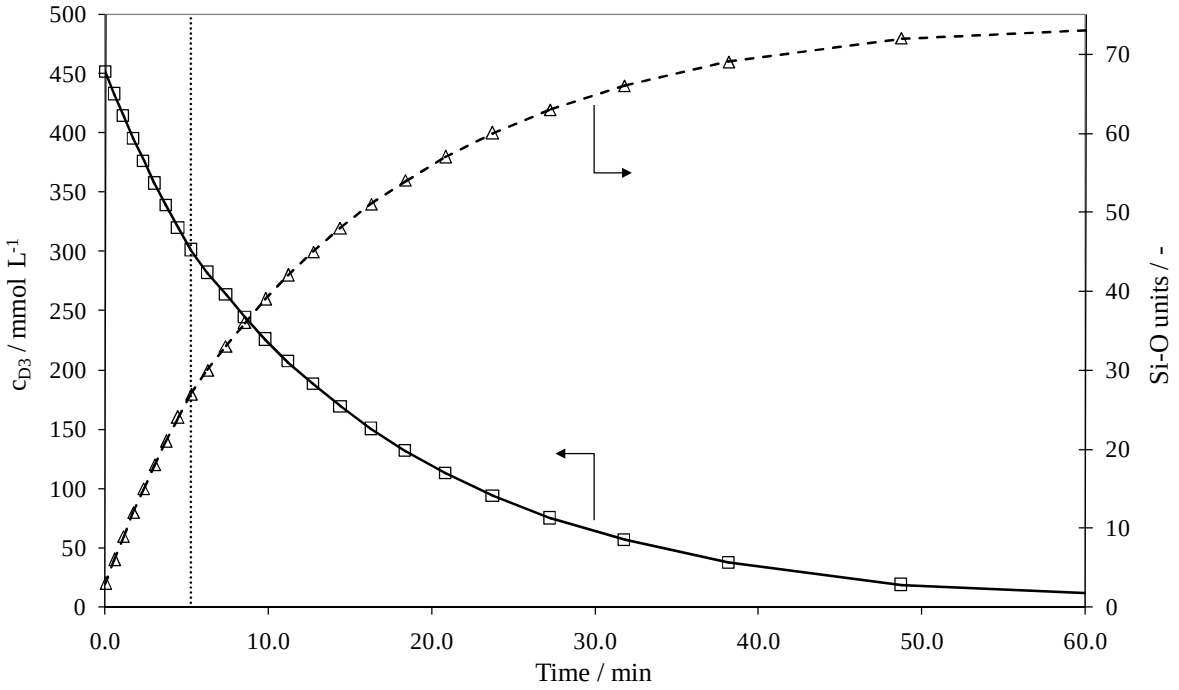


**Figure 42.** Concentration profile of monomer and PDMS repeating units (Si-O) for polymerization in the ideal PFR in dependence on the mean residence time at T = 40°C

The graphical solution of the mean residence time (t) for a monomer conversion of 88 % of a PFR (area below the dataset) in comparison to a CSTR (area of the whole square) is shown in Figure 43. In this ideal PFR curve the change from oligo- to polymerization is apparent. The reactor volume needed for the initiation reaction is insignificant and not considered at this point.

The calculated ideal residence time of the CSTR is more than six times larger than the corresponding ideal PFR residence time. Hence the PFR is the more economical type of reactor for this kind of polymerization reaction.

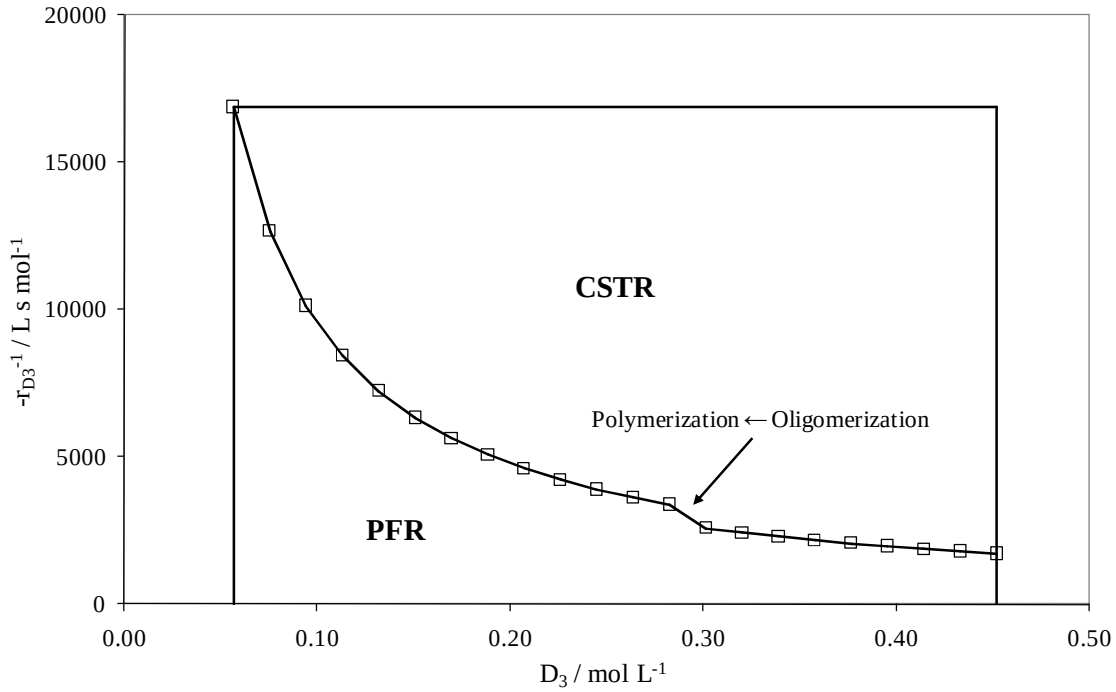


**Figure 43.** Graphical solution of the mean residence time (t) of a PFR in comparison to a CSTR at T = 40°C

### 5.4.2. SS-PFR Experiments[65]

In the continuously fed SS-PFR the first monodisperse PDMS (PDI ≤ 1.2) were already successfully synthesized. The experimental setup is shown in Figure 44.

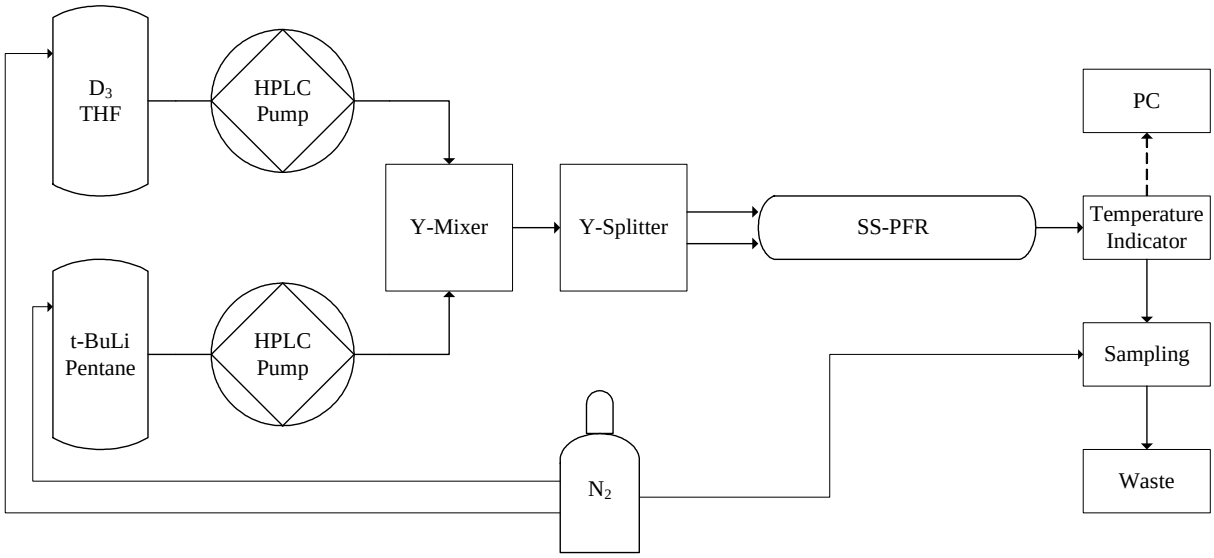


**Figure 44.** SS-PFR experimental setup for continuous ROP of $D_3$ initiated by t-BuLi

The characteristic dimensions of the SS-PFR are given in Table 14, where $L$, $D_I$, $V_{R-Mix}$ and $V_{R+Mix}$ represent the length, inner diameter and the reactor volume without and with Kenics mixer units and $F_V$ stands for the flow rate.

**Table 14.** Characteristics of the experimental setup SS-PFR

| | |
|---|---|
| **L / cm** | 40.0 |
| **$D_I$ / cm** | 1.0 |
| **$V_{R-Mix}$ / mL** | 31.4 |
| **$V_{R+Mix}$ / mL** | 27.3 |
| **$F_V$ / mL min$^{-1}$** | 1.0 – 10.0 |

Because of laminary flow conditions Kenics mixers (Figure 45) were used to induce radial mixing along the PFR. The RTD experiments showed confusing behavior as Bo-number decreased with increasing flow rate.

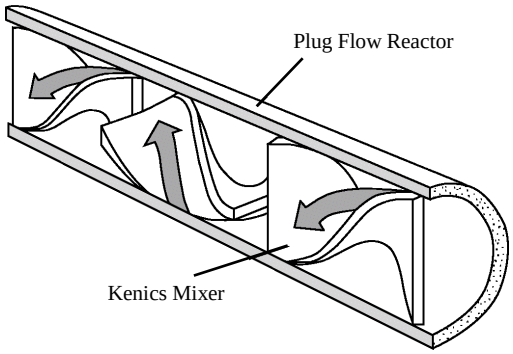


**Figure 45.** Kenics static mixer units along a PFR[66]

The polymerization reactions were performed at 40°C with a monomer to initiator ratio of $D_3$ : t-BuLi = 25 : 1 and 50 : 1. Reproducibility and control of the degree of polymerization could not be obtained with this experimental setup. In general, PDMS chains with two to seven times larger molecular weights in comparison to ideal PFR calculations were produced. The monomer conversion was generally lower than calculated. Deactivation of the initiator t-BuLi caused by interaction with the reactor material was assumed.

### 5.4.3. PTFE-PFR Experiments

To solve the problems of the SS-PFR a PTFE-PFR was constructed and operated. Radial mixing was performed by coiling the tubing up a pipe to create Dean vortices, secondary circulations perpendicular to the main flow.

#### 5.4.3.1. The Reactor

Two different PTFE tubes were used. The characteristic dimensions of these two tubings are given in Table 15, where $L$, $d_i$, $d_o$, $s$, $V_R$ represent length, inner diameter, outer diameter, wall thickness and volume of the reactor and $D_O$ the central tube diameter. The setup PTFE-PFR I was characterized at three different curvatures using $D_O$ = 2.0 cm, $D_O$ = 3.0 cm and $D_O$ = 4.0 cm. The setup PTFE-PFR II has a three times larger reactor volume than PTFE-PFR I and was used for comparison. This reactor was coiled up $D_O$ = 3.0 cm.

**Table 15.** Characteristics of the experimental setups PTFE-PFR I and II

| Parameter | PTFE-PFR I | PTFE-PFR II |
|---|---|---|
| **L / m** | 4.00 | 5.33 |
| **$d_i$ / mm** | 2.0 | 3.0 |
| **$d_o$ / mm** | 3.0 | 4.0 |
| **s / mm** | 0.5 | 0.5 |
| **$D_O$ / cm** | 2.0, 3.0, 4.0 | 3.0 |
| **$V_R$ / mL** | 12.57 | 37.71 |

The curvature diameter ($D$) of the fluid flow for calculation of the De-number is given with Equation 29.

$$D = D_O + 2 \cdot s \tag{29}$$

Figure 46 shows a picture of the reactor setup PTFE-PFR I coiled up $D_O$ = 3.0 cm. The temperature control unit, applied during continuous polymerization experiments, is not shown on this picture. The direction of the flow is from left to right hand. For RTD the second T-connector at the reactor outlet (right hand side) was not needed.

**Figure 46.** Picture of PTFE-PFR I coiled up a central tube diameter of $D_O$ = 3.0 cm for continuous experiments

The concentration profile and the number of Si-O units of the ideal PFR (Figure 42: squares, solid line and triangles, dashed line) were modified in respect to the range of the investigated flow rates in the PTFE-PFR I experiments (Figure 47). The flow rates ($F_V$) are given in Table 16. In addition, central tube diameter ($D_O$), the curvature ratio ($d_i^{0.5}\ D^{-0.5}$), Re- and De-number (*Re*, *De*) are shown. Re- and De-number were calculated for pure THF at room temperature (25°C) because the RTD experiments and the CFD calculations were performed under these conditions.

**Table 16.** Flow rates ($F_V$), central tube diameter ($D_O$), Re- and De-number for PTFE-PFR I

| $F_V$ / mL min$^{-1}$ | $D_O$ / cm | $d_i^{0.5}\ D^{-0.5}$ / - | Re / - | De / - |
|---|---|---|---|---|
| 1.50 | 2.0 | 0.309 | 31 | 14 |
| 3.00 | | | 62 | 27 |
| 5.00 | | | 103 | 45 |
| 7.50 | | | 155 | 68 |
| 1.50 | 3.0 | 0.254 | 31 | 11 |
| 3.00 | | | 62 | 22 |
| 5.00 | | | 103 | 37 |
| 7.50 | | | 155 | 56 |
| 1.50 | 4.0 | 0.221 | 31 | 10 |
| 3.00 | | | 62 | 19 |
| 5.00 | | | 103 | 32 |
| 7.50 | | | 155 | 48 |

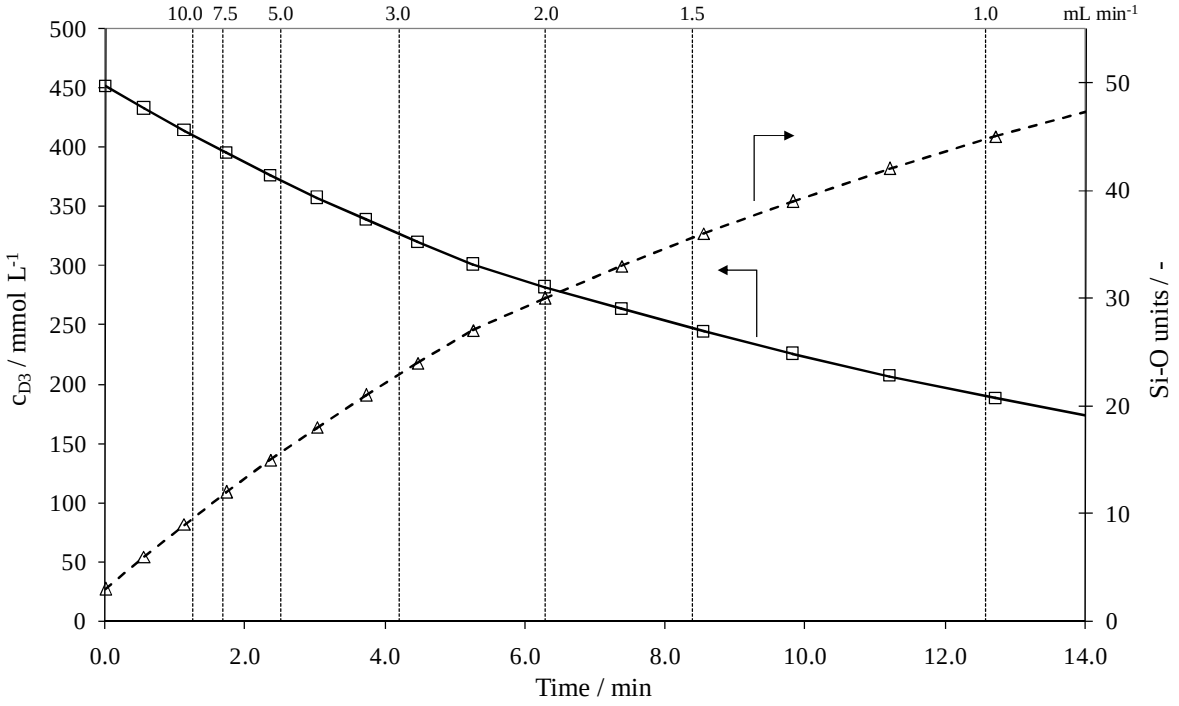


**Figure 47.** Concentration profile of monomer and PDMS repeating units (Si-O) for polymerization in ideal PTFE-PFR I in dependence on the mean residence time including the range of flow rate

#### 5.4.3.2. The Initiation Reaction in the T-Connector

At ambient temperature the highly exothermic initiation reaction occurs instantaneously when the monomer stock solution and the initiator stock solution are mixed. To prevent any enthalpy effects (e.g. hot spots) in the mixer, the adiabatic temperature increase for the initiation reaction is calculated. In this prediction only the solvents THF and Heptane are considered and the heat transfer to the mixer or any other heat loss is neglected. Hence, the temperature increase is calculated according to Equation 30.

$$\Delta T = \frac{-n_{t-BuLi} \cdot \Delta_R H_{Initiation}}{n_{THF} \cdot c_{p,THF} + n_{Heptane} \cdot c_{p,Heptane} + n_{Pentane} \cdot c_{p,Pentane}} \tag{30}$$

The temperature increase was found to be approximately **ΔT = 2.5 K**. From these calculations it was concluded that any enthalpy effects occurring in the mixer can be regarded as insignificant. However, to prevent the formation of hot spots due to non-ideal mixing neither the reaction solutions ($D_3$ stock and t-BuLi stock) nor the mixer itself are preheated in the continuous polymerization reactions. Additionally, any enthalpy effects of the termination reaction are also neglected, as the enthalpy change of reaction is even less than half of the enthalpy change of reaction of the initiation reaction.

### 5.4.3.3. RTD of the PTFE-PFR

To investigate the impact of non-idealities on the molecular weight distribution RTD experiments for PTFE-PFR I and II were performed. The experimental setup is shown in Figure 48; sampling was performed discontinuously.

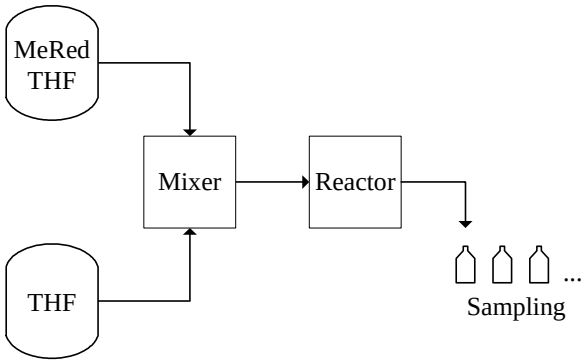


**Figure 48.** Experimental setup for determination of the RTD

A typical F-curve is shown in Figure 49. The dataset (squares) was fitted by a sigmoidal fit (grey solid line) for consecutive evaluation of the Bo-number. The dashed grey line indicates the mean residence time.

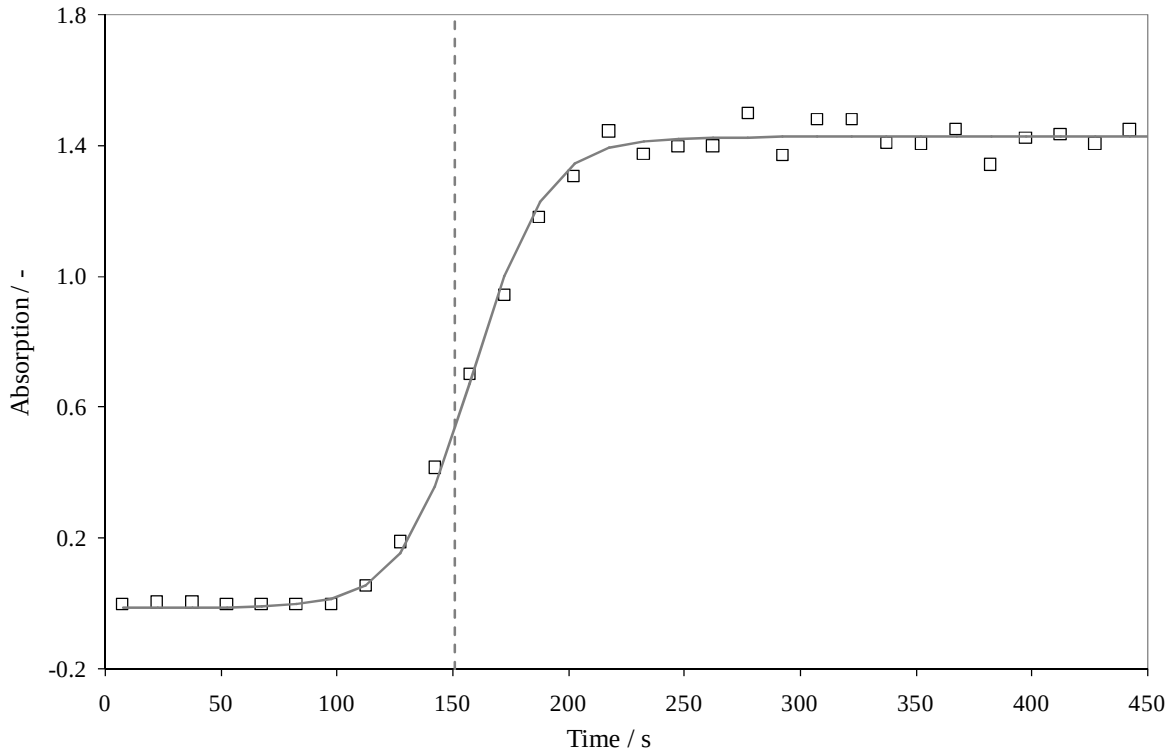


**Figure 49.** F-curve of PTFE-PFR I coiled up a central tube diameter of $D_O$ = 2.0 cm and flow rate of $F_V$ = 5.00 mL $min^{-1}$

Figure 50 shows the E-curves for the experimental setup PTFE-PFR I with a central tube diameter of $D_O$ = 2.0 cm at different flow rates ($F_V$ = 1.50 mL $min^{-1}$ grey squares;

$F_V$ = 3.00 mL min$^{-1}$ black circles; $F_V$ = 5.00 mL min$^{-1}$ grey triangles; $F_V$ = 7.50 mL min$^{-1}$ black rhombi). $\theta$ represents the dimensionless hydrodynamic residence time. The RTD curves of all experiments are summarized in Chapter 7.3.1. Figure 50 representatively shows that the distribution broadens with increasing flow rate, an unexpected hydraulic characteristic for a PFR. The results of the RTD evaluation of PTFE-PFR I are summarized in Table 17.

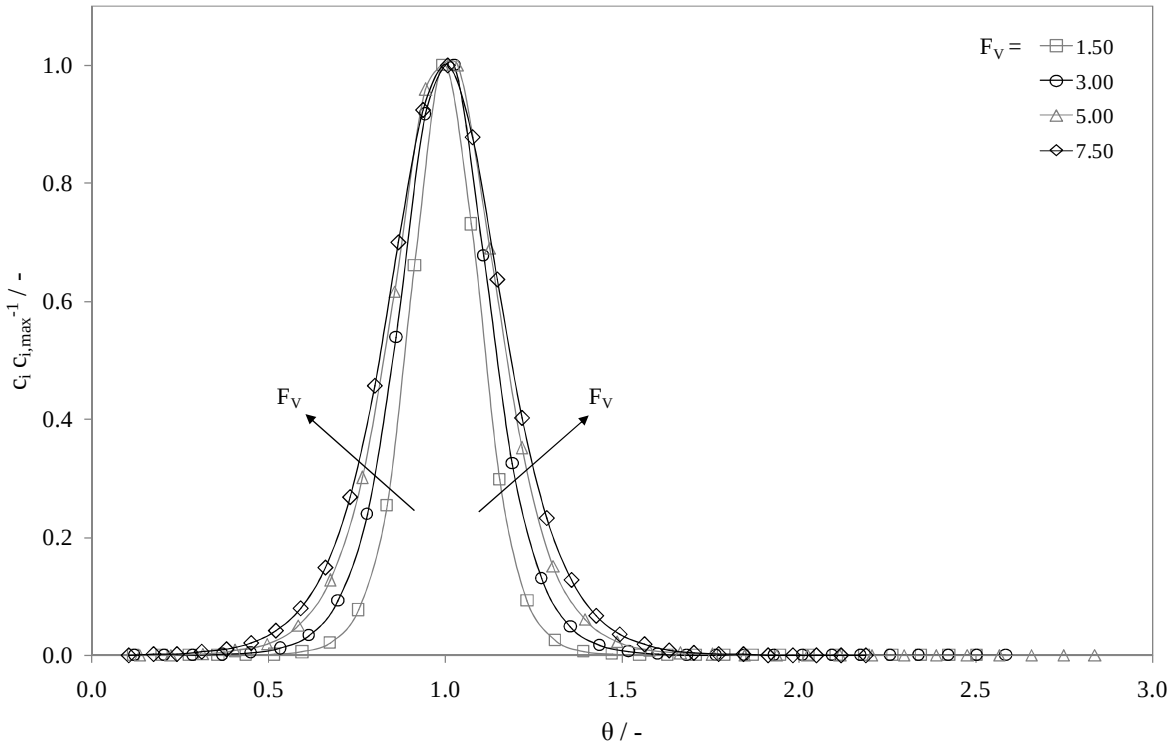


**Figure 50.** Evaluation of the RTD (E-curve) for PTFE-PFR I coiled up a central tube diameter of $D_O$ = 2.0 cm

**Table 17.** Results of the RTD experiments of PTFE-PFR I coiled up different central tube diameters $D_O$

| $D_O$ / cm | $F_V$ / mL min$^{-1}$ | Re / - | De / - | Bo / - |
|---|---|---|---|---|
| 2.0 | 1.50 | 31 | 14 | 161 |
| | 3.00 | 62 | 27 | 98 |
| | 5.00 | 103 | 45 | 72 |
| | 7.50 | 155 | 68 | 59 |
| 3.0 | 1.50 | 31 | 11 | 147 |
| | 3.00 | 62 | 22 | 72 |
| | 5.00 | 103 | 37 | 55 |
| | 7.50 | 155 | 56 | 52 |
| | 10.00 | 207 | 74 | 45 |
| 4.0 | 1.50 | 31 | 10 | 145 |
| | 3.00 | 62 | 19 | 75 |
| | 5.00 | 103 | 32 | 50 |
| | 7.50 | 155 | 48 | 48 |
| | 10.00 | 207 | 65 | 46 |

Figure 51 shows the comparison of the results of the RTD experiments (Bo-number) of PTFE-PFR I with different diameter of the central tube $D_O$ versus De-number which is proportional to the flow rate ($D_O$ = 2.0 cm, squares, solid line; $D_O$ = 3.0 cm, circles, dotted line; $D_O$ = 4.0 cm, triangles, dashed line). Bo-number is significantly decreased with increasing flow rate for all three experimental setups. This finding is in accordance with CFD simulations (Chapter 5.4.3.4). In these calculations first eddies were formed at $F_V$ = 3.00 mL min$^{-1}$. When De-number obtains $De_{crit}$ the Bo-number reaches a constant value. Generally, with increasing curvature diameter the Bo-number is decreased and the fluid flow is less stable.

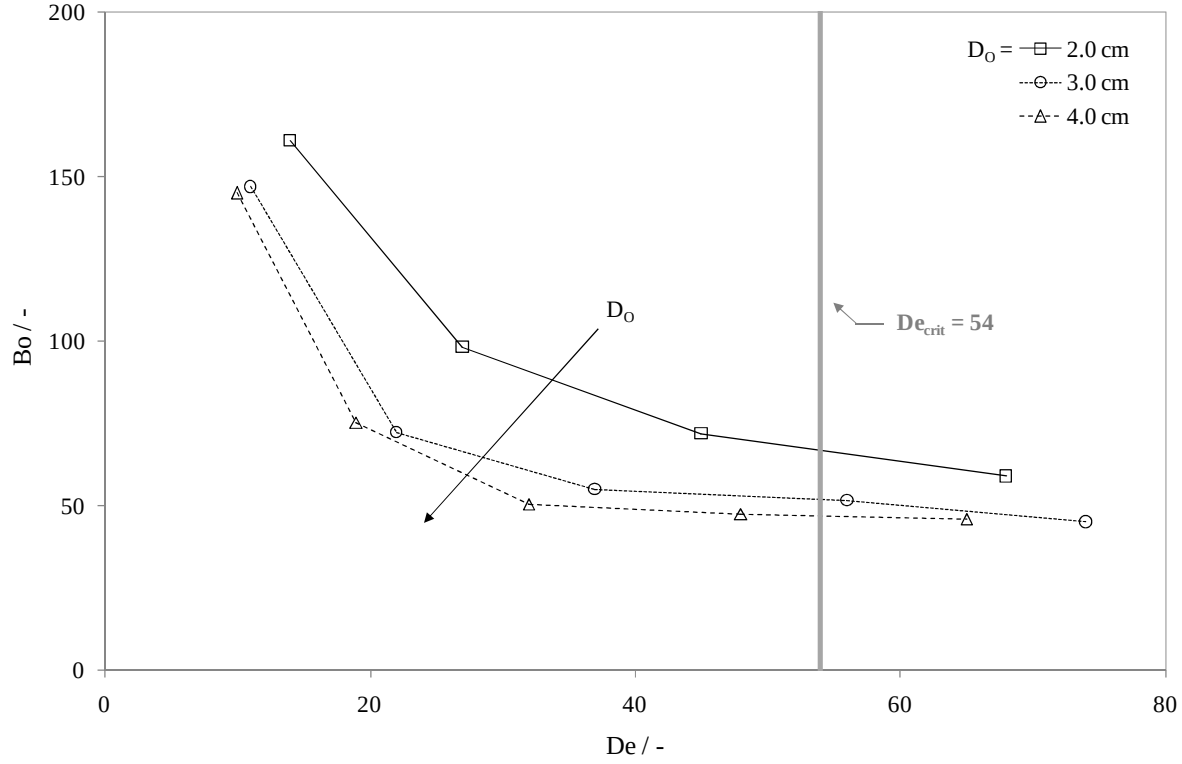


**Figure 51.** Bo- versus De-number for PTFE-PFR I: Comparison and influence of different central tube diameters $D_O$

The experimental results of the RTD experiments of PTFE-PFR II coiled up a central tube diameter of $D_O$ = 3.0 cm and different flow rate are summarized in Table 18.

**Table 18.** Results of the RTD experiments of PTFE-PFR II coiled up a central tube diameter of $D_O$ = 3.0 cm

| $D_O$ / cm | $F_V$ / mL min$^{-1}$ | Re / - | De / - | Bo / - |
|---|---|---|---|---|
| 3.0 | 1.50 | 21 | 9 | 170 |
| | 3.00 | 41 | 18 | 117 |
| | 5.00 | 69 | 30 | 88 |
| | 7.50 | 103 | 46 | 71 |
| | 10.00 | 138 | 61 | 63 |

Figure 52 shows the comparison of PTFE-PFR I ($d_i$ = 2.0 mm; squares, solid line) and PTFE-PFR II ($d_i$ = 3.0 mm; circles, dotted line); both coiled up a central tube diameter of $D_O$ = 3.0 cm. The Bo-numbers of PTFE-PFR I are significantly lower than the corresponding values of PTFE-PFR II. Hence, an increase of $d_i$, which results in a decrease of De- and Re-number, shows a positive effect on the stability of the system.

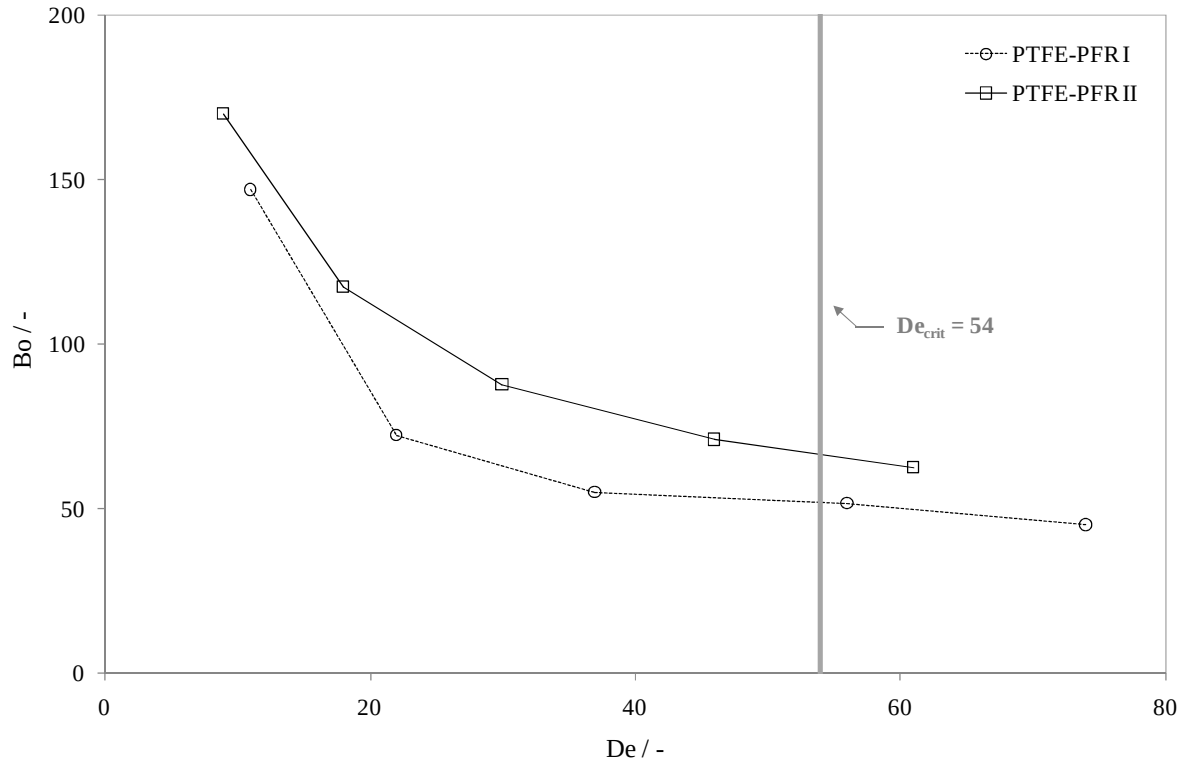


**Figure 52.** Bo- versus De-number: Comparison of different diameters of the reactor (PTFE-PFR I and PTFE-PFR II) coiled up a central tube diameter of $D_O$ = 3.0 cm

#### 5.4.3.4. CFD Simulation of PTFE-PFR I

The experimental results of the RTD investigations were compared with CFD calculations. The case scenario for simulation was the experimental setup PTFE-PFR I coiled up a central tube diameter of $D_O$ = 2.0 cm (Table 15). Ten coils of the reactor were meshed according to Figure 53.

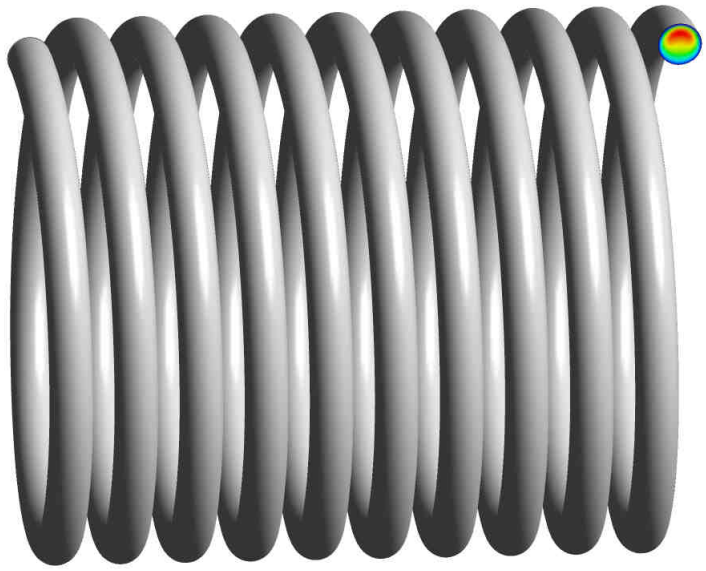

**Figure 53.** Simulated reactor setup (PTFE-PFR I) for CFD calculations

The mesh grid consists of approximately $1.2 \cdot 10^6$ cells; partially shown in Figure 54. Laminary flow conditions (Re << 2300) and the physical properties of THF (viscous Newtonian fluid) were used.

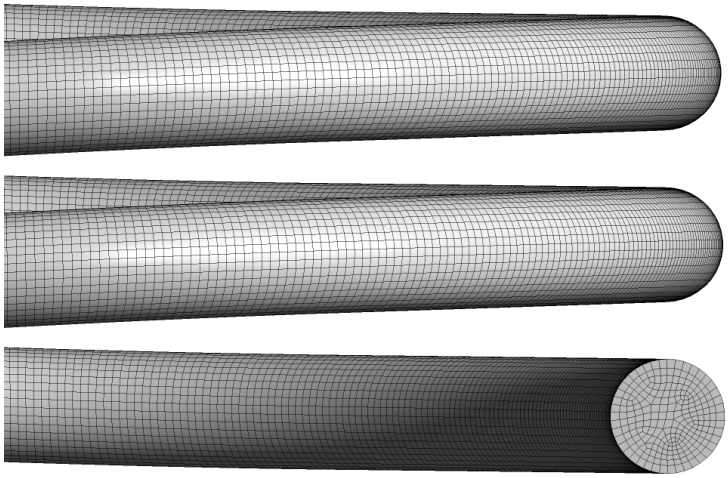

**Figure 54.** Mesh grid of the simulated reactor (PTFE-PFR I) for CFD simulations

Figure 55 shows the cross section of PTFE-PFR I for the flow rate of $F_V$ = 1.50 mL min$^{-1}$, $F_V$ = 3.00 mL min$^{-1}$, $F_V$ = 5.00 mL min$^{-1}$ and $F_V$ = 7.50 mL min$^{-1}$. The flow rate values were fixed in accordance with polymerization experiments.

At $F_V$ = 1.50 mL min$^{-1}$ the fluid flow generally equals basic laminary flow conditions, with the maximum flow velocity (orange-red) in the center of the reactor. The flow rate decreases radially towards the reactor wall (yellow, green, light blue, blue are representing the negative trend). However, a secondary flow field is induced by centrifugal forces; the inner stream filaments flowing outwards from the right to the left hand side, as represented by vectors. For this reason the maximum velocity is shifted to the outside (left hand side) with increasing flow rate. At $F_V$ = 3.00 mL min$^{-1}$ (De = 27) two toroidal eddies are formed and the flux is unstable. In this region axial backmixing affects the fluid flow and Bo-number is expected to decrease.

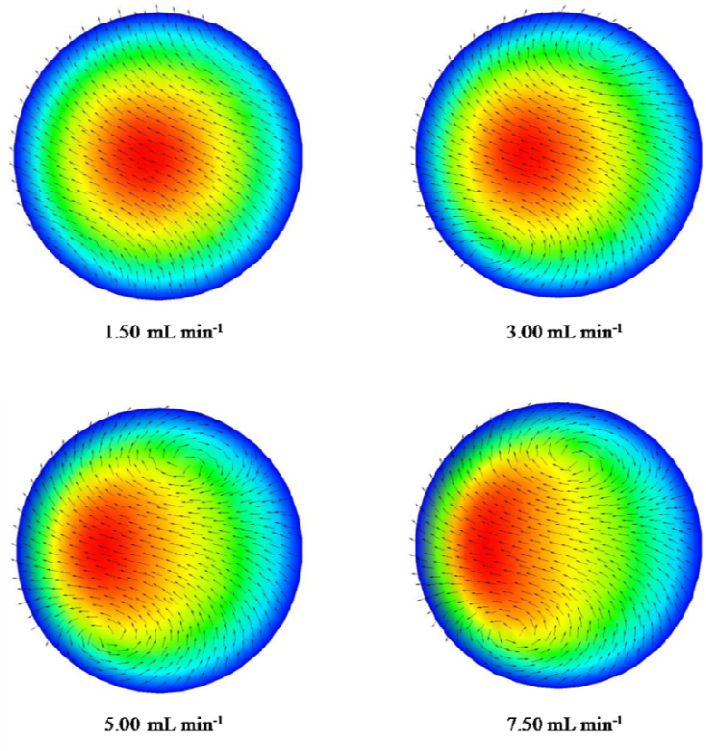


**Figure 55.** CFD simulations of fluid flow in the experimental setup PTFE-PFR I coiled up a central tube diameter of $D_O$ = 2.0 cm and flow rate of $F_V$ = 1.5 mL min$^{-1}$ to $F_V$ = 7.5 mL min$^{-1}$

The CFD-calculations were extended to higher flow rate (up to $F_V$ = 30.00 mL min$^{-1}$) as shown in Figure 56. The maximum flow velocity is shifted closer to the reactor wall and, starting at 10.00 mL min$^{-1}$, the velocity profile becomes U-shaped. However, this flow range simulation does not indicate additional eddies or instabilities. Hence, an increase of the Bo-number is expected. This assumption was validated with a turbulence model (Reynolds stress), which is strictly spoken not valid for the investigated flow regime.

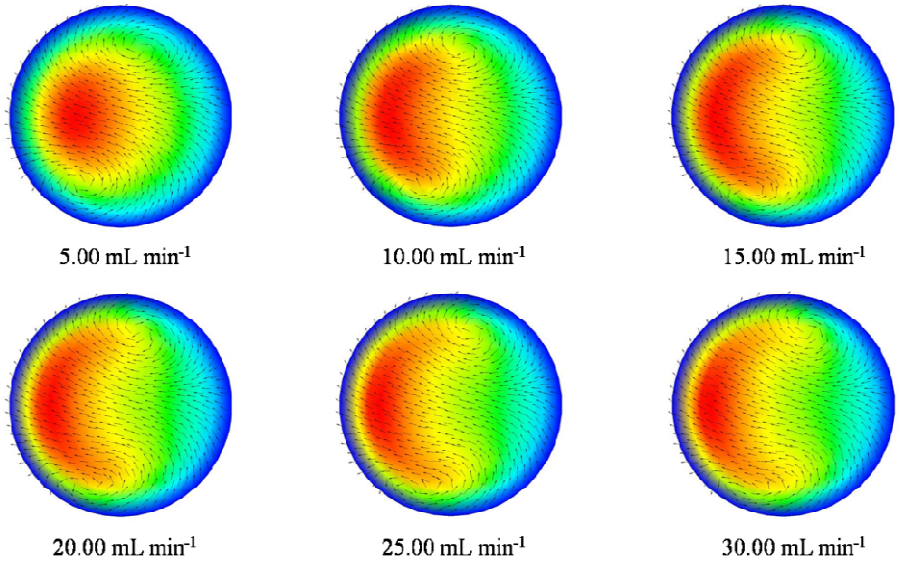


**Figure 56.** CFD simulations of fluid flow in the experimental setup PTFE-PFR I coiled up a central tube diameter of $D_O$ = 2.0 cm and flow rate of $F_V$ = 5.0 mL min$^{-1}$ to $F_V$ = 30.0 mL min$^{-1}$

#### 5.4.3.5. Continuous ROP of $D_3$

The ROP of D3 was performed in two different PTFE-tubings: PTFE-PFR I and II. PTFE-PFR I was used to investigate the influence of the flow rate and the curvature on the PDMS chain length and the polydispersity. The termination reaction was performed in batch mode. The experimental setup PTFE-PFR II was used for comparison. This reactor has a three times larger reactor volume and the CTMS stock solution was continuously dispensed to the reaction solution.

##### 5.4.3.5.1. PTFE-PFR I

Figure 57 shows the experimental setup PTFE-PFR I for the continuous ROP of $D_3$. The monomer is delivered by an HPLC-pump and t-BuLi is dispensed by a syringe pump. The two fluxes are mixed in a T-connector at quasi-adiabatic conditions (see Chapter 5.4.3.2). The mixed fluxes enter the PTFE-PFR which is located in a temperature controlled water bath to obtain quasi-isothermal conditions. The ROP of $D_3$ was performed at T = 40°C. At the reactor outlet the reaction solution was rapidly cooled down to T ≤ -10°C to quench the polymerization reaction and to prevent mass loss in the sampling flask. Afterwards, samples of the reaction solution were taken and the PDMS chains were terminated in a CTMS stock solution in batch mode.

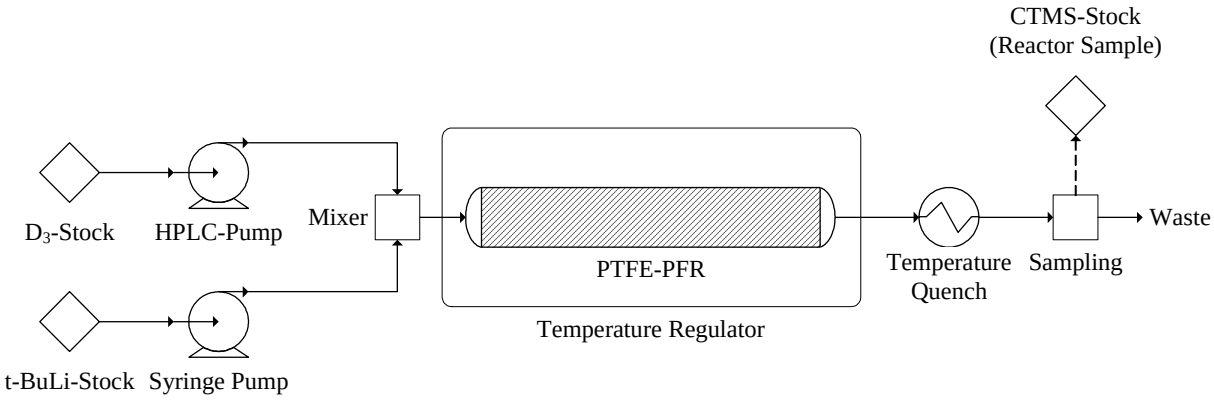


**Figure 57.** Flowsheet of the experimental setup PTFE-PFR I for the continuous ROP of $D_3$ initiated by t-BuLi and stopped by CTMS

The results of the continuous ROP of $D_3$ in PTFE-PFR I are summarized in Table 19; Re- and De-number were determined for flow conditions with pure THF at room temperature (25°C) because the RTD experiments and CFD calculations were performed under these conditions.

**Table 19.** Experimental results of the continuous ROP of $D_3$ in PTFE-PFR I

| $D_O$ / cm | $d_i^{0.5} D^{-0.5}$ / - | $F_V$ / mL min$^{-1}$ | Re / - | De / - | $M_n$ / g mol$^{-1}$ | PDI / - |
|---|---|---|---|---|---|---|
| 2.0 | 0.309 | 1.50 | 31 | 14 | 2680 | 1.243 |
| | | 3.00 | 62 | 27 | 1965 | 1.262 |
| | | 5.00 | 103 | 45 | 1520 | 1.227 |
| | | 7.50 | 155 | 68 | 1215 | 1.148 |
| 3.0 | 0.254 | 1.50 | 31 | 11 | 2825 | 1.230 |
| | | 3.00 | 62 | 22 | 1980 | 1.204 |
| | | 5.00 | 103 | 37 | 1433 | 1.181 |
| | | 7.50 | 155 | 56 | 1337 | 1.146 |
| 4.0 | 0.221 | 1.50 | 31 | 10 | 2850 | 1.179 |
| | | 3.00 | 62 | 19 | 2110 | 1.237 |
| | | 5.00 | 103 | 32 | 1560 | 1.189 |
| | | 7.50 | 155 | 48 | 1195 | 1.134 |

Figure 58 shows the correlation of $M_n$ from SEC measurements in dependence of the adjusted flow rate for the three different experimental setups of PTFE-PFR I ($D_O$ = 2.0 cm: squares, solid line; $D_O$ = 3.0 cm: circles, dotted line; $D_O$ = 4.0 cm: triangles, dashed line). As expected an exponential decay was observed; the molecular weight decreases with increasing flow rate. At low flow rate, the exponential fits show a higher dependence on the experimental setup. At high flow rate the fits are approximately the same.

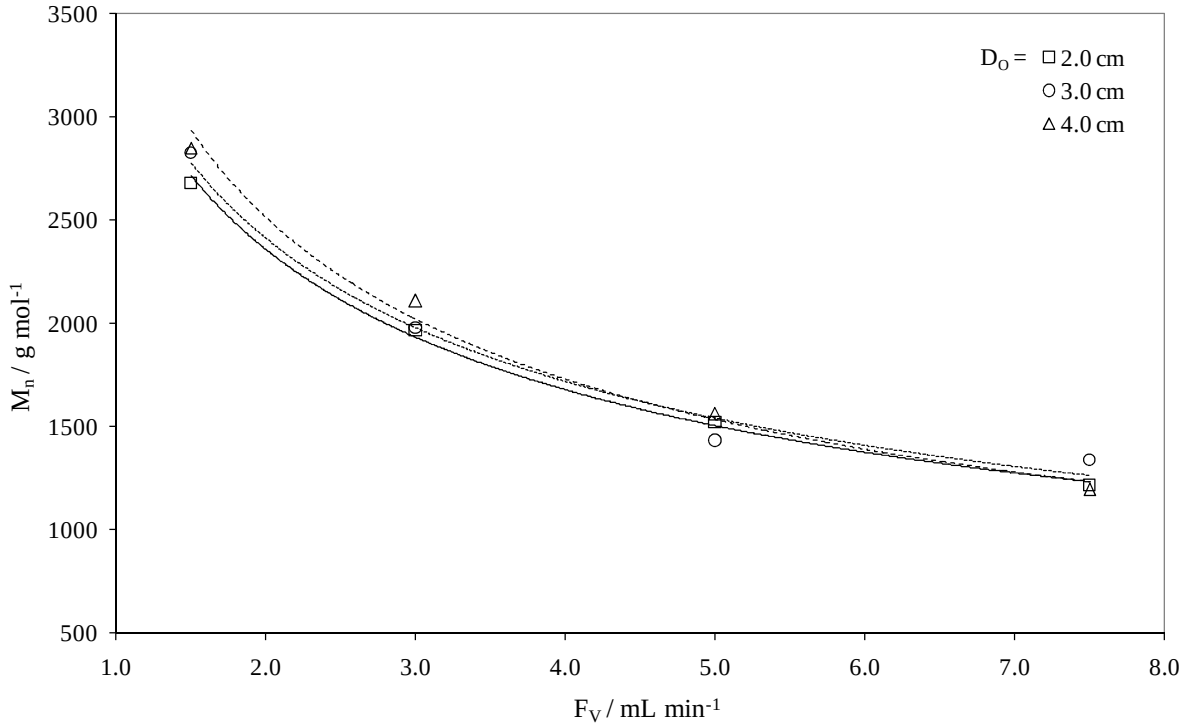


**Figure 58.** Results of the continuous ROP of $D_3$ in the experimental setup PTFE-PFR I: Molecular weight $M_n$ versus flow rate $F_V$ at different coiling diameters of the central tube $D_O$

Figure 59 shows the correlation of $M_n$ from SEC measurements in dependence on De-number of the three different experimental setups of PTFE-PFR I ($D_O$ = 2.0 cm: squares; $D_O$ = 3.0 cm: circles; $D_O$ = 4.0 cm: triangles). Furthermore, the corresponding flow rate, a linear trend for each flow velocity (dashed lines) and $De_{crit}$ = 54 (vertical grey dotted line) are mentioned.

In accordance with Figure 58, it can also be seen, that at low flow rate $M_n$ depends on the diameter of the central tube as shown by the trends which have a significant slope. The slope decreases with increasing flow rate. At a flow rate of $F_V$ = 7.5 mL min$^{-1}$ ($48 \leq De \leq 68$) the slope is horizontal and therefore, the effect of centrifugal force on the molecular weight becomes negligible. Even at flow rate of $F_V$ = 5.0 mL min$^{-1}$ ($32 \leq De \leq 45$) the slope is nearly horizontal which corresponds with the results from the CFD calculations (Chapter 5.4.3.4) which indicated toroidal eddy formation at flow rate of $F_V$ = 3.0 mL min$^{-1}$ (De = 27).

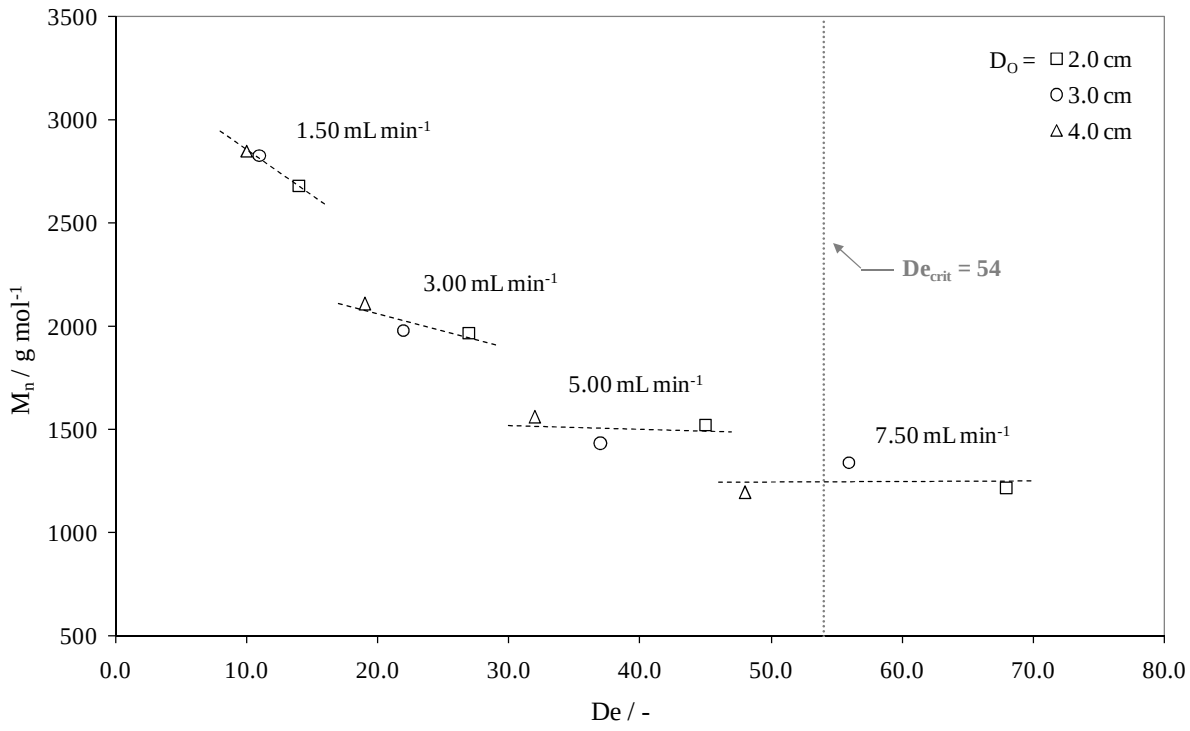


**Figure 59.** Results of the continuous ROP of $D_3$ in the experimental setup PTFE-PFR I: Molecular weight $M_n$ versus De-number at different coiling diameters of the central tube $D_O$ with different flow rates

The PDI of the PDMS chains depending on the flow rate of the three different experimental setups of PTFE-PFR I is shown in Figure 60 ($D_O$ = 2.0 cm: squares, solid line; $D_O$ = 3.0 cm: circles, dotted line; $D_O$ = 4.0 cm: triangles, dashed line). Linear fits are used to show the trend of the polydispersity which decreases with increasing flow rate. At high flow rate the PDMS chains approach uniform chain lengths.

These results do not correlate with the RTD experiments. Within the investigated flow range the Bo-number decreases with increasing flow rate (Chapter 5.4.3.3). Generally, polymers show low polydispersity at high Bo-number (insignificant or no back-mixing) and vice versa.

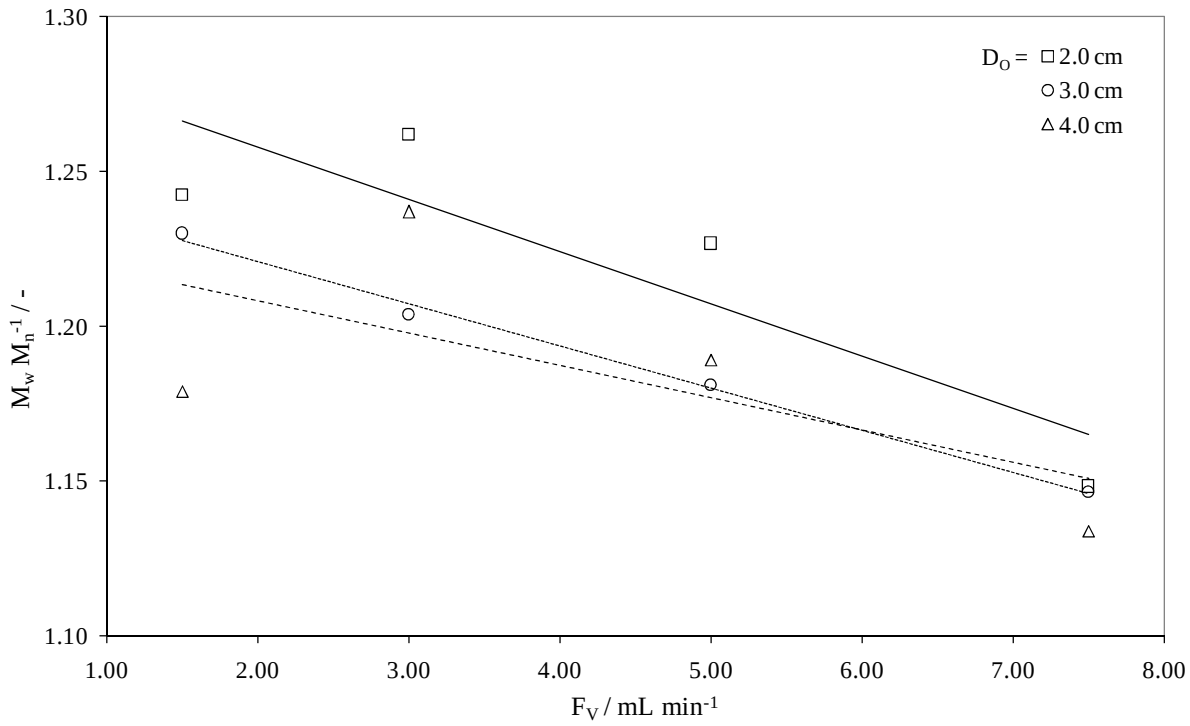


**Figure 60.** Results of the continuous ROP of $D_3$ in the experimental setup PTFE-PFR I: Molecular weight distribution (PDI) versus flow rate ($F_V$) at different coiling diameters of the central tube $D_O$

Table 20 shows the theoretical molecular mass ($M_{th}$) calculated from the ideal PFR equation and the molecular mass calculated from the monomer conversion of the $^1$H NMR spectra ($M_{NMR}$ and $X_{NMR}$) for the experimental setup PTFE-PFR I coiled up a central tube diameter of $D_O$ = 4.0 cm in comparison the molecular mass of the SEC measurements ($M_n$).

**Table 20.** Results of $M_{th}$ from ideal PFR and $M_{NMR}$ from $^1$H NMR spectroscopy for PTFE-PFR I coiled up a central tube diameter of $D_O$ = 4.0 cm in comparison to $M_n$ from SEC

| $F_V$ / mL min$^{-1}$ | $M_{th}$ / g mol$^{-1}$ | $X_{NMR}$ / % | $M_{NMR}$ / g mol$^{-1}$ | $M_n$ / g mol$^{-1}$ |
|---|---|---|---|---|
| 1.50 | 2768 | 40.6 | 2390 | 2850 |
| 3.00 | 1827 | 34.1 | 2025 | 2110 |
| 5.00 | 1294 | 17.7 | 1112 | 1560 |
| 7.50 | 1000 | 7.5 | 547 | 1195 |

A comparison of the theoretical molecular weight (from ideal PFR equations, squares, solid line), calculated molecular weight from $^1$H NMR spectroscopy (circles, dotted line) and measured $M_n$ from SEC (triangles, dashed line) for a central coiling diameter of $D_O$ = 4.0 cm is illustrated in Figure 61.

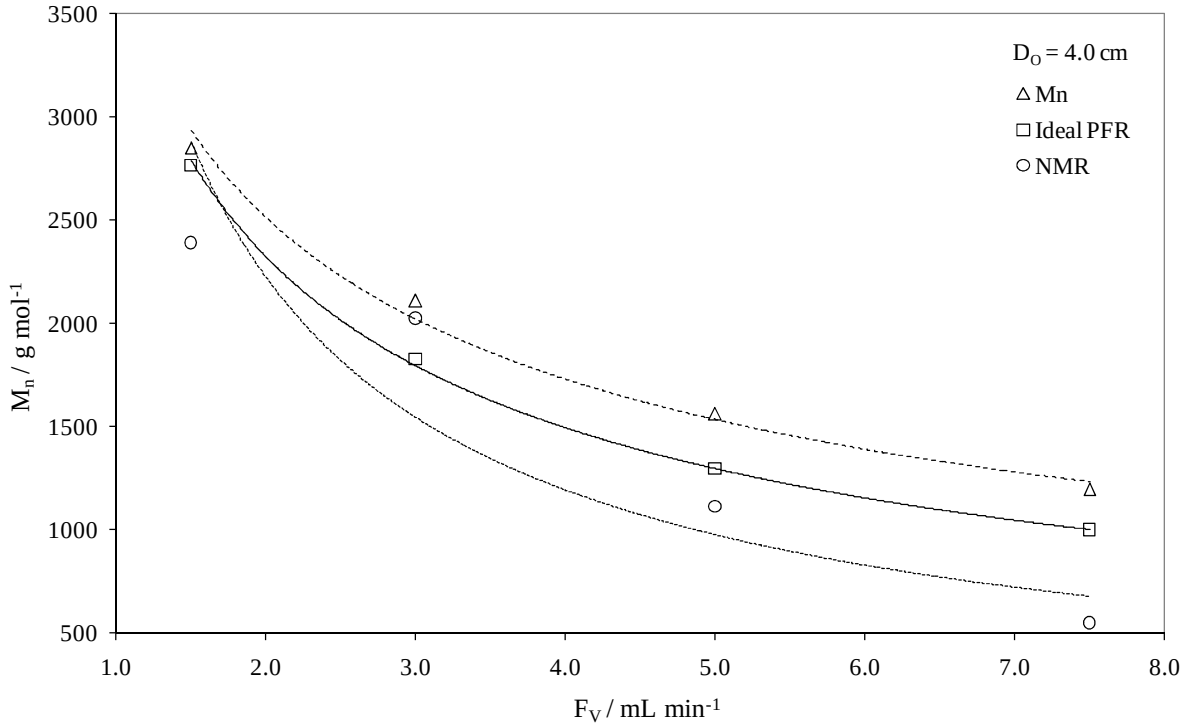


**Figure 61.** Comparison of the molecular weights from ideal PFR, from $^1$H NMR and $M_n$ from SEC of PTFE-PFR I coiled up a central tube diameter of $D_O$ = 4.0 cm

Both, the theoretical (ideal PFR) and the calculated (NMR) molecular weights underestimate the effective measured PDMS chain lengths from SEC measurements. The deviation of $M_n$ from the ideal PFR calculation is basically insignificant and within the experimental error. It is assumed that the deviation of the NMR data results from a mass loss of the internal standard benzene in the sampling flask. The monomer concentration appears to be higher when the benzene concentration is decreased and therefore the calculated chain length is shorter.

#### 5.4.3.5.2. PTFE-PFR II

Figure 62 shows the experimental setup PTFE-PFR II for the continuous ROP of $D_3$. The reactor volume of PTFE-PFR II is three times larger than PTFE-PFR I; hence, the continuous polymerization can be performed with higher conversions. Additionally, the CTMS stock solution was continuously mixed to the reaction solution in a T-connector at the reactor outlet at quasi-adiabatic conditions. The dispensing of the monomer and initiator stock solutions was equal to PTFE-PFR I. The fluid flow was cooled down after the termination reaction to $T \leq -10$°C to prevent mass loss in the sampling flask.

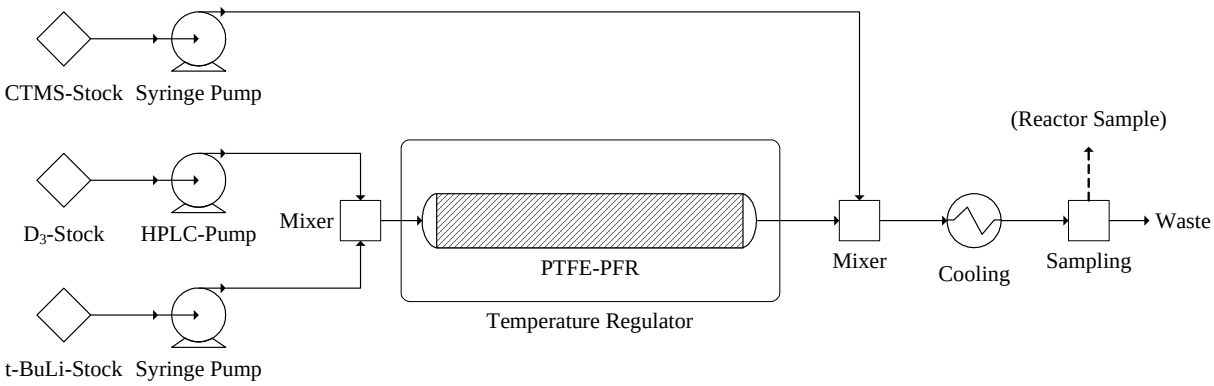


**Figure 62.** Flowsheet of the continuous ROP of $D_3$ initiated by t-BuLi and stopped by CTMS: PTFE-PFR II

The concentration profile and the number of Si-O units from polymerization in the ideal PFR (Figure 42: squares, solid line and triangles, dashed line) were modified to obtain a correlation for the range of the flow rate in the PTFE-PFR II experiments (Figure 63).

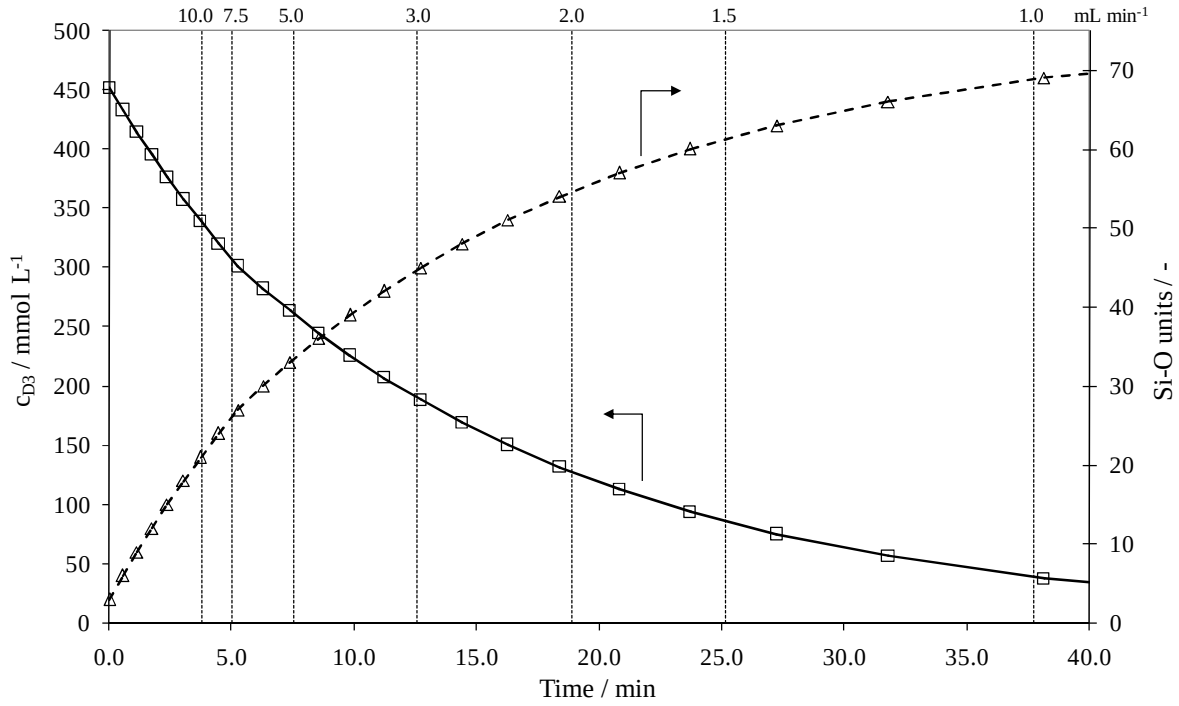


**Figure 63.** Concentration profile of monomer and PDMS repeating units (Si-O) for polymerization in ideal PTFE-PFR II in dependence on the mean residence time including the range of flow rate

The investigated flow rates ($F_V$) and the results of the continuous ROP of $D_3$ in PTFE-PFR II are given in Table 21. In addition, the central curvature diameter ($D_O$), the curvature ratio ($d_i^{0.5}\ D^{-0.5}$), Re- and De-number (*Re*, *De*) are shown. Re- and De-number were determined for pure THF at room temperature (25°C) because the RTD experiments and CFD calculations were performed under these conditions. A comparison with theoretical data (ideal PFR) and $^1$H NMR data in comparison to $M_n$ from SEC measurements is given in Table 22.

**Table 21.** Experimental results of the continuous ROP of $D_3$ in PTFE-PFR II

| $D_O$ / cm | $d_i^{0.5} D^{-0.5}$ / - | $F_V$ / mL min$^{-1}$ | Re / - | De / - | $M_n$ / g mol$^{-1}$ | PDI / - |
|---|---|---|---|---|---|---|
| 3.0 | 0.311 | 3.00 | 41 | 18 | 3777 | 1.157 |
| | | 10.00 | 138 | 61 | 1638 | 1.186 |

**Table 22.** $M_{th}$ from ideal PFR and $M_{NMR}$ from $^1$H NMR spectroscopy for PTFE-PFR II on $D_O$ = 3.0 cm

| $F_V$ / mL min$^{-1}$ | $M_{th}$ / g mol$^{-1}$ | $X_{NMR}$ / % | $M_{NMR}$ / g mol$^{-1}$ | $M_n$ / g mol$^{-1}$ |
|---|---|---|---|---|
| 3.00 | 1702 | 17.8 | 1119 | 3777 |
| 10.00 | 3446 | 53.1 | 3084 | 1638 |

A comparison of the theoretical molecular weight (from ideal PFR design equation, squares, solid line), calculated molecular weight from $^1$H NMR spectroscopy (circles, dotted line) and measured $M_n$ from SEC (triangles, dashed line) for $D_O$ = 3.0 cm is illustrated in Figure 64. The theoretical molecular weight (ideal PFR) is in accurate accordance to $M_n$ from SEC measurements. Again, the NMR data underestimate the experimental chain length (see PTFE-PFR I in Chapter 5.4.3.5.1). Again, a mass loss of the internal standard benzene in the sampling flask is assumed.

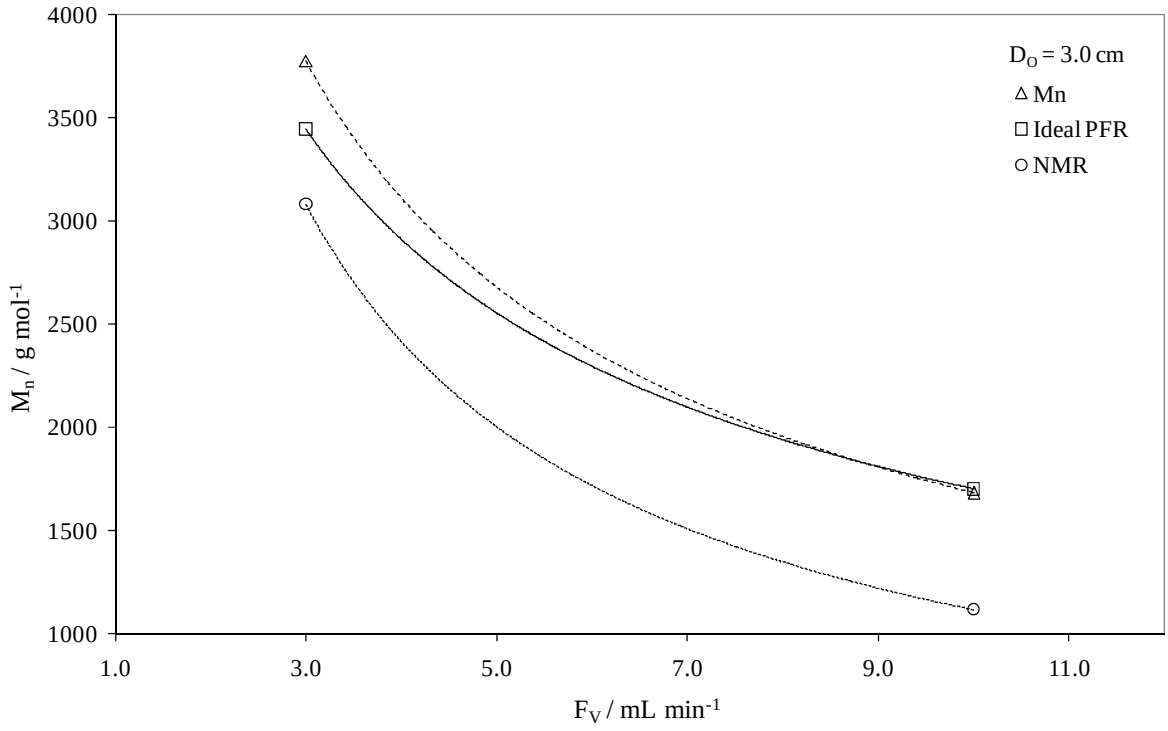


**Figure 64.** Comparison of the molecular weights from ideal PFR, from $^1$H NMR and $M_n$ from SEC of PTFE-PFR II coiled up a central tube diameter of $D_O$ = 3.0 cm

# 6. Summary

Target of this work was the development of a continuously operated reactor for the production of monofunctional oligo- and polysiloxanes from hexamethylcyclotrisiloxane ($D_3$). The polymerization is initiated by *tert*-butyllithium (t-BuLi) and stopped by chlorodimethylsilane (CDMS) in order to acquire the desired substance. The individual reactions – initiation-, propagation- and termination reaction – were kinetically and thermodynamically characterized for adequate scale-up.

The initiation and termination reaction are irreversible and rather exothermic. Latter property and the general hazardous risks of organolithium reagents are future key issues for operability and safety management in terms of a pilot plant.

Chain growth is best described by anionic ring-opening polymerization (ROP). The ROP is highly selective towards the monomer $D_3$ in respect to other cyclic oligosiloxanes. Side reactions such as backbiting or rearrangement reactions were found to be insignificant under the investigated reaction conditions. The propagation rate was divided into two sections, oligo- and polymerization. However, an overall rate of polymerization can be used for simplified reactor calculations. It was found that matrix ions may negatively influence the ion pair equilibrium and therefore decrease the rate of reaction. Hence, the choice of the reactor material may crucially influence the reactor's performance.

The PFR is the preferential type of reactor for ionic polymerization reactions. Thus, a PFR on lab scale consisting of PTFE-tubing was designed, modeled and operated with the collected data from investigation of kinetics and thermodynamics. The whole PFR was coiled up a central tube to induce radial mixing along the reactor due to Dean vortices. The effect of coiling on reactor hydraulics was confirmed by CFD calculations. Within the investigated flow range the Bo-number seemingly showed uncommon behavior as the value decreased with increasing flow rate. This effect is mainly caused by the effect of coiling on the flow pattern.

With the experimental setup, monofunctional polydimethylsiloxanes (PDMS) with a narrow molecular weight distribution ($PDI \leq 1.2$) were produced. The chain length of these substances was adjustable by altering the flow rate and therefore the residence time of the reaction solution. PDMS consisting of 15 to 50 Si-O units were produced according to the specification of the project target.

With the acquired knowledge, a pilot plant for the continuous production of monofunctional PDMS from the monomer $D_3$, using organolithium reagents as initiator and corresponding chlorosilanes as termination reagent, can be planned and adequately operated.

# 7. Experimental

Herein, the experimental procedures are described. All experiments were carried out under nitrogen atmosphere either using a drybox or standard Schlenk technique. All chemicals were extensively dried prior to use unless otherwise stated. Additional supportive information of the experiments may be found in Chapter 8.1.

## 7.1. Chemicals

Hexamethylcyclotrisiloxane ($D_3$) was received from ABCR (solid, 95 %) or GE Bayer Silicones in a liquid mixture (~ 10 %) with other cyclic and linear oligo- and polysiloxanes. These mixtures were distilled several times for purification. Quality was checked with $^{1}H$ and $^{29}Si$-INEPT NMR spectroscopy and GC/MS. Pure $D_3$ was stirred over $CaH_2$ for several hours at 80°C and distilled from the flask. Octamethylcyclotetrasiloxane ($D_4$) was obtained from the same liquid siloxane mixture from GE Bayer Silicones. Purification of $D_4$ was generally equal to $D_3$: distillation of $D_4$ was performed under reduced pressure.

*tert*-Butyllithium (t-BuLi) solution (1.6 M in pentane) was received from Acros Organics and used as received and stored at -20°C. Concentration was checked by titration according to Gilman.[67,68] The residual basic content was regularly checked and was assured to be at least less than 2 %.

Chlorodimethylsilane (CDMS) and chlorotrimethylsilane (CTMS) were received from ABCR (95 %). Both chlorosilanes were heated to reflux for several hours and distilled twice. Quality was checked by $^{1}H$ and $^{29}Si$-INEPT NMR spectroscopy.

Tetrahydrofurane (THF) was received from Acros Organics. The solvent was either deoxygenized and dried over molecular sieves in a commercial available apparatus from Innovative Technology Inc. or distilled from purple ketyl radical solution (sodium/benzophenone).

Benzene and alkanes were deoxygenized and dried over molecular sieves equal to THF.

Chloroform ($CHCl_3$) was received from Fisher Scientific (analytical reagent grade) and deuterochloroform ($CDCl_3$) from Aldrich or Deutero GmbH (both 99.8 % D). $CHCl_3$ was pre-dried over anhydrous $CaCl_2$ and heated to reflux with $P_2O_5$ for several hours and distilled from the flask. $CDCl_3$ was only dried by refluxing with $P_2O_5$ and subsequent distillation.

All metal compounds for matrix ion studies are commercially available substances either as pure metals or in hydrated form and converted according to standard methods.[69,70]

Methyl red and other dyes were used as received from Merck.

## 7.2. Kinetics and Thermodynamic Characterization

The kinetics and thermodynamic properties of a chemical reaction are essential for scale-up and further process development. The three elementary reactions – initiation, propagation and termination reaction – were separately characterized.

### 7.2.1. Initiation and Termination Reaction

The ROR of $D_3$ and $D_4$ initiated by t-BuLi in THF was kinetically and thermodynamically characterized. For the termination reaction only latter characterization was performed.

#### 7.2.1.1. Kinetics of the ROR of $D_3$ and $D_4$

The temperature of the reaction mixture was continuously recorded for each single experiment. The experiments were performed in a temperature window of -70°C to -45°C. 0.10 g $D_3$ (0.45 mmol, 1 eq) in 8.0 mL THF was cooled to the desired reaction temperature. 0.28 mL t-BuLi solution (0.45 mmol, 1 eq) was added slowly. The resulting temperature increase did not exceed more than 2 K; hence, isothermal conditions were maintained over the whole experiment. A mixture of 0.31 mL CDMS in 20.0 mL $CHCl_3$ was prepared. A 4.0 mL aliquot ($CHCl_3$: 49.7 mmol, 111 eq; CDMS: 0.56 mmol, 1.25 eq) of this solution was used to instantly stop the initiation reaction at a desired time of reaction. This procedure was repeated many times to get the corresponding conversion curve. The ratio of reacted to unreacted $D_3$ molecules was quantified by $^{1}H$ NMR spectroscopy. Qualitative analysis was performed by $^{29}Si$-INEPT NMR spectroscopy.

The same experimental procedure was repeated for the monomer $D_4$ instead of $D_3$; the temperature window for these experiments was extended to 25°C. No conversion could be detected in $^{1}H$ and $^{29}Si$ NMR spectroscopy.

Table 23 to Table 29 show the concentration profiles of the kinetic experiments of the ROR of $D_3$ initiated by t-BuLi in THF.

**Table 23.** ROR of $D_3$ at -40.8°C

| **-40.8°C** Time / h | $D_3$ / mmol $L^{-1}$ |
|---|---|
| 0 | 54.29 |
| 0.100 | 22.46 |
| 0.167 | 17.07 |
| 0.250 | 11.26 |
| 0.333 | 9.38 |
| 0.417 | 13.02 |
| 0.500 | 5.98 |
| 0.583 | 6.40 |
| 0.667 | 4.10 |
| 0.833 | 2.97 |
| 1.00 | 0.00 |

**Table 24.** ROR of $D_3$ at -45.3°C

| **-45.3°C** Time / h | $D_3$ / mmol $L^{-1}$ |
|---|---|
| 0 | 54.29 |
| 0.075 | 31.27 |
| 0.167 | 25.84 |
| 0.250 | 16.73 |
| 0.317 | 15.42 |
| 0.333 | 17.64 |
| 0.500 | 12.29 |
| 0.583 | 6.84 |
| 0.583 | 6.93 |
| 0.75 | 4.58 |
| 1.00 | 4.43 |
| 1.00 | 3.23 |
| 1.17 | 0.00 |

**Table 25.** ROR of $D_3$ at -50.7°C

| **-50.7°C** Time / h | $D_3$ / mmol $L^{-1}$ |
|---|---|
| 0 | 54.29 |
| 0.083 | 38.93 |
| 0.167 | 29.13 |
| 0.250 | 24.29 |
| 0.333 | 22.70 |
| 0.500 | 16.90 |
| 0.500 | 15.24 |
| 0.500 | 17.35 |
| 0.667 | 12.27 |
| 0.833 | 11.52 |
| 1.00 | 7.30 |
| 1.33 | 7.77 |
| 1.67 | 4.80 |
| 2.00 | 5.49 |
| 2.50 | 0.00 |

**Table 26.** ROR of $D_3$ at -50.8°C

| **-50.8°C** Time / h | $D_3$ / mmol $L^{-1}$ |
|---|---|
| 0 | 54.29 |
| 0.033 | 38.36 |
| 0.083 | 29.46 |
| 0.167 | 24.12 |
| 0.250 | 22.26 |
| 0.500 | 15.11 |
| 0.750 | 11.21 |
| 1.00 | 10.03 |
| 1.20 | 8.40 |
| 1.40 | 6.12 |
| 1.50 | 6.39 |
| 1.60 | 6.14 |
| 1.80 | 5.17 |
| 2.00 | 3.77 |
| 2.20 | 3.93 |
| 2.50 | 2.94 |
| 3.00 | 2.94 |
| 12.0 | 0.00 |

**Table 27.** ROR of $D_3$ at -55.5°C

| **-55.5°C** Time / h | $D_3$ / mmol $L^{-1}$ |
|---|---|
| 0 | 54.29 |
| 0.250 | 32.68 |
| 0.500 | 21.49 |
| 0.750 | 18.07 |
| 1.00 | 13.31 |
| 1.25 | 14.19 |
| 1.50 | 9.77 |
| 1.75 | 9.31 |
| 2.00 | 5.83 |
| 3.00 | 5.84 |

**Table 28.** ROR of $D_3$ at -60.6°C

| **-60.6°C** Time / h | $D_3$ / mmol $L^{-1}$ |
|---|---|
| 0 | 54.29 |
| 0.500 | 30.17 |
| 1.00 | 21.93 |
| 1.50 | 18.25 |
| 2.00 | 12.73 |
| 2.50 | 12.21 |
| 3.00 | 9.58 |
| 5.00 | 4.69 |
| 8.00 | 3.06 |

**Table 29.** ROR of $D_3$ at -70.0°C

| **-70.0°C** Time / h | $D_3$ / mmol $L^{-1}$ |
|---|---|
| 0 | 54.29 |
| 1.00 | 34.77 |
| 1.50 | 29.15 |
| 2.00 | 25.44 |
| 2.50 | 23.51 |
| 3.00 | 24.43 |
| 4.00 | 19.09 |
| 6.00 | 12.22 |
| 8.00 | 10.10 |

#### 7.2.1.2. Thermodynamics of the ROR of $D_3$ and Termination Reaction

All experiments were carried out in a Dewar vessel under adiabatic conditions. The temperature of the reaction solution was continuously recorded. 3.00 g $D_3$ (13.5 mmol, 1 eq) was dissolved in 150.0 mL THF. The $D_3$-THF mixture was cooled to a certain temperature between -20°C to -5°C. Afterwards 8.4 mL of t-BuLi solution (13.5 mmol, 1 eq) was slowly added. The solution was stirred for at least 30 min assuring the completion of the initiation reaction. In the end 1.5 mL CDMS (13.5 mmol, 1 eq) was slowly added and the solution was stirred for another 30 min. $^{1}H$ and $^{29}Si$-INEPT NMR spectroscopy was used for qualitative and quantitative analysis.

### 7.2.2. Propagation Reaction

In this section all experimental details for the characterization of the kinetics and thermodynamic properties of the propagation reaction are described. First, product characterization and comparison of the analytical methods were performed. With this data, kinetics of the propagation reaction in dependence on the molar ratio of $D_3$ to t-BuLi was investigated.

#### 7.2.2.1. Polymer Characterization and Analytics

A solution consisting of 6.00 g $D_3$ (27.0 mmol, 31 eq) and 2.40 mL benzene (27.0 mmol, 31 eq) in 50.0 mL THF was cooled to 0°C. 0.54 mL t-BuLi solution (0.86 mmol, 1 eq) was slowly added. After stirring for 7.0 h at 0°C, 0.12 mL CTMS (0.94 mmol, 1.1 eq) was added to stop the ROP and stirred for another 0.5 h. A sample for $^{1}H$ and $^{29}Si$ NMR spectroscopy was taken and afterwards all volatiles were vacuum evaporated for several hours at 40°C. The residue, a colorless oily liquid with a white precipitate, was centrifuged at 5000 rpm for > 30 min and the clear liquid phase was used for further analyses. $^{1}H$ NMR spectroscopy of the reaction solution, SEC and gravimetric analyses of the product were performed for calculation of the monomer conversion and comparison of these methods. The product was further characterized by $^{1}H$, $^{29}Si$ NMR spectroscopy, viscosity, density and MALDI-TOF-MS measurements.

#### 7.2.2.2. Kinetics of the Propagation Reaction

##### 7.2.2.2.1. Molar Ratio of $D_3$ : t-BuLi = 2 : 1

*Reaction:* The temperature of the reaction mixture was continuously recorded for each single experiment to ensure that isothermal conditions were maintained throughout the experiment. The experiments were performed in a temperature window of -10°C to 30°C. 0.20 g $D_3$ (0.90 mmol, 2 eq) in 8.0 mL THF was cooled to the desired reaction temperature. 0.28 mL t-BuLi solution (0.45 mmol, 1 eq) was slowly added. *Sampling:* A mixture of 0.1 mL CDMS (85.5 mg, 0.90 mmol) in 20.0 mL $CDCl_3$ was prepared. A 0.6 mL to 1.0 mL aliquot of this solution (CDMS: 0.027 mmol to 0.045 mmol, $\geq$ 4 eq) was filled in an NMR tube. A cooled syringe (-20°C) was used to take a < 0.1 mL sample of the reaction solution (max. 0.006 mmol t-BuLi initiated chains, 1 eq) which was immediately quenched in the prepared NMR tube at desired reaction times. The ratio of reacted to unreacted $D_3$ molecules was quantified by $^{1}H$ NMR spectroscopy. Qualitative analysis was performed by $^{29}Si$-INEPT NMR spectroscopy.

Table 30 to Table 39 show the concentration profiles of the kinetic experiments of the ROP of $D_3$ initiated by t-BuLi in THF with a molar ratio of 2 : 1.

**Table 30.** ROP of $D_3$ (2:1) at -10.0°C

| **-10.0°C** Time / h | $D_3$ / mmol $L^{-1}$ |
|---|---|
| 0 | 108.6 |
| 0.500 | 27.8 |
| 1.00 | 26.9 |
| 1.50 | 26.5 |
| 2.00 | 24.9 |
| 3.00 | 23.5 |
| 4.00 | 21.7 |
| 5.00 | 19.8 |
| 6.00 | 18.8 |
| 8.00 | 15.2 |
| 10.0 | 13.0 |
| 12.0 | 10.4 |
| 24.0 | 4.5 |

**Table 31.** ROP of $D_3$ (2:1) at -0.79°C

| **-0.79°C** Time / h | $D_3$ / mmol $L^{-1}$ |
|---|---|
| 0 | 210.1 |
| 0.500 | 59.9 |
| 1.00 | 50.9 |
| 2.00 | 41.0 |
| 4.00 | 25.6 |
| 6.00 | 18.0 |
| 8.00 | 11.3 |

**Table 32.** ROP of $D_3$ (2:1) at 0.0°C

| **0.0°C** Time / h | $D_3$ / mmol $L^{-1}$ |
|---|---|
| 0 | 108.6 |
| 0.250 | 47.4 |
| 0.500 | 45.1 |
| 0.750 | 43.6 |
| 1.00 | 40.9 |
| 1.50 | 38.7 |
| 2.00 | 31.9 |
| 3.00 | 28.6 |
| 4.00 | 22.2 |
| 5.00 | 17.9 |
| 6.00 | 15.0 |
| 7.00 | 11.5 |
| 8.00 | 6.2 |

**Table 33.** ROP of $D_3$ (2:1) at 10.1°C

| **10.1°C** Time / h | $D_3$ / mmol $L^{-1}$ |
|---|---|
| 0 | 108.6 |
| 0.250 | 35.8 |
| 0.500 | 30.3 |
| 0.750 | 26.0 |
| 1.00 | 24.0 |
| 1.50 | 20.3 |
| 2.00 | 13.9 |
| 3.00 | 10.7 |
| 4.00 | 6.3 |

**Table 34.** ROP of $D_3$ (2:1) at 14.8°C

| **14.8°C** Time / h | $D_3$ / mmol $L^{-1}$ |
|---|---|
| 0 | 108.6 |
| 0.083 | 37.7 |
| 0.167 | 34.3 |
| 0.330 | 31.8 |
| 0.500 | 28.1 |
| 0.750 | 24.0 |
| 1.00 | 18.4 |
| 1.33 | 15.1 |
| 1.67 | 11.9 |
| 2.33 | 8.4 |
| 3.00 | 5.8 |

**Table 35.** ROP of $D_3$ (2:1) at 14.9°C

| **14.9°C** Time / h | $D_3$ / mmol $L^{-1}$ |
|---|---|
| 0 | 108.6 |
| 0.250 | 32.3 |
| 0.500 | 26.8 |
| 0.750 | 23.6 |
| 1.00 | 20.8 |
| 1.50 | 13.9 |
| 2.00 | 10.2 |
| 2.50 | 6.9 |

**Table 36.** ROP of $D_3$ (2:1) at 19.9°C

| **19.9°C** Time / h | $D_3$ / mmol $L^{-1}$ |
|---|---|
| 0 | 108.6 |
| 0.167 | 38.5 |
| 0.333 | 34.1 |
| 0.500 | 25.5 |
| 0.667 | 20.8 |
| 0.833 | 19.9 |
| 1.00 | 15.7 |
| 1.33 | 13.3 |
| 1.67 | 7.7 |
| 2.00 | 5.9 |
| 2.50 | 3.8 |
| 3.00 | 3.1 |

**Table 37.** ROP of $D_3$ (2:1) at 24.8°C

| **24.8°C** Time / h | $D_3$ / mmol $L^{-1}$ |
|---|---|
| 0 | 108.6 |
| 0.033 | 39.2 |
| 0.083 | 37.1 |
| 0.167 | 31.6 |
| 0.250 | 28.4 |
| 0.333 | 25.8 |
| 0.417 | 21.7 |
| 0.500 | 19.8 |
| 0.667 | 15.3 |
| 0.833 | 11.6 |
| 1.00 | 10.5 |

**Table 38.** ROP of $D_3$ (2:1) at 29.8°C

| **29.8°C** Time / h | $D_3$ / mmol $L^{-1}$ |
|---|---|
| 0 | 108.6 |
| 0.033 | 40.9 |
| 0.083 | 36.1 |
| 0.167 | 29.5 |
| 0.250 | 26.8 |
| 0.330 | 21.1 |
| 0.417 | 20.1 |
| 0.500 | 15.3 |
| 0.667 | 11.3 |
| 0.833 | 8.6 |
| 1.00 | 6.5 |

**Table 39.** ROP of $D_3$ (2:1) at 30.4°C

| **30.4°C** Time / h | $D_3$ / mmol $L^{-1}$ |
|---|---|
| 0 | 108.6 |
| 0.033 | 34.7 |
| 0.067 | 32.4 |
| 0.100 | 30.0 |
| 0.133 | 28.2 |
| 0.167 | 25.8 |
| 0.250 | 18.9 |
| 0.333 | 15.8 |
| 0.417 | 13.0 |

#### 7.2.2.2.2. Molar Ratio of $D_3$ : t-BuLi = 4 : 1

*Reaction:* The temperature of the reaction mixture was continuously recorded for each single experiment to ensure that isothermal conditions were maintained throughout the experiment. The experiments were performed in a temperature window of 10°C to 30°C. For preparation of a monomer stock solution 27.05 g $D_3$ (121.6 mmol, 1 eq) and 10.8 mL benzene (9.5 g, 121.6 mmol, 1 eq) was put in a 100 mL volumetric flask and filled up with THF. A 2.0 mL aliquot of the monomer stock solution ($D_3$: 541 mg, 2.43 mmol, 4 eq; benzene: 0.216 mL, 0.19 g, 2.43 mmol, 4 eq) was put into a Schlenk flask and diluted with 8.0 mL THF. The temperature of the reaction solution was adjusted to the desired reaction temperature. 0.38 mL t-BuLi solution (0.61 mmol, 1 eq) was slowly added. *Sampling:* A quench stock solution containing 0.1 mL CTMS (85.4 mg, 0.79 mmol) in 5.0 mL $CDCl_3$ was prepared. A 0.6 mL aliquot of the quench stock solution (CTMS: 0.094 mmol, ≥ 15 eq) was filled in an NMR tube. A cooled syringe (-20°C) was used to take a < 0.1 mL sample of the reaction solution (max. 0.006 mmol t-BuLi initiated chains, 1 eq) which was immediately quenched in the prepared NMR tube at desired reaction times. The amount of unreacted $D_3$ molecules was quantified by $^{1}H$ NMR spectroscopy using benzene as the internal standard. Qualitative analysis was performed by $^{29}Si$-INEPT NMR spectroscopy.

Table 40 to Table 42 show the concentration profiles of the kinetic experiments of the ROP of $D_3$ initiated by t-BuLi in THF with a molar ratio of 4 : 1.

**Table 40.** ROP of $D_3$ (4:1) at 10.0°C

| **10.0°C** Time / h | $D_3$ / mmol $L^{-1}$ |
|---|---|
| 0 | 234.3 |
| 0.500 | 120.9 |
| 1.00 | 91.1 |
| 1.50 | 82.8 |
| 2.00 | 62.9 |
| 2.50 | 41.4 |
| 3.00 | 32.3 |
| 4.00 | 19.9 |
| 6.00 | 74.5 |

**Table 41.** ROP of $D_3$ (4:1) at 20.0°C

| **20.0°C** Time / h | $D_3$ / mmol $L^{-1}$ |
|---|---|
| 0 | 234.3 |
| 0.333 | 119.2 |
| 0.667 | 68.4 |
| 1.00 | 43.5 |
| 1.50 | 30.6 |
| 2.00 | 14.5 |
| 2.50 | 9.7 |
| 3.00 | 6.4 |

**Table 42.** ROP of $D_3$ (4:1) at 30.0°C

| **30.0°C** Time / h | $D_3$ / mmol $L^{-1}$ |
|---|---|
| 0 | 234.3 |
| 0.333 | 66.5 |
| 0.500 | 40.1 |
| 0.667 | 31.9 |
| 1.00 | 15.5 |
| 1.33 | 8.2 |
| 1.67 | 3.6 |

#### 7.2.2.2.3. Molar Ratio of $D_3$ : t-BuLi = 7 : 1

*Reaction:* The temperature of the reaction mixture was continuously recorded for each single experiment to ensure that isothermal conditions were maintained throughout the experiment. The experiments were performed in a temperature window of 0°C to 30°C. For preparation of a monomer stock solution 27.05 g $D_3$ (121.6 mmol, 1 eq) and 10.8 mL benzene (9.5 g, 121.6 mmol, 1 eq) was put in a 100 mL volumetric flask and filled up with THF. A 3.0 mL aliquot of the monomer stock solution ($D_3$: 812 mg, 3.65 mmol, 7 eq; benzene: 0.324 mL, 0.28 g, 3.65 mmol, 7 eq) was put into a Schlenk flask and diluted with 7.0 mL THF. The temperature of the reaction solution was adjusted to the desired reaction temperature. 0.33 mL t-BuLi solution (0.52 mmol, 1 eq) was slowly added. *Sampling:* A quench stock solution containing 0.1 mL CTMS (85.4 mg, 0.79 mmol) in 5.0 mL $CDCl_3$ was prepared. A 0.6 mL aliquot of the quench stock solution (CTMS: 0.094 mmol, ≥ 15 eq) was filled in an NMR tube. A cooled syringe (-20°C) was used to take a < 0.1 mL sample of the reaction solution (max. 0.005 mmol t-BuLi initiated chains, 1 eq) which was immediately quenched in the prepared NMR tube at desired reaction times. The amount of unreacted $D_3$ molecules was quantified by $^{1}H$ NMR spectroscopy using benzene as the internal standard. Qualitative analysis was performed by $^{29}Si$-INEPT NMR spectroscopy.

Table 43 to Table 46 show the concentration profiles of the kinetic experiments of the ROP of $D_3$ initiated by t-BuLi in THF with a molar ratio of 7 : 1.

**Table 43.** ROP of $D_3$ (7:1) at 0.0°C

| **0.0°C** Time / h | $D_3$ / mmol $L^{-1}$ |
|---|---|
| 0 | 353.1 |
| 0.500 | 295.4 |
| 1.00 | 280.0 |
| 2.00 | 243.4 |
| 3.00 | 194.2 |
| 4.00 | 151.9 |
| 6.00 | 108.3 |
| 9.00 | 46.4 |
| 12.0 | 26.7 |

**Table 44.** ROP of $D_3$ (7:1) at 10.0°C

| **10.0°C** Time / h | $D_3$ / mmol $L^{-1}$ |
|---|---|
| 0 | 353.1 |
| 0.500 | 248.7 |
| 1.00 | 193.0 |
| 1.50 | 148.7 |
| 2.00 | 120.4 |
| 3.00 | 76.1 |
| 4.00 | 47.7 |
| 6.00 | 17.0 |
| 8.00 | 6.8 |

**Table 45.** ROP of $D_3$ (7:1) at 20.0°C

| **20.0°C** Time / h | $D_3$ / mmol $L^{-1}$ |
|---|---|
| 0 | 353.1 |
| 0.333 | 208.3 |
| 0.667 | 138.9 |
| 1.00 | 87.4 |
| 1.50 | 51.5 |
| 2.00 | 32.3 |
| 2.50 | 19.2 |
| 3.00 | 9.6 |
| 4.00 | 3.6 |

**Table 46.** ROP of $D_3$ (7:1) at 30.0°C

| **30.0°C** Time / h | $D_3$ / mmol $L^{-1}$ |
|---|---|
| 0 | 353.1 |
| 0.167 | 195.1 |
| 0.333 | 132.9 |
| 0.500 | 99.4 |
| 0.667 | 62.2 |
| 1.00 | 29.9 |
| 1.33 | 15.6 |
| 1.67 | 8.4 |
| 2.00 | 3.6 |

#### 7.2.2.2.4. Molar Ratio of $D_3$ : t-BuLi = 10 : 1

*Reaction:* The temperature of the reaction mixture was continuously recorded for each single experiment to ensure that isothermal conditions were maintained throughout the experiment. The experiments were performed in a temperature window of 0°C to 30°C. For preparation of a monomer stock solution 27.05 g $D_3$ (121.6 mmol, 1 eq) and 10.8 mL benzene (9.5 g, 121.6 mmol, 1 eq) was put in a 100 mL volumetric flask and filled up with THF. A 5.0 mL aliquot of the monomer stock solution ($D_3$: 1.35 g, 6.08 mmol, 10 eq; benzene: 0.54 mL, 0.48 g, 6.08 mmol, 10 eq) was put into a Schlenk flask and diluted with 5.0 mL THF. The temperature of the reaction solution was adjusted to the desired reaction temperature. 0.38 mL t-BuLi solution (0.61 mmol, 1 eq) was slowly added. *Sampling:* A quench stock solution containing 0.1 mL CTMS (85.4 mg, 0.79 mmol) in 5.0 mL $CDCl_3$ was prepared. A 0.6 mL aliquot of the quench stock solution (CTMS: 0.094 mmol, ≥ 15 eq) was filled in an NMR tube. A cooled syringe (-20°C) was used to take a < 0.1 mL sample of the reaction solution (max. 0.006 mmol t-BuLi initiated chains, 1 eq) which was immediately quenched in the prepared NMR tube at desired reaction times. The amount of unreacted $D_3$ molecules was quantified by $^{1}H$ NMR spectroscopy using benzene as the internal standard. Qualitative analysis was performed by $^{29}Si$-INEPT NMR spectroscopy. Alternatively, the same procedure was repeated using 2.0 mL of the monomer stock solution ($D_3$: 541 mg, 2.43 mmol, 10 eq; benzene: 0.216 mL, 0.19 g, 2.43 mmol, 10 eq) diluted with 8.0 mL THF and initiated by 0.15 mL t-BuLi solution (0.24 mmol, 1 eq) at 10°C.

Table 47 to Table 50 show the concentration profiles of the kinetic experiments of the ROP of $D_3$ initiated by t-BuLi in THF with a molar ratio of 10 : 1.

**Table 47.** ROP of $D_3$ (10:1) at 0.0°C

| **0.0°C** Time / h | $D_3$ / mmol $L^{-1}$ |
|---|---|
| 0 | 585.7 |
| 0.500 | 371.0 |
| 1.00 | 322.9 |
| 2.00 | 259.8 |
| 3.00 | 229.8 |
| 4.00 | 187.7 |
| 6.00 | 123.2 |
| 8.00 | 79.6 |
| 10.0 | 61.6 |

**Table 48.** ROP of $D_3$ (10:1) at 10.0°C

| **10.0°C** Time / h | $D_3$ / mmol $L^{-1}$ |
|---|---|
| 0 | 585.7 |
| 0.500 | 420.7 |
| 1.00 | 340.2 |
| 1.50 | 263.7 |
| 2.00 | 219.4 |
| 3.00 | 132.8 |
| 4.00 | 825.2 |
| 6.00 | 322.0 |
| 8.00 | 120.8 |

**Table 49.** ROP of $D_3$ (10:1) at 10.0°C

| **10.0°C** Time / h | $D_3$ / mmol $L^{-1}$ |
|---|---|
| 0 | 239.6 |
| 0.500 | 155.0 |
| 1.00 | 132.4 |
| 1.50 | 112.3 |
| 2.00 | 81.3 |
| 3.00 | 55.3 |
| 4.00 | 33.5 |
| 6.00 | 14.2 |
| 8.00 | 6.7 |

**Table 50.** ROP of $D_3$ (10:1) at 30.0°C

| **30.0°C** Time / h | $D_3$ / mmol $L^{-1}$ |
|---|---|
| 0 | 585.7 |
| 0.250 | 304.2 |
| 0.500 | 204.9 |
| 0.750 | 107.6 |
| 1.00 | 70.4 |
| 1.50 | 31.0 |
| 2.00 | 10.3 |

#### 7.2.2.2.5. Molar Ratio of $D_3$ : t-BuLi = 19 : 1

*Reaction:* The temperature of the reaction mixture was continuously recorded for each single experiment to ensure that isothermal conditions were maintained throughout the experiment. The experiments were performed in a temperature window of 0°C to 20°C. For preparation of a monomer stock solution 27.05 g $D_3$ (121.6 mmol, 1 eq) and 10.8 mL benzene (9.5 g, 121.6 mmol, 1 eq) was put in a 100 mL volumetric flask and filled up with THF. A 5.0 mL aliquot of the monomer stock solution ($D_3$: 1.35 g, 6.08 mmol, 19 eq; benzene: 0.54 mL, 0.48 g, 6.08 mmol, 19 eq) was put into a Schlenk flask and diluted with 5.0 mL THF. The temperature of the reaction solution was adjusted to the desired reaction temperature. 0.20 mL t-BuLi solution (0.32 mmol, 1 eq) was slowly added. *Sampling:* A quench stock solution containing 0.1 mL CTMS (85.4 mg, 0.79 mmol) in 5.0 mL $CDCl_3$ was prepared. A 0.6 mL aliquot of the quench stock solution (CTMS: 0.094 mmol, ≥ 20 eq) was filled in an NMR tube. A cooled syringe (-20°C) was used to take a < 0.1 mL sample of the reaction solution (max. 0.004 mmol t-BuLi initiated chains, 1 eq) which was immediately quenched in the prepared NMR tube at desired reaction times. The amount of unreacted $D_3$ molecules was

quantified by $^{1}H$ NMR spectroscopy using benzene as the internal standard. Qualitative analysis was performed by $^{29}Si$-INEPT NMR spectroscopy.

Table 51 to Table 53 show the concentration profiles of the kinetic experiments of the ROP of $D_3$ initiated by t-BuLi in THF with a molar ratio of 19 : 1.

**Table 51.** ROP of $D_3$ (19:1) at 0.0°C

| **0.0°C** Time / h | $D_3$ / mmol $L^{-1}$ |
|---|---|
| 0 | 596.1 |
| 0.500 | 548.9 |
| 1.00 | 518.2 |
| 2.00 | 419.9 |
| 3.00 | 374.8 |
| 4.00 | 305.2 |
| 6.00 | 223.3 |
| 9.00 | 122.9 |
| 12.0 | 71.7 |

**Table 52.** ROP of $D_3$ (19:1) at 20.0°C

| **20.0°C** Time / h | $D_3$ / mmol $L^{-1}$ |
|---|---|
| 0 | 596.1 |
| 0.500 | 358.4 |
| 1.00 | 257.8 |
| 1.50 | 141.0 |
| 2.00 | 84.6 |
| 3.00 | 30.2 |
| 4.00 | 14.1 |
| 5.00 | 6.0 |

**Table 53.** ROP of $D_3$ (19:1) at 20.0°C

| **20.0°C** Time / h | $D_3$ / mmol $L^{-1}$ |
|---|---|
| 0 | 596.1 |
| 1.50 | 110.6 |
| 2.00 | 65.5 |
| 2.50 | 51.2 |
| 3.00 | 20.5 |
| 4.00 | 12.3 |

#### 7.2.2.2.6. ROP of $D_3$: Further Kinetic Characterization

For additional characterization, the polymerization reaction of $D_3$ initiated by t-BuLi was carried out with addition of the monomer $D_4$ and under the influence of matrix ions. Furthermore, the ROP was characterized using the method of initial rates.

##### 7.2.2.2.6.1. ROP of $D_3$ from $D_3$-$D_4$-Mixtures

*Reaction:* The temperature of the reaction mixture was continuously recorded for each single experiment to ensure that isothermal conditions were maintained throughout the experiment. The two experiments were performed at 10°C and 15°C. For preparation of a monomer stock solution 2.00 g $D_3$ (8.99 mmol, 1 eq) and 2.67 g $D_4$ (8.99 mmol, 1 eq) was dissolved in 40 mL THF. A 12.0 mL aliquot of the monomer stock solution ($D_3$: 0.60 g, 2.70 mmol, 10 eq; $D_4$:

0.80 g, 2.70 mmol, 10 eq) was put into a Schlenk flask. The temperature of the reaction solution was adjusted to the desired reaction temperature. 0.17 mL t-BuLi solution (0.27 mmol, 1 eq) was slowly added. *Sampling:* A quench stock solution containing 0.1 mL CDMS (85.5 mg, 0.90 mmol) in 10.0 mL $CDCl_3$ was prepared. A 0.6 mL aliquot of the quench stock solution (CDMS: 0.054 mmol, ≥ 20 eq) was filled in an NMR tube. A cooled syringe (-20°C) was used to take a < 0.1 mL sample of the reaction solution (max. 0.003 mmol t-BuLi initiated chains, 1 eq) which was immediately quenched in the prepared NMR tube at desired reaction times. The ratio of reacted to unreacted $D_3$ molecules was quantified by $^1$H NMR spectroscopy. Qualitative analysis was performed by $^{29}$Si-INEPT NMR spectroscopy.

#### 7.2.2.2.6.2. ROP of $D_3$: The Influence of Matrix Ions

*Reaction:* The temperature of the reaction mixture was continuously recorded for each single experiment to ensure that isothermal conditions were maintained throughout the experiment. The experiments were generally carried out at 10°C or 20°C. For preparation of a monomer stock solution 10.0 g $D_3$ (45.0 mmol, 1 eq) and 4.0 mL benzene (3.5 g, 45.0 mmol, 1 eq) was put in a 50 mL volumetric flask and filled up with THF. A 10.0 mL aliquot of the monomer stock solution ($D_3$: 2.00 g, 8.99 mmol, 19 eq; benzene: 0.80 mL, 0.70 g, 9.00 mmol, 19 eq) was put into a Schlenk flask. The temperature of the reaction solution was adjusted to the desired reaction temperature. 0.29 mL t-BuLi solution (0.47 mmol, 1 eq) was slowly added. After successful initiation an equimolar amount of a metal compound was immediately added to the reaction solution by rinsing with small amounts THF. The metal compounds used in this study were: $CrCl_3$, $CrCl_2 \cdot 2$ THF, $Cr(acac)_3$, $NiSO_4$, $NiCl_2 \cdot 1.65$ THF, $FeCl_2 \cdot 1.5$ THF, $MgBr_2$, $MnSO_4$ and two stainless steel samples (1.4571 and 1.4301). *Sampling for NMR spectroscopic analyses:* A quench stock solution containing 0.1 mL CTMS (85.4 mg, 0.79 mmol) in 20.0 mL $CDCl_3$ was prepared. A 0.6 mL aliquot of the quench stock solution (CTMS: 0.024 mmol, ~ 5 eq) was filled in an NMR tube. A cooled syringe (-20°C) was used to take a < 0.1 mL sample of the reaction solution (max. 0.005 mmol t-BuLi initiated chains, 1 eq) which was immediately quenched in the prepared NMR tube at desired reaction times. The amount of unreacted $D_3$ molecules was quantified by $^1$H NMR spectroscopy using benzene as the internal standard. Qualitative analysis was performed by $^{29}$Si-INEPT NMR spectroscopy. *Sampling for gravimetric analyses:* When metal compounds which inhibit NMR spectroscopic measurements were used, the ROP of $D_3$ was stopped by adding 0.12 mL CTMS (0.10 g, 0.94 mmol, 2 eq). All volatiles of the reaction solution were evaporated under vacuum and gravimetric analysis – equimolar amounts of PDMS and LiCl – was performed.

Table 54 to Table 58 show the concentration profiles of the kinetic experiments of the ROP of $D_3$ initiated by t-BuLi in THF with a molar ratio of 19 : 1 under the influence of $CrCl_2 \cdot 2$ THF and $CrCl_3$ at 10.0°C.

**Table 54.** ROP of $D_3$ (19:1) at 10.0°C, no metal salt

| **10.0°C** Time / h | $D_3$ / mmol $L^{-1}$ |
|---|---|
| 0 | 875.8 |
| 0.500 | 680.8 |
| 1.00 | 628.5 |
| 1.50 | 491.7 |
| 2.00 | 456.8 |
| 3.00 | 232.8 |
| 4.00 | 194.9 |
| 6.00 | 101.8 |

**Table 55.** ROP of $D_3$ + 1.00 eq $CrCl_2 \cdot 2$ THF

| **10.0°C** Time / h | $D_3$ / mmol $L^{-1}$ |
|---|---|
| 0 | 872.9 |
| 0.500 | 794.3 |
| 1.00 | 782.7 |
| 1.50 | 803.0 |
| 2.00 | 797.2 |
| 3.00 | 805.9 |
| 4.00 | 797.2 |
| 6.00 | 808.8 |

**Table 56.** ROP of $D_3$ + 1.00 eq $CrCl_3$

| **10.0°C** Time / h | $D_3$ / mmol $L^{-1}$ |
|---|---|
| 0 | 872.9 |
| 0.500 | 835.0 |
| 1.00 | 715.7 |
| 1.50 | 672.1 |
| 2.00 | 619.7 |
| 3.00 | 552.8 |
| 4.00 | 503.3 |

**Table 57.** ROP of $D_3$ + 0.50 eq $CrCl_3$

| **10.0°C** Time / h | $D_3$ / mmol $L^{-1}$ |
|---|---|
| 0 | 875.8 |
| 0.500 | 736.1 |
| 1.00 | 645.9 |
| 1.50 | 622.6 |
| 2.00 | 547.0 |
| 3.00 | 421.9 |
| 4.00 | 343.3 |
| 6.00 | 296.8 |

**Table 58.** ROP of $D_3$ + 0.25 eq $CrCl_3$

| **10.0°C** Time / h | $D_3$ / mmol $L^{-1}$ |
|---|---|
| 0 | 875.8 |
| 0.500 | 741.9 |
| 1.00 | 590.6 |
| 1.50 | 445.2 |
| 2.00 | 413.2 |
| 3.00 | 311.3 |
| 4.00 | 212.4 |
| 6.00 | 75.6 |

#### 7.2.2.2.6.3. ROP of $D_3$: Method of Initial Rates

*Reaction:* The temperature of the reaction mixture was continuously recorded for each single experiment to ensure that isothermal conditions are maintained throughout the experiment. The experiments were performed at 0°C, 10°C or 20°C with a molar ratio of $D_3$ : t-BuLi of 4 : 1 or 10 : 1. For preparation of a the 10 : 1 monomer stock solution 11.0 g $D_3$ (49.4 mmol) was dissolved in 50 mL THF and for preparation of the 4 : 1 monomer stock solution 4.27 g $D_3$ (19.2 mmol) was dissolved in the same amount of THF. For variation of the concentration different aliquots of the 10 : 1 monomer stock solution between 2.0 mL (0.44 g, 1.98 mmol) and 10.0 mL (2.20 g, 9.89 mmol) or of the 4 : 1 monomer stock solution between 2.5 mL (0.21 g, 0.96 mmol) and 10.0 mL (0.85 g, 3.84 mmol) was put into a Schlenk flask and diluted with THF to a resulting end volume of 10.0 mL. The temperature of the reaction solution was adjusted to the desired reaction temperature. For initiation of 10 : 1 experiments between 0.12 mL (0.20 mmol) and 0.62 mL (0.99 mmol) and for initiation of 4 : 1 experiments between 0.15 mL (0.24 mmol) and 0.60 mL (0.96 mmol) t-BuLi solution was slowly added. For both molar ratios a quench stock solution containing 2.6 mL CDMS (2.22 g, 23.5 mmol) in 30.0 mL THF was prepared. An aliquot of 2.0 mL (CDMS: 1.57 mmol, > 1.5 eq) of the quench stock solution was added to the reaction solution after 0.5 h or 1.0 h of reaction time to stop the ROP. The ratio of reacted to unreacted $D_3$ molecules was quantified by $^{1}$H NMR spectroscopy. Qualitative analysis was performed by $^{29}$Si-INEPT NMR spectroscopy.

Table 59 to Table 61 show the method of initial rates (MIR) for $D_3$ : t-BuLi = 10 : 1 for a reaction time of $t_R$ = 1.0 h at a temperature of T = 0°C, $t_R$ = 0.5 h at T = 10°C and $t_R$ = 0.5 h at T = 20°C.

**Table 59.** MIR 10 : 1, 1.0 h at 0°C

| $D_{3,S}$ / mol $L^{-1}$ | $D_{3,E}$ / mol $L^{-1}$ |
|---|---|
| 0.198 | 0.160 |
| 0.297 | 0.199 |
| 0.494 | 0.408 |
| 0.593 | 0.491 |
| 0.989 | 0.794 |

**Table 60.** MIR 10 : 1, 0.5 h at 10°C

| $D_{3,S}$ / mol $L^{-1}$ | $D_{3,E}$ / mol $L^{-1}$ |
|---|---|
| 0.198 | 0.164 |
| 0.297 | 0.230 |
| 0.297 | 0.240 |
| 0.494 | 0.392 |
| 0.593 | 0.467 |
| 0.989 | 0.803 |

**Table 61.** MIR 10 : 1, 0.5 h at 20°C

| $D_{3,S}$ / mol $L^{-1}$ | $D_{3,E}$ / mol $L^{-1}$ |
|---|---|
| 0.198 | 0.145 |
| 0.297 | 0.202 |
| 0.494 | 0.350 |
| 0.593 | 0.428 |

Table 62 and Table 63 show the MIR for $D_3$ : t-BuLi = 4 : 1 for a reaction time of $t_R$ = 1.0 h at a temperature of T = 0°C and $t_R$ = 0.5 h at T = 20°C.

**Table 62.** MIR 4 : 1, 1.0 h at 0°C

| $D_{3,S}$ / mol $L^{-1}$ | $D_{3,E}$ / mol $L^{-1}$ |
|---|---|
| 0.096 | 0.062 |
| 0.192 | 0.112 |
| 0.192 | 0.130 |
| 0.269 | 0.165 |
| 0.319 | 0.201 |
| 0.384 | 0.250 |

**Table 63.** MIR 4 : 1, 0.5 h at 20°C

| $D_{3,S}$ / mol $L^{-1}$ | $D_{3,E}$ / mol $L^{-1}$ |
|---|---|
| 0.096 | 0.055 |
| 0.192 | 0.110 |
| 0.269 | 0.144 |
| 0.319 | 0.182 |
| 0.384 | 0.193 |
| 0.384 | 0.207 |

### 7.2.2.3. Thermodynamics of the ROP of $D_3$

All experiments were carried out in a Dewar vessel under adiabatic conditions. The temperature of the reaction solution was continuously recorded. For preparation of a monomer stock solution 25.00 g $D_3$ (112.4 mmol, 1 eq) and 8.78 g benzene (10.0 mL, 112.4 mmol, 1 eq) was put in a 50 mL volumetric flask and filled up with THF. A 10.0 mL aliquot of the monomer stock solution ($D_3$: 5.00 g, 22.48 mmol, 1 eq; benzene: 1.76 g, 2.00 mL, 22.48 mmol, 1 eq) was put in the Dewar vessel and diluted with 140.0 mL THF. This solution was cooled to about 5°C with a copper cooling coil connected to a cryostatic temperature control unit. 14.0 mL t-BuLi solution (22.4 mmol, 1 eq) was slowly added and the mixture was stirred for about 1 h. Afterwards, a second 10.0 mL aliquot of the monomer stock solution ($D_3$: 5.00 g, 22.48 mmol, 1 eq; benzene: 1.76 g, 2.00 mL, 22.48 mmol, 1 eq) was added. The reaction solution was stirred for more than 4 h. In the end, 2.9 mL CTMS (2.5 g, 22.8 mmol, 1.02 eq) were added to stop the ROP and the solution was stirred for 30 min. $^{1}H$ and $^{29}Si$-INEPT NMR spectroscopy was used for qualitative and quantitative analysis.

## 7.3. PFR Experiments

The ROP of $D_3$ was performed in a PTFE-PFR as described in Chapter 5.4.3. Herein, the experimental procedures are described.

### 7.3.1. Determination of the RTD

The experimental setup is shown in Figure 48.

An approximate amount of 37.5 mg to 42.0 mg of methyl red (MeRed) was put in a 250 mL volumetric flask and filled up with THF. A 100 mL Hamilton 1100TLL gastight syringe was filled with the dye solution and a second syringe of the same type was filled with pure THF. Before starting the experiment the whole experimental setup was purged with these solutions to create bubble free conditions. The end of purging was reached when the reactor was filled with pure THF and no inhomogeneities were present. Furthermore, the charging level of the syringe containing the dye solution had to be lower than the corresponding level of the syringe containing pure THF. Then, both syringes were loaded in the syringe pump kdScientific KDS200 and the flow rate was adjusted to half of its value (two syringes!). The experiment started when both syringes were dispensing. *Sampling*: Several vials were filled with 5.0 mL THF and the solution leaving the reactor was continuously collected for a certain period of time in these vials (sampling interval). 32 samples were collected for PTFE-PFR I and 40 or 48 samples for PTFE-PFR II. Additionally, when latter experimental setup was used, an interval which started at the beginning of the RTD experiment was defined where no sample was taken (waste interval). The flow rates and their corresponding intervals are summarized in Table 64.

**Table 64.** Sampling intervals and waster intervals for RTD experiments

| Flow rate / mL min$^{-1}$ | Sampling interval / s | Waste interval / min:s |
|---|---|---|
| 1.50 | 45.0 | 12:00 |
| 3.00 | 23.0 | 6:00 |
| 5.00 | 15.0 | 3:00 |
| 7.50 | 8.0 | 2:30 |
| 10.00 | 5.0 | 1:45 |

UV-VIS spectra of the samples were measured and the increase of the absorption at 487 nm was determined which resulted in a step response (F-curve). For correction the data set was fitted with a sigmoidal fit using the analysis software Origin 7.5 from OriginLab. This fit was evaluated for calculation of the Bo-number.

The evaluations of the RTD experiments for PTFE-PFR I on $D_O$ = 2.0 cm to $D_O$ = 4.0 cm are shown in Figure 65 to Figure 67 and the evaluation of the RTD experiments for PTFE-PFR II on $D_O$ = 3.0 cm is shown in Figure 68. ($F_V$ = 1.50 mL min$^{-1}$ grey squares; $F_V$ = 3.00 mL min$^{-1}$ black circles; $F_V$ = 5.00 mL min$^{-1}$ grey triangles; $F_V$ = 7.50 mL min$^{-1}$ black rhombi; $F_V$ = 10.00 mL min$^{-1}$ grey crosses). The distribution broadens with increasing flow rate for all experimental setups.

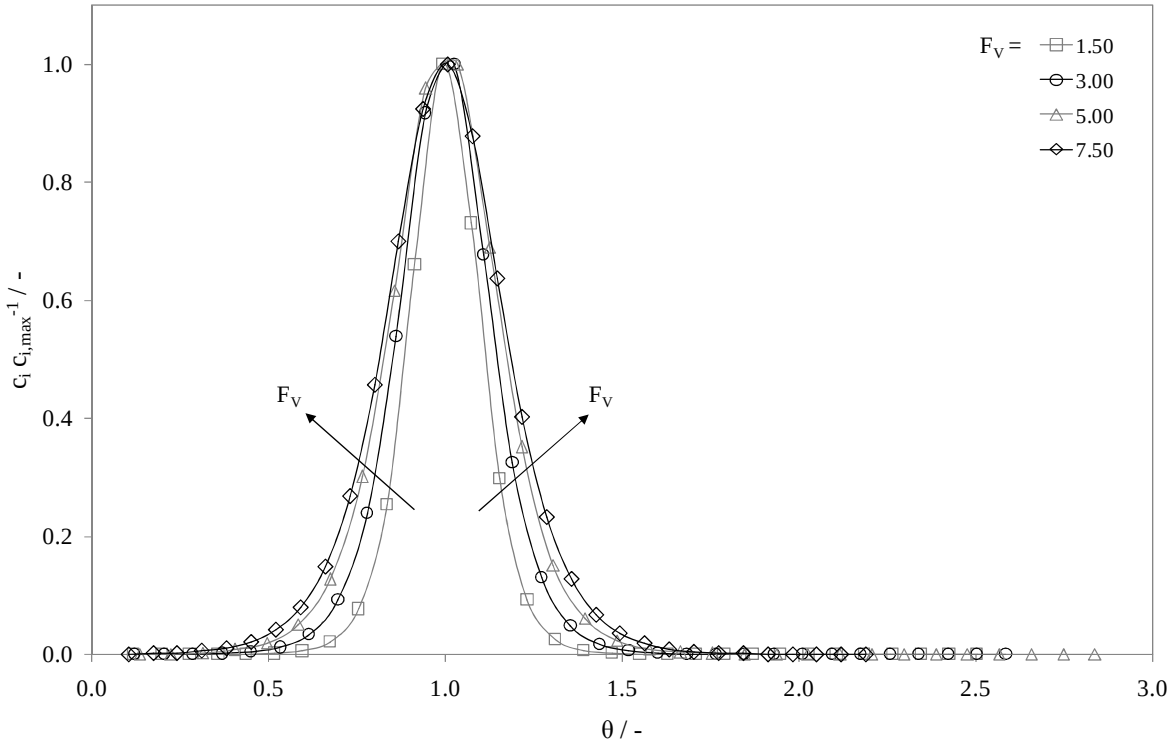


**Figure 65.** Evaluation of the RTD (E-curve) for PTFE-PFR I coiled up a central tube diameter of $D_O$ = 2.0 cm

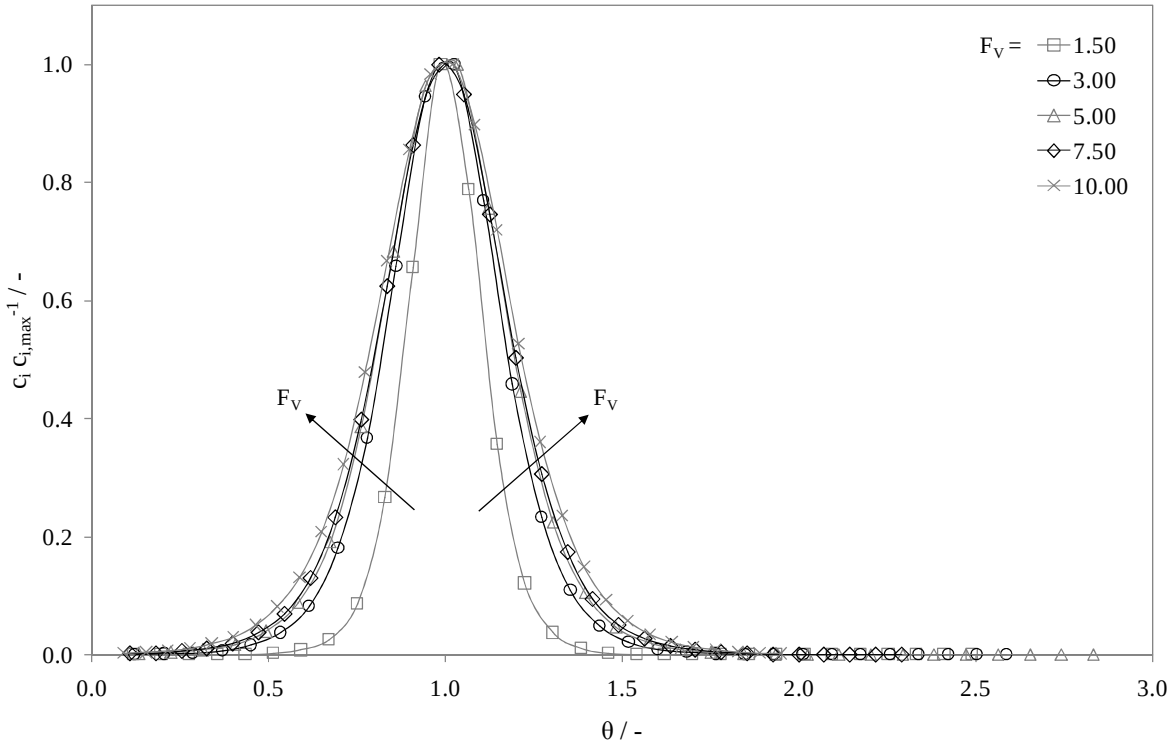


**Figure 66.** Evaluation of the RTD (E-curve) for PTFE-PFR I coiled up a central tube diameter of $D_O$ = 3.0 cm

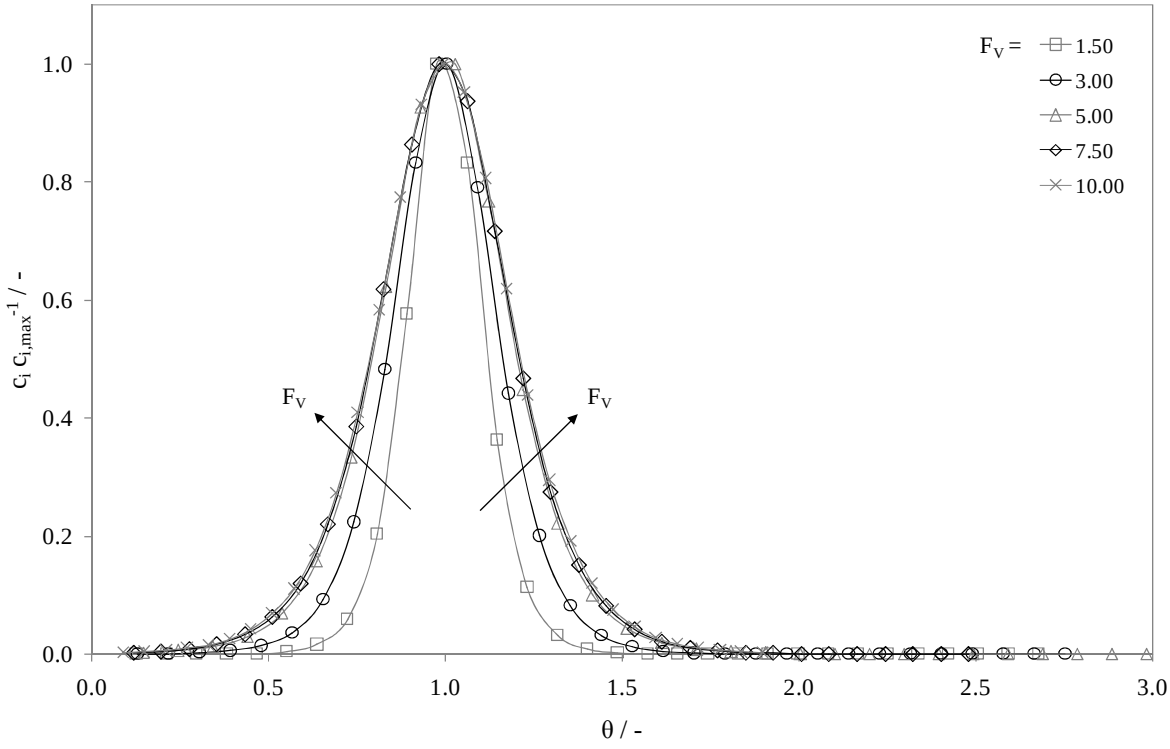


**Figure 67.** Evaluation of the RTD (E-curve) for PTFE-PFR I coiled up a central tube diameter of $D_O$ = 4.0 cm

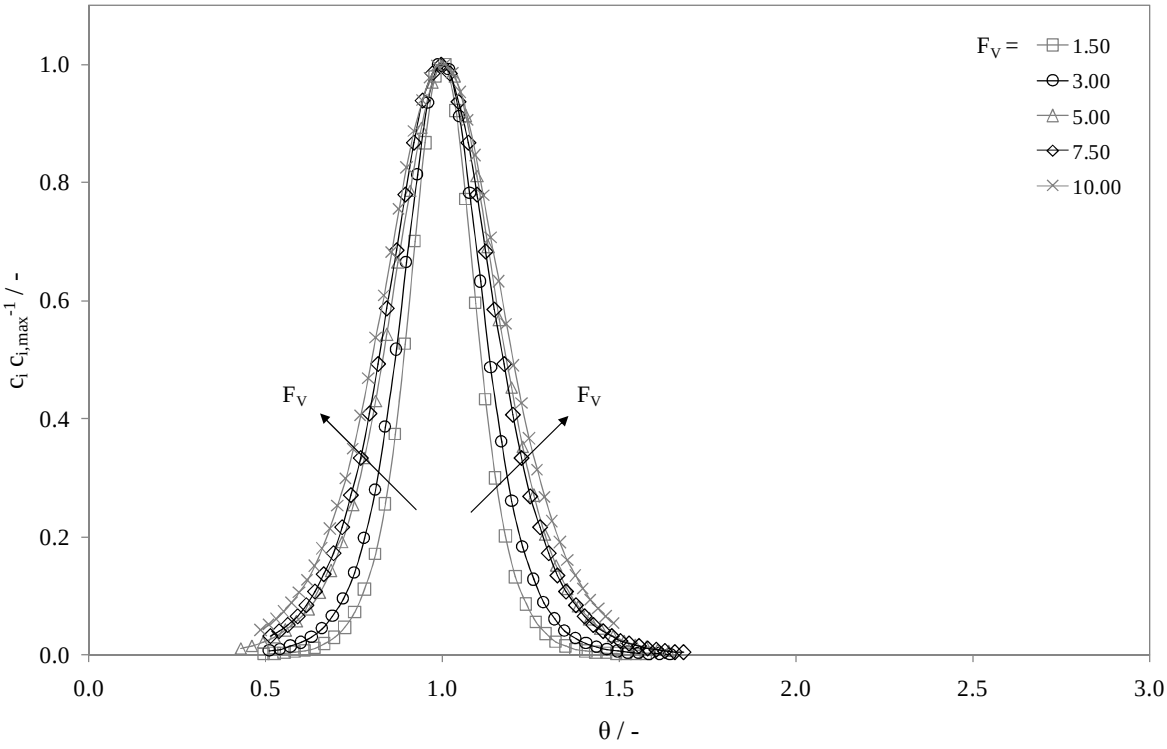


**Figure 68.** Evaluation of the RTD (E-curve) for PTFE-PFR II coiled up a central tube diameter of $D_O$ = 3.0 cm

### 7.3.2. CFD calculations of PTFE-PFR I

The commercially available CFD-code *Ansys 12.1* was used for modeling. *Laminary Flow* conditions were used according to Re regime. 1,119,080 unstructured cubic cells with a side length of 0.15 mm (cross section) were used for meshing. The boundary conditions are *velocity inlet, pressure outlet* (*0 bar overpressure*) and *no slip condition* at the reactor wall. For steric discretization, *PRESTO!* was used for calculation of the pressure and *QUICK* for calculation of the momentum.

### 7.3.3. Continuous ROP of $D_3$ in PTFE-PFR I

The experimental setup is shown Figure 57. The PFR consists of a PTFE-tubing with $d_i$ = 2.00 mm, $d_o$ = 3.00 mm and L = 4.0 m which was coiled up a pipe with $D_O$ = 2.0 cm, 3.0 cm or 4.0 cm. The total volumetric flow rate in the reactor was adjusted to $F_V$ = 1.50 mL min$^{-1}$, 3.00 mL min$^{-1}$, 5.00 mL min$^{-1}$ or 7.50 mL min$^{-1}$. *Reaction:* All preparation steps of the experimental setup were performed in the drybox, afterwards the setup was locked out of the drybox and the experiment was carried out under standard Schlenk technique. For preparation of the monomer stock solution 27.81 g $D_3$ (125.0 mmol, 1 eq) and 11.1 mL benzene (9.76 g, 125.0 mmol, 1 eq) were put in a 250 mL volumetric flask

and filled up with THF. This procedure was repeated to have at least 400 mL to 500 mL of the monomer stock solution, which was put in a Schlenk flask for the continuous experiments. This amount was approximately used for each run. For preparation of an initiator stock solution 5.0 mL t-BuLi solution (8.0 mmol) was put in a 25 mL volumetric flask and filled up with heptane. The initiator stock solution was put in a 100 mL gastight syringe (Hamilton 1100 TLL) and connected to the experimental setup, when locked out of the drybox the syringe was placed in the syringe pump. The reactor was put into the temperature controlled water bath. The temperature of it was adjusted to 40°C; hence, quasi-isothermal conditions were maintained throughout the experiment. The $D_3$-stock solution was connected to the HPLC pump and the pump was purged with several mL of the stock solution prior to the experiment. The reactor outlet was connected to a PTFE tube with an inner diameter of 0.8 mm and a length of approximately 1.0 m. This tubing was placed in a methanol / $N_{2,l}$ cooling bath which was adjusted to a temperature of < -10°C to drastically decrease the rate of polymerization in the reaction solution leaving the reactor. This tube ended in a 100 mL three necked flask which was equipped with a magnetic stir bar. The flask itself was additionally placed in an ice bath and used for discontinuous sampling. Downstream, another tube with an inner diameter of 0.8 mm leaving the flask (= waste) was used to adjust the charging level of the flask to about 6 mL to 10 mL. The flow rates of the stock solutions were adjusted according to a molar ratio of $D_3$ : t-BuLi = 25 : 1, which equals a flow rate ratio of $F_{V,D3} : F_{V,t\text{-}BuLi} = 16 : 1$. *Sampling:* 2 to 3 samples were taken; starting when a total volume of approximately 8 times the reactor volume passed through the PTFE-PFR and ending when one of the stock solutions was nearly depleted. For each sample, a quench stock solution containing 0.12 mL CTMS (102.5 mg, 0.94 mmol, 10 eq) in 3.0 mL THF was filled in a Schlenk flask. A gastight syringe was used to take a 5.0 mL aliquot of the reaction solution (0.094 mmol t-BuLi initiated chains, 1 eq) out of the three necked flask which was immediately quenched in the CTMS-THF mixture (reactor sample). An NMR sample from the reactor sample was taken. The amount of unreacted $D_3$ molecules was quantified by $^{1}H$ NMR spectroscopy using benzene as the internal standard. Qualitative analysis was performed by $^{29}Si$-INEPT NMR spectroscopy. All volatiles of the reactor sample were vacuum evaporated for several hours at 40°C. $CH_2Cl_2$, pentane or diethylether was added to the residue, a colorless oily liquid with a white precipitate, and the mixture was centrifuged at 5000 rpm for > 30 min. The clear liquid phase was separated from the white precipitate and the solvent was evaporated. The product, a colorless oily liquid, was analyzed by SEC.

### 7.3.4. Continuous ROP of $D_3$ in PTFE-PFR II

The experimental setup is shown in Figure 62. Basically, the same procedure as for PTFE-PFR I was used ($D_3$ : t-BuLi = 25 : 1 and $F_{V,D3}$ : $F_{V,t\text{-}BuLi}$ = 16 : 1.). The PFR consists of a PTFE-tubing with $d_i$ = 3.00 mm, $d_o$ = 4.00 mm and L = 5.33 m which was coiled up a pipe with $D_O$ = 3.0 cm. The total volumetric flow rate in the reactor was adjusted to $F_V$ = 3.00 mL $min^{-1}$ or 10.00 mL $min^{-1}$. CTMS was continuously dispensed to the reactions solution at the reactor outlet to quench the polymerization reaction. For preparation of the quench-stock solution 5.1 mL CTMS (4.35 g, 40.0 mmol) was put in a 100 mL volumetric flask and filled up with THF. The quench stock solution was put in a 100 mL gastight syringe (Hamilton 1100 TLL) and connected to the experimental setup, when locked out of the drybox the quench stock and the initiator stock were placed in the same syringe pump. Hence, both stock solutions were dispensed at the same $F_V$ and the molar ratio was automatically adjusted to CTMS : t-BuLi = 1.25 : 1 (t-BuLi = 320 mmol $L^{-1}$ and CTMS = 400 mmol $L^{-1}$). *Sampling:* 3 samples were taken; starting when a total volume of approximately 6 times the reactor volume passed through the PTFE-PFR and ending when one of the stock solutions was nearly depleted. A gastight syringe was used to take a 5.0 mL aliquot of the reaction solution out of the three necked flask which was put in a separate Schlenk flask (reactor sample). $^{1}$H NMR, $^{29}$Si-INEPT NMR spectroscopy and work up for SEC measurements was performed according to procedure described in Chapter 7.3.3.

# 8. Appendix

## 8.1. Additional Experimental Details

In this section auxiliary information of the performed experiments is described.

### 8.1.1. Thermodynamics: Heat Capacity of the System ($C_{p,Sys}$)

For determination of thermodynamic properties of the individual reactions, the heat capacity of the system (Dewar vessel, magnetic stir bar, Pt-100 temperature sensor) was found to be $\mathbf{C_{p,Sys} = 59.1\ J\ K^{-1}}$ with a standard deviation of 19.3 %. The measurements were performed using two aliquots of THF at different temperatures according to literature[71].

**Table 65.** Determination of $C_{p,Sys}$

| Experiment No. | $C_{p,Sys}$ / J $K^{-1}$ |
|---|---|
| # 1 | 47.0 |
| # 2 | 70.3 |
| # 3 | 44.1 |
| # 4 | 46.9 |
| # 5 | 57.7 |
| # 6 | 68.2 |
| # 7 | 79.5 |
| # 8 | 55.9 |
| # 9 | 60.6 |
| # 10 | 60.6 |
| **Average** | **59.1** |
| **Deviation** | **11.4** |

### 8.1.2. ROP of $D_3$: MALDI-TOF-MS Isotope Pattern

Figure 69 shows the theoretical and experimental MALDI-TOF-MS isotope pattern of $[t\text{-}Bu((SiOMe_2)_3)_6SiMe_3+Ag]^+$.

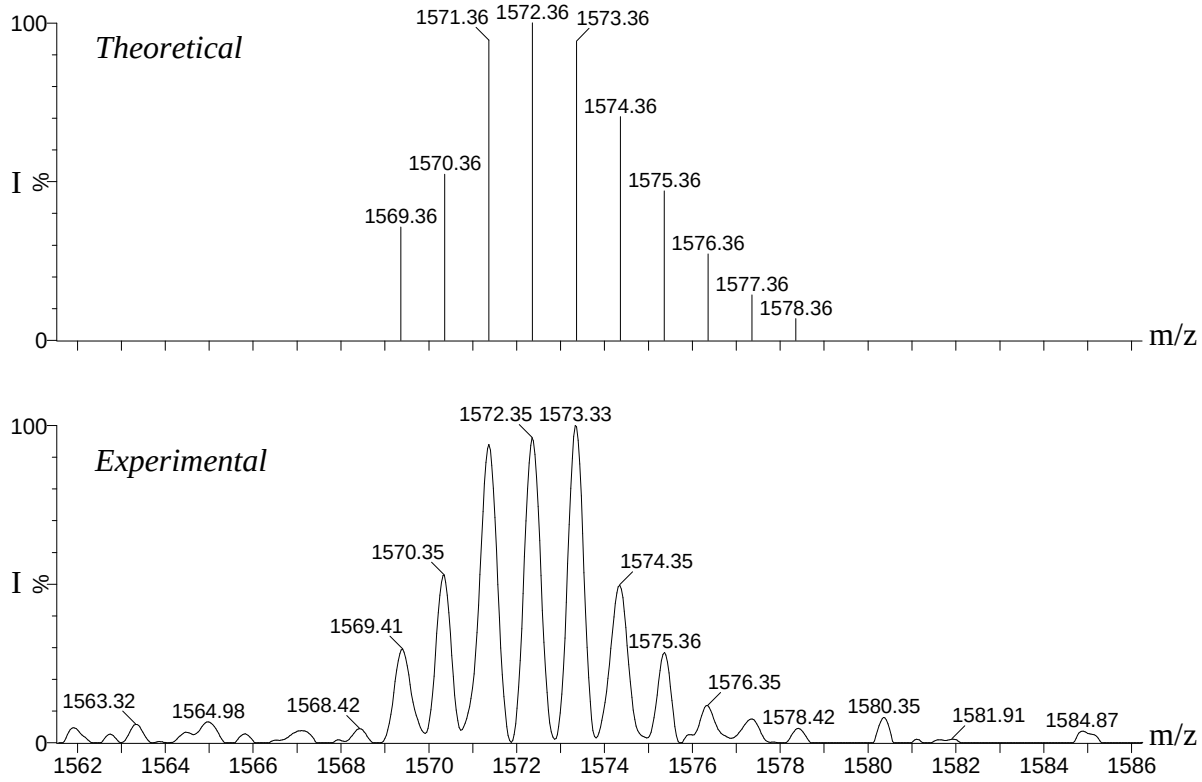


**Figure 69.** Theoretical and experimental MALDI-TOF-MS isotope pattern of a CTMS terminated PDMS

### 8.1.3. Continuous Experiments: Calibration of the HPLC Pump

The HPLC pump Milton Roy CM 4000 was used for continuously operated polymerization reaction experiments. The flow rate was calibrated according to Figure 70.

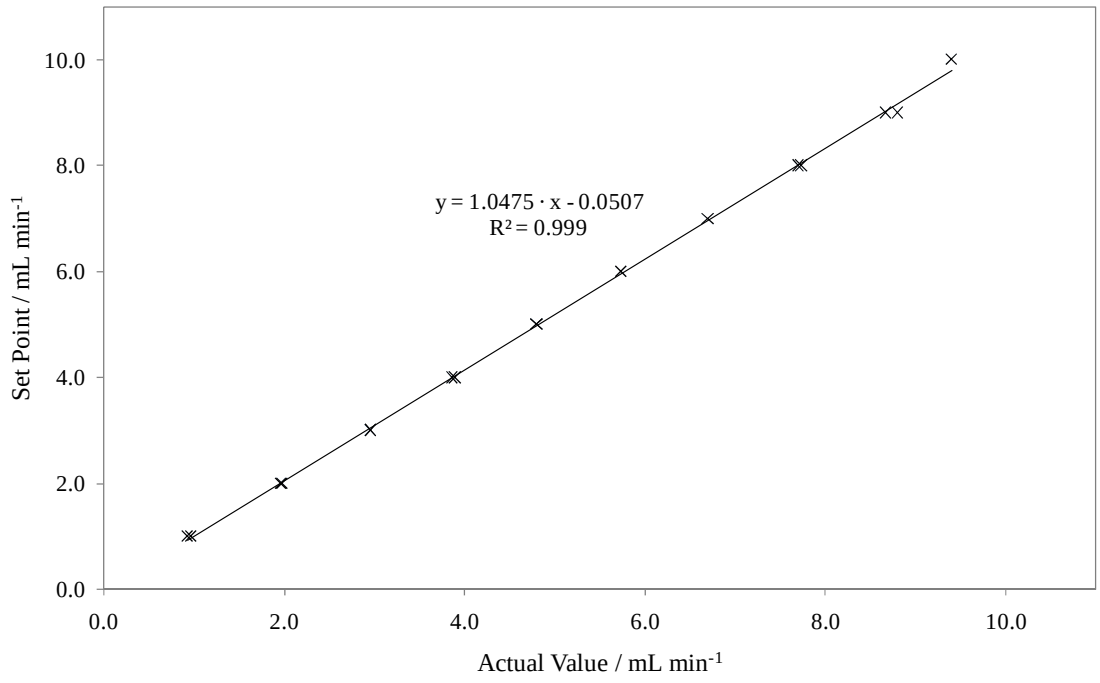


**Figure 70.** Calibration of the HPLC pump Milton Roy CM 4000

### 8.1.4. RTD: Solubility of Dyes

The solubility of different dyes in THF at room temperature was investigated. Only methyl red and 4-nitrophenol showed sufficient solubility. Furthermore, only methyl red showed strong absorbance in the VIS region. Hence, this dye was used for all RTD experiments. The results of this investigation are given in Table 66.

**Table 66.** Solubility of dyes in THF at room temperature

| Dye | Description |
|---|---|
| Methyl red | soluble, strong VIS absorption (orange-red) |
| 4-Nitrophenol | soluble, VIS absorption (slightly yellow) |
| Benzophenone<br>Phenolphthalein<br>Thymolphthalein | soluble, no VIS absorption |
| Alizarin<br>Alizarin S<br>Bromophenol blue<br>Methyl orange<br>Methyl violet<br>Metanil yellow | slightly soluble |
| Indigo carmine<br>Luminol<br>Methylene blue<br>Potassium permanganate | insoluble |

The molar absorption coefficient of methyl red in THF was determined to be $\varepsilon$ = **26900 L mol$^{-1}$ cm$^{-1}$**.

## 8.2. Analytics

### 8.2.1. NMR Spectroscopy

All NMR spectra were measured on *Varian Mercury 300*. All measurements were performed at 25°C in $CDCl_3$ and the NMR signals are given in *ppm* in respect to $Si(CH_3)_4$ unless otherwise stated. The $^{29}Si$ spectra were recorded using the Insensitive Nuclei Enhancement by Polarization Transfer (INEPT) method. The frequencies of the nuclei are given in Table 67.

**Table 67.** NMR spectroscopy: nuclei and their corresponding frequencies

| Nucleus | Frequency / MHz |
|---|---|
| $^{1}H$ | 300.224 |
| $^{13}C$ | 75.499 |
| $^{29}Si$ | 59.641 |

### 8.2.2. UV-VIS Spectroscopy

The UV-Vis spectra were recorded on *Lambda 35 UV/VIS Spectrometer* from *Perkin Elmer Instruments* with the software *UV WinLab Version 2.85.04*. The spectra were evaluated with the software *SpekWin 32 Version 1.70.5*. The blank for RTD experiments was pure THF.

### 8.2.3. IR Spectroscopy

The IR spectra were recorded on *883 Infrared Spectrophotometer* from *Perkin Elmer*. The liquid polymers were put between two KBr pellets. The spectra were evaluated with the software *SpekWin 32 Version 1.70.5*.

### 8.2.4. SEC

The SEC measurements were performed in degassed THF with a flow rate of 1.0 mL $min^{-1}$. Solvent degassing was performed with *ERC 3315a* and solvent dispensing with *L6000A* from *Merck-Hitachi*. A pre-column with 5 µm (8 mm · 50 mm) and three analytical columns – $1 \cdot 10^6$ Å, $1 \cdot 10^4$ Å and $1 \cdot 10^3$ Å (all 8 mm · 300 mm) – of type *SDV* from *Polymer Standards Service (PSS)* were used. Detection was performed with a differential refractometer / viscometer from *Viscotek*. Calibration was performed with polystyrene standards from *PSS*.

### 8.2.5. Viscosity and Density

The dynamic and kinematic viscosity and the density were simultaneously determined on a Stabinger Viscometer *SVM 3000* from *Anton Paar* according to the ASTM standard test method.[72]

### 8.2.6. MALDI-TOF-MS

MALDI-TOF-MS was performed on a *Micromass TofSpec 2E* Time-of-Flight Mass Spectrometer. The instrument is equipped with a nitrogen laser (337 nm wavelength, operated at a frequency of 5 Hz), and a time lag focusing unit. Ions were generated by irradiation slightly above the threshold laser power. Positive ion spectra were recorded in reflectron mode applying an accelerating voltage of 20 kV and externally calibrated with a suitable mixture of poly(ethyleneglycol)s (PEG). The spectra of 100 – 150 shots were averaged to improve the signal-to-noise ratio. Analysis of data was done with *MassLynx-Software V3.5* (*Micromass/Waters*, Manchester, UK). Sample solutions were prepared by mixing a solution of dithranol ($c = 10\ g\ L^{-1}$ in THF), a solution of the analyte ($c = 1\ g\ L^{-1}$ in THF), and a solution of $CF_3COOAg$ (AgTFA; $c = 0.1\ g\ L^{-1}$ in THF), in a volumetric ratio of 10 : 1 : 1. 0.5 µL of the resulting mixture were deposited on the sample plate (stainless steel) and allowed to dry under air.

### 8.2.7. GC-MS

The measurements were performed on *7890A GC System* coupled with a *5975 C VL MSD*; both from *Agilent Technologies*. He was used as the carrier gas. 1 µL of a solution of the analyte in THF ($c = 1\ g\ L^{-1}$) was used for analysis.

## 8.3. Laboratory Equipment

### 8.3.1. Cryostatic Temperature Regulator

The cryostatic temperature regulator *RUL-80* from *LAUDA* was used for isothermal conditions in the batch experiments and kinetic investigations. The device was coupled to a homemade copper coil for heat transfer. Methanol was used as the heat carrier.

### 8.3.2. Temperature Regulator

The PTFE-PFR was put in a *RML 6 B* from *LAUDA* filled with temperature regulated water to maintain isothermal conditions throughout the continuous polymerization experiments.

### 8.3.3. Temperature Recording

A glass coated *Pt-100* from *Testo* attached to a *testo 735-2* was used for continuous temperature recording during the kinetic and thermodynamic experiments.

### 8.3.4. Dispensing

For continuous ROP of $D_3$ the HPLC pump *CM 4000* from *Milton Roy* was used for dispensing the monomer stock-solution and the syringe pump *kds200* from *kdScientific* equipped with one or two *1100 TLL* 100 mL gastight syringes from *Hamilton* was used for dispensing the initiator and/or termination stock solutions. The same syringe pump equipped with two 100 mL gastight syringes of the same type (*1100 TLL* from *Hamilton*) was used for RTD experiments.

## 8.4. Nomenclature of Abbreviations

| Abbreviation | Meaning / unit |
|---|---|
| acac | Acetylacetonate |
| Bo | Bodenstein number / - |
| Bo-number | Bodenstein number / - |
| BR | Batch Reactor |
| c | Concentration / mol $L^{-1}$ |
| c | Heat capacity / J $mol^{-1}$ $K^{-1}$ (Single substance) |
| C | Heat capacity / J $K^{-1}$ (Overall, System) |
| CDMS | Chlorodimethylsilane |
| CDMS | Concentration of CDMS / mol $L^{-1}$ |
| CFD | Computational Fluid Dynamics |
| CSTR | Continuously Stirred Tank Reactor |
| CTMS | Chlorotrimethylsilane |
| CTMS | Concentration of CTMS / mol $L^{-1}$ |
| d | Diameter / m (PTFE-PFR) |
| D | Diameter / m (Central tube) |
| D | Dispersion coefficient / $m^2$ $s^{-1}$ |
| D | Di-O-substituted Si (Chemical nomenclature) |
| $D_3$ | Concentration of $D_3$ / mol $L^{-1}$ |
| $D_3$ | Hexamethylcyclotrisiloxane |
| $D_4$ | Octamethylcyclotetrasiloxane |
| $D_5$ | Decamethylcyclopentasiloxane |
| $D_6$ | Dodecamethylcyclohexasiloxane |
| De | Dean number / - |
| De-number | Dean number / - |
| E | Energy / J $mol^{-1}$ |
| eq | Equivalent |
| F | Flow rate / L $s^{-1}$ |
| F | Flow rate / mol $s^{-1}$ |
| GPC | Gelpermeationschromatographie |
| H | Enthalpy / J $mol^{-1}$ |
| HPLC | High Pressure/Performance Liquid Chromatography |
| INEPT | Insensitive Nuclei Enhancement by Polarization Transfer |
| IR | Infrared |
| k | Rate constant / $M^{1-n}$ $s^{-1}$ |
| L | Characteristic length / m (Dimensionless number) |
| L | Reactor length / m |
| m | Order of reaction |
| M | Molar / mol $L^{-1}$ (Concentration) |
| M | Molecular mass / g $mol^{-1}$ |
| M | Mono-O-substituted Si (Chemical nomenclature) |
| MALDI | Matrix Assisted Laser Desorption Ionization |

| | |
|---|---|
| MeRed | Methyl red |
| MIR | Method of Initial Rates |
| MS | Mass spectrometry |
| n | Molar number / mol |
| n | Degree of Polymerization (repeating unit in PDMS chain) |
| n | Order of reaction |
| NMR | Nuclear Magnetic Resonance |
| PDI | Polydispersity Index |
| PDMS | Polydimethylsiloxane(s) |
| $Pé_{ax}$ | Péclet number / - |
| $Pé_{ax}$-number | Péclet number / - |
| PFR | Plug Flow Reactor |
| PTFE | Polytetrafluoroethylene (Teflon) |
| Q | Heat / J $mol^{-1}$ |
| Q | Tetra-O-substituted or quaternary Si (Chemical nomenclature) |
| r | Rate of reaction / mol $L^{-1}$ $s^{-1}$ |
| R | Ideal gas constant / 8.314 J $mol^{-1}$ $K^{-1}$ |
| Re | Reynolds number / - |
| Re-number | Reynolds number / - |
| ROP | Ring-Opening Polymerization |
| ROR | Ring-Opening Reaction |
| RR | Rohrreaktor |
| RTD | Residence Time Distribution |
| s | Wall thickness / m |
| SEC | Size Exclusion Chromatography |
| SS | Stainless Steel |
| t | Mean residence time / s (RTD) |
| t | Time / s |
| T | Temperature / °C / K |
| T | Tri-O-substituted Si (Chemical nomenclature) |
| t-BuLi | Concentration of t-BuLi / mol $L^{-1}$ |
| t-BuLi | *tert*-Butyllithium |
| TfOH | Trifluoromethane sulfonic acid |
| THF | Tetrahydrofurane |
| TMS | Trimethylsilyl |
| TOF | Time Of Flight |
| u | Flow velocity / m $s^{-1}$ |
| UV | Ultra Violet |
| V | Volume / L |
| VIS | Visible |
| VZV | Verweilzeitverteilung |
| x | Order of reaction |
| X | Conversion / - / % |
| δ | Chemical shift / ppm |

| | |
|---|---|
| $\eta$ | Dynamic viscosity / Pa s |
| $\theta$ | Dimensionless hydrodynamic residence time / - |
| $\nu$ | Kinematic viscosity / $m^2\ s^{-1}$ |
| $\nu$ | Stoichometric coefficient |

## 8.5. Nomenclature of Indices

| **Indices** | **Meaning** |
|---|---|
| 0 | Infinitely (Arrhenius) |
| 0 | Initial value (Concentration) |
| 0 | Standard… (Enthalpies, …) |
| 1 | Condition 1 |
| 2 | Condition 2 |
| A | Activation (Energy) |
| A | Component A (Reactant) |
| av | Average |
| ax | Axial |
| crit | Critical |
| E | End |
| F | Formation |
| grav | Gravimetric |
| i | Component i |
| i | Inner (PTFE-PFR) |
| I | Inner (Central tube) |
| n | Number average |
| NMR | Calculated from $^1$H NMR data |
| o | Outer (PTFE-PFR) |
| O | Outer (Central tube) |
| p | Constant pressure |
| R | Reaction |
| R | Reactor |
| S | Start |
| SEC | Calculated from SEC |
| Sys | System |
| (T) | Temperature dependent |
| th | Theoretical |
| V | Volumetric |
| w | Weight average |
| * | After successful initiation |

## 8.6. Figures

## 8.7. Tables

## 8.8. Literature


(1) H.-H. Moretto, M. Schulze, G. Wagner In *Ullmann's Encyclopedia of Industrial Chemistry*; Wiley VCH: 2005; Vol. 7th Edition.

(2) G. Maaß, B. Degen *GE Bayer Silicones GmbH & Co. KG* **2000**, *DE19934374C1*.

(3) G. Fleischmann, H. Eck, P. Wenzeler *Wacker-Chemie GmbH* **1988**, *EP0302492*.

(4) Selin, T. G. *General Electric Company* **1969**, *US3481965*.

(5) J. G. Zilliox, J. E. L. Roovers, S. Bywater *Macromolecules* **1975**, *8*, 573-578.

(6) Y. Kawakami, et al. *Polymer Journal* **1982**, *14*, 913-917.

(7) Y. Gnanou, P. Rempp *Makromolekulare Chemie - Macromolecular Chemistry and Physics* **1988**, *189*, 1997-2005.

(8) Boileau, S. *ACS Symposium Series* **1985**, *286*, 23-35.

(9) T. Uozumi, et al. *Journal of Polymer Science Part A: Polymer Chemistry* **2000**, *38*, 1844-1847.

(10) C. L. Frye, et al. *The Journal of Organic Chemistry* **1969**, *35*, 1308-1314.

(11) S. M. Sieburth, W. Mu *Journal of Organic Chemistry* **1993**, *58*, 7584-7586.

(12) Boileau, S. *Makromolekulare Chemie - Macromolecular Symposia* **1993**, *73*, 177-181.

(13) S. Boileau, et al. *Macromolecular Symposia* **1994**, *88*, 177-189.

(14) Z. Zhang, N. Zhou, C. Xu, Z. Xie *Chinese Journal of Polymer Science* **2001**, *19*, 7-11.

(15) K. Yoshinaga, Y. Iida *Chemistry Letters* **1991**, 1057-1058.

(16) A. Molenberg, M. Möller *Macromolecular Rapid Communications* **1995**, *16*, 449-453.

(17) J. Chojnowski, et al. *Journal of Inorganic and Organometallic Polymers* **2004**, *14*, 85-99.

(18) B. Esswein, A. Molenberg, M. Möller *Macromolecular Symposia* **1996**, *107*, 331-340.

(19) R. Drake, I. MacKinnon, R. Taylor In *The Chemistry of Organic Silicon Compounds*; Z. Rappaport, Y. A., Ed. 1998; Vol. 2, p 2217-2244.

(20) A. M. Hawkridge, J. A. Gardella Jr. *Journal of the American Society for Mass Spectrometry* **2003**, *14*, 95-101.

(21) J. D. Kress, P. C. Leung, G. J. Tawa, P. J. Hay *JACS* **1997**, *119*, 1954-1960.

(22) G. Toskas, M. Moreau, P. Sigwalt *Macromolecular Symposia* **2006**, *240*, 68-77.

(23) B. Arkles, G. Larson *Gelest Catalog 3000-A; Silicon Compounds: Silanes and Silicones* **2004**.

(24) Saam, J. C. *Silicon Based Polymers: A Comprehensive Resource*; American Chemical Society, 1990.

(25) Pop, C. *PhD-Thesis: Herstellung von monodispersen Polydimethylsiloxan-Netzwerken und Charakterisierung der Mikrostruktur und der Permeationseigenschaften* **2006**, Bayerische Julius-Maximilians-Universität Würzburg.

(26) W. Fortuniak, J. Chojnowski, G. Sauvet *Macromolecular Chemistry and Physics* **2001**, *202*, 2306-2313.

(27) S. O. Hammouch, G. J. Beinert, J. G. Zilliox, J. E. Herz *Polymer* **1995**, *36*, 421-426.

(28) A. Baceiredo, et al. *Journal of Organometallic Chemistry* **2007**, *692*, 705-708.

(29) J. Chojnowski, S. Rubinsztajn, W. Fortuniak, J. Kurjata *Journal of Inorganic and Organometallic Polymers and Materials* **2007**, *17*, 173-187.

(30) C. L. Lee, O. W. Marko, O. K. Johannson *Journal of Polymer Science* **1976**, *14*, 743-758.

(31) J. Pfeiffer, O. Schäfer *5th European Silicon Days: Oral Presentation* **2009**, *Vienna, Austria*.

(32) G. Richard, A.-F. Mingotaud, D. Cardinaud, A. Soum *Polymer Bulletin* **1997**, *39*, 581-588.

(33) P. J. Miller, K. Matyjaszewski *Macromolecules* **1999**, *32*, 8760-8767.

(34) J. Chojnowski, et al. *Polymer* **2004**, *45*, 6111-6121.

(35) J. Chojnowski, et al. *Macromolecules* **2003**, *36*, 3890-3897.

(36) J. K. Paulasaari, W. P. Weber *Macromolecules* **1999**, *32*, 6574-6577.

(37) Brandstätter, M. *PhD-Thesis: Funktionelle Silikone und Siloxane* **2010**, Graz University of Technology.

(38) P. J. Wang, Y. J. Zeng, C. T. Huang, I. Lin *Journal of Polymer Science* **1958**, *30*, 525-532.

(39) R. M. Waymouth, et al. *Organic Letters* **2006**, *8*, 4683-4686.

(40) C. Brochon, A. F. Mingotaud, M. Schappacher, A. Soum *Macromolecules* **2007**, *40*, 3547-3553.

(41) T. Akimoto, K. Kawahara, Y. Nagase, T. Aoyagi *Macromolecular Chemistry and Physics* **2000**, *201*, 2729-2734.

(42) Y. Poojari, S. J. Clarson *Journal of Inorganic and Organometallic Polymers and Materials* **2010**, *20*, 46-52.

(43) J. Zhao, A. Sakthivel, A. M. Santos, F. E. Kühn *Inorganica Chimica Acta* **2005**, *358*, 4201-4207.

(44) G. Sauvet, S. Dupond, K. Kazmierski, J. Chojnowski *Journal of Applied Polymer Science* **2000**, *75*, 1005-1012.

(45) G. Lohmann, K. Rühlmann *Plaste und Kautschuk* **1985**, *32*, 206-210.

(46) Y. Poojari, S. J. Clarson *Macromolecules* **2010**, *43*, 4616-4622.

(47) M. S. Owen, T. C. Kendrick, B. M. Kingston, N. C. Lloyd *Journal of Colloid and Interface Science* **1967**, *24*, 135-140.

(48) Vaughn, H. A. *Journal of Polymer Science Part B: Polymer Letters* **1969**, *7*, 569-572.

(49) Kambour, R. P. *Journal of Polymer Science Part B: Polymer Letters* **1969**, *7*, 573-577.

(50) G. Emig, E. Klemm *Technische Chemie*; 5 ed.; Springer-Verlag, 2005.

(51) Siebenhofer, M. *VU-Skriptum, LV-Nr. 667.500* **2007**, *Reaktionstechnik I*.

(52) Siebenhofer, M. *VU-Skriptum, LV-Nr. 667.550* **2008**, *Reaktionstechnik II*.

(53) Tilton, J. N. In *Perry's Chemical Engineers' Handbook*; McGraw-Hill: 2004.

(54) Dean, W. R. *Proceedings of the Royal Society of London* **1928**, *121*, 402-420.

(55) P. G. Drazin, W. H. Reid *Hydrodynamic Stability*; 2nd ed.; Cambridge Mathematical Library, 2004.

(56) Gschwind, P. *PhD-Thesis: Strömungs- und Transportvorgänge in gewellten Kanälen mit ineinanderliegender Anordnung der Wände* **2000**, Institut für Lebensmitteltechnologie, Universität Hohenheim.

(57) M. Hesse, H. Meier, B. Zeeh *Spektroskopische Methoden in der organischen Chemie* **2005**, *7., überarbeitete Auflage*.

(58) Walas, S. M. In *Perry's Chemical Engineers' Handbook*; McGraw-Hill: 2004.

(59) Brandstätter, M. *Diploma Thesis: Monofunktionelle Oligosiloxane* **2006**, Graz University of Technology.

(60) Muresanu, C. *PC LU Skriptum, LV-Nr. 635.021* **2004**, *Kalorimetrie*.

(61) R. W. LaRochelle, J. D. Cargioli, E. A. Williams *Macromolecules* **1976**, *9*, 85-88.

(62) Wilcock, D. F. *JACS* **1946**, *68*, 691-696.

(63) S. Meth, C. N. Sukenik *Thin Solid Films* **2003**, *425*, 49-58.

(64) Y. Azuma, K. Nogami, N. Ohshima *Journal of Ceramic Society of Japan, International Edition* **1992**, *100*, 646-651.

(65) Pschera, C. *Diploma Thesis: Herstellung monodisperser Polydimethylsiloxane: Bau, Planung und Inbetriebnahme eines Rohrreaktors* **2009**, Graz University of Technology.

(66) Römpp *www.roempp.com* **2010**, *Stichwort: "statische Mischer"*.

(67) H. Gilman, A. H. Haubein *JACS* **1944**, *66*, 1515-1516.

(68) H. Gilman, F. K. Cartledge *J. Organometal. Chem.* **1964**, *2*, 447-454.

(69) B. Heyn, B. Hipler, G. Kreisel, H. Schreer, D. Walther *Anorganische Synthesechemie*; Springer-Verlag, 1986.

(70) A. Golloch, H. M. Kuß, P. Sartori *Anorganisch Chemische Präparate*; de Gruyter, 1985.

(71) Markert, A. *Chemische Affinität - Warum laufen chemische Reaktionen ab* **1978**, *Otto Salle Verlag*.

(72) *ASTM - D7042 - 04 2004*, Standard Test Method for Dynamic Viscosity and Density of Liquids by Stabinger Viscometer (and the Calculation of Kinematic Viscosity).